



National Library
of Canada

Acquisitions and
Bibliographic Services Branch

395 Wellington Street
Ottawa, Ontario
K1A 0N4

Bibliothèque nationale
du Canada

Direction des acquisitions et
des services bibliographiques

395, rue Wellington
Ottawa (Ontario)
K1A 0N4

Your file - Votre référence

Our file - Notre référence

NOTICE

The quality of this microform is heavily dependent upon the quality of the original thesis submitted for microfilming. Every effort has been made to ensure the highest quality of reproduction possible.

If pages are missing, contact the university which granted the degree.

Some pages may have indistinct print especially if the original pages were typed with a poor typewriter ribbon or if the university sent us an inferior photocopy.

Reproduction in full or in part of this microform is governed by the Canadian Copyright Act, R.S.C. 1970, c. C-30, and subsequent amendments.

AVIS

La qualité de cette microforme dépend grandement de la qualité de la thèse soumise au microfilmage. Nous avons tout fait pour assurer une qualité supérieure de reproduction.

S'il manque des pages, veuillez communiquer avec l'université qui a conféré le grade.

La qualité d'impression de certaines pages peut laisser à désirer, surtout si les pages originales ont été dactylographiées à l'aide d'un ruban usé ou si l'université nous a fait parvenir une photocopie de qualité inférieure.

La reproduction, même partielle, de cette microforme est soumise à la Loi canadienne sur le droit d'auteur, SRC 1970, c. C-30, et ses amendements subséquents.

Canada

UNIVERSITY OF ALBERTA

ACTIVATED CARBON
FROM SYNTHETIC
PETROLEUM COKE

BY

ROBERT DI PANFILO ©

A THESIS

SUBMITTED TO THE FACULTY OF
GRADUATE STUDIES AND RESEARCH
IN PARTIAL FULFILLMENT OF THE
REQUIREMENT FOR THE DEGREE OF
MASTER OF SCIENCE
IN
MINERAL ENGINEERING

DEPARTMENT OF MINING
METALLURGICAL AND PETROLEUM
ENGINEERING

EDMONTON, ALBERTA
SPRING 1995



National Library
of Canada

Acquisitions and
Bibliographic Services Branch

395 Wellington Street
Ottawa, Ontario
K1A 0N4

Bibliothèque nationale
du Canada

Direction des acquisitions et
des services bibliographiques

395, rue Wellington
Ottawa (Ontario)
K1A 0N4

Your file *Votre référence*

Our file *Notre référence*

THE AUTHOR HAS GRANTED AN IRREVOCABLE NON-EXCLUSIVE LICENCE ALLOWING THE NATIONAL LIBRARY OF CANADA TO REPRODUCE, LOAN, DISTRIBUTE OR SELL COPIES OF HIS/HER THESIS BY ANY MEANS AND IN ANY FORM OR FORMAT, MAKING THIS THESIS AVAILABLE TO INTERESTED PERSONS.

L'AUTEUR A ACCORDE UNE LICENCE IRREVOCABLE ET NON EXCLUSIVE PERMETTANT A LA BIBLIOTHEQUE NATIONALE DU CANADA DE REPRODUIRE, PRETER, DISTRIBUER OU VENDRE DES COPIES DE SA THESE DE QUELQUE MANIERE ET SOUS QUELQUE FORME QUE CE SOIT POUR METTRE DES EXEMPLAIRES DE CETTE THESE A LA DISPOSITION DES PERSONNE INTERESSEES.

THE AUTHOR RETAINS OWNERSHIP OF THE COPYRIGHT IN HIS/HER THESIS. NEITHER THE THESIS NOR SUBSTANTIAL EXTRACTS FROM IT MAY BE PRINTED OR OTHERWISE REPRODUCED WITHOUT HIS/HER PERMISSION.

L'AUTEUR CONSERVE LA PROPRIETE DU DROIT D'AUTEUR QUI PROTEGE SA THESE. NI LA THESE NI DES EXTRAITS SUBSTANTIELS DE CELLE-CI NE DOIVENT ETRE IMPRIMES OU AUTREMENT REPRODUITS SANS SON AUTORISATION.

ISBN 0-612-01597-1

Canada

UNIVERSITY OF ALBERTA

Library Release Form

Name of Author: Robert Di Panfilo

Title of Thesis: Activated Carbon From Synthetic Petroleum Residue

Degree: Master of Science

Year this Degree Granted: 1995

Permission is hereby granted to the University of Alberta Library to reproduce single copies of this thesis and to lend or sell such copies for private, scholarly, or scientific research purposes only.

The author reserves all other publication and other rights in association with the copyright in the thesis, and except as hereinbefore provided, neither the thesis nor any substantial thereof may be printed or otherwise reproduced in any material form whatever without the author's prior written permission.


Robert Di Panfilo

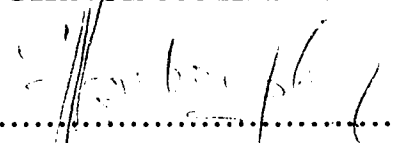
Permanent Address: 14120 - 96 Street
Edmonton, Alberta
T5E 5Z2


Date Submitted: January 27, 1995.

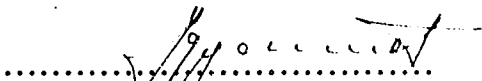
UNIVERSITY OF ALBERTA

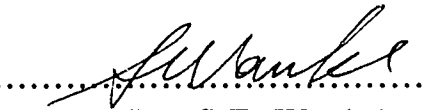
FACULTY OF GRADUATE STUDIES AND RESEARCH

The undersigned certify that they have read, and recommend to the Faculty of Graduate Studies and Research, for acceptance, a thesis entitled **ACTIVATED CARBON FROM SYNTHETIC PETROLEUM COKE** submitted by **ROBERT DI PANFILO** in partial fulfillment of the requirements for the degree of **MASTER OF SCIENCE** in **MINERAL ENGINEERING**.


.....
(Dr. N.O. Egiebor)
Supervisor


.....
(Prof. L.R. Plitt)


.....
(Dr. J. Szymanski)


.....
(Dr. S.E. Wanke)

Date: *January 26*....., 1995

DEDICATION

This thesis is dedicated to the memory
of my father, **Carlo Di Panfilo**, who
unfortunately did not live long enough
to see its completion. To my mother,
Iolanda Di Panfilo, thank you for
all your support and understanding.

ABSTRACT

The production of activated carbon from synthetic fluid petroleum coke was investigated. A simple two-step pyrolysis/activation procedure was found to be sufficient to convert raw fluid coke and potassium treated fluid coke into activated cokes with properties comparable to commercial grade activated carbon.

The activated carbon produced was found to have adsorptive capacities 20 to 50 times greater than raw fluid coke and roughly one quarter of the adsorptive capacity of the best commercial grade activated carbon. The activated coke has the ability to adsorb large molecular molecules, light hydrocarbons and ions from a liquid stream. The adsorptive capacity is attributable to the large surface area and porosity developed from the activation. The maximum N₂ BET surface area developed was 318 m² g⁻¹ at a porosity of 0.24 cm³ g⁻¹, and was produced by steam activation of raw coke at a temperature of 850°C with a soak time of 6 hours.

Potassium treatment was observed to increase the rate of carbon conversion by steam activation which in turn developed more microporosity than the untreated coke. However, faster carbon conversion did not lead to higher surface areas due to excessive carbon loss and ash poisoning of the coke surface. The untreated activated coke had the highest surface area and correspondingly the highest adsorptive capacity for large

organic molecules such as methylene blue dye; however both the potassium and untreated coke had the same adsorptive capacity for aqueous iodine.

Scanning electron microscopy revealed a novel mechanism of activation. The physical structure of the fluid coke along with its reaction to the pyrolysis/activation caused a density change which initially leads to tension cracking of the coke particle. Activation then proceeded into the interior of the coke particle where it migrated along highly reactive contact surfaces present as concentric spheres. The resulting activated carbon consisted of concentric spheres of porous carbon.

ACKNOWLEDGEMENT

I would like to thank my supervisor, Dr. N. O. Egiebor for all his assistance and encouragement in the completion of this thesis.

The author also wishes to acknowledge the support provided by the technical, academic and administrative staff of the Mining, Metallurgical and Petroleum Engineering Department, especially Mr. Bashir Mohamedhai and Ms. Tina Barker.

TABLE OF CONTENTS

CHAPTER	PAGE
1. INTRODUCTION.....	1
2. LITERATURE SURVEY.....	8
2.1 Petroleum Coke From Athabasca Oil Sands Bitumen.....	8
2.1.1 Delayed Petroleum Coke.....	8
2.1.2 Fluid Petroleum Coke.....	9
2.1.2.1 Gasification.....	10
2.1.3 Flexicoke.....	11
2.1.4 Adsorption Properties of Petroleum Coke.....	11
2.1.4.1 High Surface Area Activated Cokes.....	12
2.2 Activated Carbon.....	13
2.2.1 General Properties.....	15
2.2.1.1 Physical Structure.....	16
2.2.1.2 Surface Chemistry.....	25
2.2.1.3 Catalytic Properties.....	29
2.2.1.4 Adsorption Models.....	32
2.2.1.3.1 Gas Adsorption.....	32
2.2.1.3.2 Liquid Adsorption.....	36
2.2.2 Production of Activated Carbon.....	36
2.2.2.1 Raw Material.....	39
2.2.2.2 Granulation.....	43

CHAPTER	PAGE
2.2.2.3 Carbonization.....	44
2.2.2.4 Activation.....	47
2.2.2.5 Regeneration.....	56
3. EXPERIMENTAL.....	58
3.1 Materials.....	58
3.2 Analysis.....	59
3.2.1 Size Analysis.....	60
3.2.2 Proximate and Ultimate Analysis.....	60
3.2.3 Density Analysis.....	60
3.2.4 Scanning Electron Microscope Analysis.....	61
3.2.5 BET Surface Area Analysis.....	62
3.2.6 Zeta Potential and pH Analysis.....	62
3.2.7 Gas Chromotography.....	64
3.2.8 Adsorption Analysis.....	64
3.2.8.1 Methylene Blue Adsorption.....	64
3.2.8.2 Iodine Adsorption.....	65
3.3 Pyrolysis and Activation.....	66
3.3.1 Pyrolysis.....	66
3.3.2 Activation.....	67
4. RESULTS AND DISCUSSION.....	71
4.1 Analysis.....	71
4.1.i Pyrolysis of Fluid Petroleum Coke.....	71

CHAPTER	PAGE
4.1.2 Activation of Fluid Petroleum Coke.....	79
4.1.3 Proximate and Ultimate Analysis.....	93
4.1.4 Size Analysis.....	98
4.1.5 Density Analysis.....	104
4.1.5.1 Bulk Density.....	104
4.1.5.2 Absolute Density.....	115
4.1.6 BET Surface Area and Porosity Analysis.....	120
4.1.6.1 Surface Area.....	120
4.1.6.2 Surface Area and Porosity Distribution.....	125
4.1.6.3 Adsorption Isotherms.....	132
4.1.7 pH and Zeta Potential.....	143
4.1.7.1 pH.....	143
4.1.7.2 Zeta Potential.....	144
4.1.8 Aqueous Adsorption.....	155
4.1.9 Gas Analysis.....	158
4.1.10 Scanning Electron Microscopy.....	162
4.1.10.1 Raw Fluid Coke.....	162
4.1.10.2 Activated Coke.....	164
4.1.10.3 Activated Potassium Coke.....	174
4.2 General Discussion.....	183
4.2.1 Evolution of Pore Structure.....	183
4.2.2 Surface Chemistry.....	188

CHAPTER	PAGE
5. CONCLUSIONS.....	189
6. REFERENCES.....	192
7. APPENDIX A.....	207

LIST OF TABLES

TABLE		PAGE
1	Pyrolysis Analysis of Raw Fluid Petroleum Coke at 200°C, 400°C, 600°C, and 800°C, (As Recieved).....	72
2	Pyrolysis Analysis of Raw Fluid Petroleum Coke at 400°C, (As Recieved and Crushed).....	74
3	Recovery, Burnoff and Water Efficiency of Activated Fluid Petroleum Coke.....	80
4	Recovery, Burnoff and Water Efficiency of Activated Potassium (4% KOH) Fluid Coke.....	87
5	Proximate and Ultimate Analysis of Raw Coke, Untreated Activated Coke (B-1), and Potassium Treated (4% KOH) Activated Coke (B-7).....	94
6	Particle Size Analysis of Raw Fluid Petroleum Coke.....	99
7	Particle Size Analysis of Activated Fluid Petroleum Coke (Sample B-2).....	100
8	Particle Size Analysis of Potassium Treated (4% KOH) Fluid Coke (Sample B-8).....	101
9	Bulk Densities of Raw Coke and Activated Fluid Petroleum Coke.....	105
10	Bulk Densities of Activated Potassium (4% KOH) Fluid Petroleum Coke and Coconut Charcoal.....	107
11	Absolute Densities of Raw Coke, Activated Untreated Coke and Coconut Charcoal.....	116
12	Specific Surface Area of Raw Coke, Untreated Activated Coke, Potassium Treated (4% KOH) Activated Coke and Coconut Charcoal.....	121

TABLE	PAGE
13	Surface Area and Porosity Characteristics of Raw Coke, Untreated Activated Coke, Potassium Treated (4% KOH) Activated Coke and Coconut Charcoal.....127
14	Surface Area and Porosity Distribution of Untreated and Potassium Treated (4% KOH) Activated Fluid Petroleum Coke.....128
15	Zeta Potential of Untreated Activated Coke (Sample B-4) as a Function of pH.....145
16	Zeta Potential of Potassium Activated Coke (Sample B-7) as a Function of pH.....147
17	Zeta Potential of Fisher Coconut Charcoal as a Function of pH.....149
18	Summary of Aqueous Adsorption of Methylene Blue and Iodine.....156
19	Gas Composition from the Steam Activation of Untreated Coke at 850°C.....159

LIST OF FIGURES

FIGURE		PAGE
1	Schematic of the Pyrolysis/Activation Reactor and Experimental Setup.....	68
2	The Pyrolysis Recoveries of Raw Fluid Petroleum Coke at 200°C, 400°C, 600°C and 800°C.....	73
3	The Pyrolysis Recoveries of Crushed and Uncrushed Raw Fluid Petroleum Coke at 400°C.....	75
4	The Burnoff of Untreated Activated Coke as a Function of Activation Time.....	81
5	The Water Efficiency of the Activation of Untreated Coke as a Function of Activation Time.....	82
6	The Water Efficiency of the Activation of Untreated Coke as a Function of Burnoff.....	83
7	The Burnoff of Potassium Treated (4% KOH) Activated Coke as a Function of Activation Time.....	88
8	The Water Efficiency of the Activation of Potassium Treated (4% KOH) Coke as a Function of Activation Time.....	89
9	The Water Efficiency of the Activation of Potassium Treated (4% KOH) Coke as a Function of Burnoff.....	90
10	Comparison of the Recoveries of Untreated Activated Coke and Potassium Treated (4% KOH) Coke as a Function of Activation Time.....	92
11	The Particle Size Analysis of Raw Coke, Activated Coke (Sample B-2), and Potassium Treated (4% KOH) Activated Coke (Sample B-8).....	102
12	The Bulk Densities of Untreated Activated Coke as a Function of Activation Time.....	106

FIGURE	PAGE
13	The Bulk Densities of Untreated Activated Coke as a Function of Burnoff.....107
14	The Bulk Densities of Potassium Treated (4% KOH) Activated Coke as a Function of Activation Time.....110
15	The Bulk Densities of Potassium Treated (4% KOH) Activated Coke as a Function of Burnoff.....111
16	Comparison of the Bulk Densities of Untreated Activated Coke and Potassium Treated (4% KOH) Activated Coke as a Function of Activation Time.....112
17	Comparison of the Bulk Densities of Untreated Activated Coke and Potassium Treated (4% KOH) Activated Coke as a Function of Burnoff.....113
18	The Absolute Density of Untreated Activated Coke as a Function of Activation Time.....117
19	The Absolute Density of Untreated Activated Coke as a Function of Burnoff.....118
20	The BET Surface Areas of Untreated and Potassium Treated (4% KOH) Cokes as a Function of Activation Time.....122
21	The BET Surface Areas of Untreated and Potassium Treated (4% KOH) Cokes as a Function of Burnoff.....124
22	The Specific Surface Area Distribution Between Micro and MesoPores For Raw Coke, Untreated Activated Coke, Potassium Treated (4% KOH) Coke and Fisher Coconut Charcoal.....129
23	The Specific Pore Volume Distribution Between Micro and MesoPores For Raw Coke, Untreated Activated Coke, Potassium Treated (4% KOH) Coke and Fisher Coconut Charcoal.....130

FIGURE	PAGE
24 Adsorption and Desorption Isotherms for Raw Petroleum Coke, (Sample C-1).....	133
25 Adsorption and Desorption Isotherms for Raw Petroleum Coke, (Sample C-2).....	134
26 Adsorption and Desorption Isotherms for Untreated Activated Coke, (Sample A-9).....	136
27 Adsorption and Desorption Isotherms for Untreated Activated Coke, (Sample A-12).....	137
28 Adsorption and Desorption isotherms for Untreated Activated Coke, (Sample A-17).....	138
29 Adsorption and Desorption Isotherms for Potassium Treated (4% KOH) Coke, (Sample A-11).....	139
30 Adsorption and Desorption Isotherms for Potassium Treated (4% KOH) Coke, (Sample A-14).....	140
31 Adsorption and Desorption Isotherms for Potassium Treated (4% KOH) Coke, (Sample A-18).....	141
32 Adsorption and Desorption Isotherms for Fisher Coconut Charcoal.....	142
33 The Relative Zeta Potential of Untreated Activated Coke (Sample B-4) as a Function of pH.....	146
34 The Relative Zeta Potential of Potassium Treated (4% KOH) Activated Coke (Sample B-7) as a Function of pH.....	148
35 The Relative Zeta Potential of Fisher Coconut Charcoal as a Function of pH.....	150
28 The Gas Composition from the Steam Activation of Untreated Coke at 850°C.....	160

LISTS OF PLATES

PLATE	PAGE
1	SEM Micrograph of Raw Fluid Petroleum Coke, (x200).....163
2	SEM Micrograph of Raw Fluid Petroleum Coke (x1000).....163
3	SEM Micrograph of a Cross Section of Raw Fluid Petroleum Coke, (x200).....165
4	SEM Micrograph of a Cross Section of Raw Fluid Petroleum Coke, (x1000).....165
5	SEM Micrograph of a Cross Section of Untreated Coke Activated for 0 Hours, Sample B-13, (x200).....166
6	SEM Micrograph of a Cross Section of Untreated Coke Activated for 0 Hours, Sample B-13, (x1000).....166
7	SEM Micrograph of Untreated Coke Activated for 2 Hours, Sample A-9, (x200).....168
8	SEM Micrograph of Untreated Coke Activated for 2 Hours, Sample A-9, (x1000).....168
9	SEM Micrograph of Untreated Coke Activated for 2 Hours, Sample A-9, (x5000).....169
10	SEM Micrograph of Untreated Coke Activated for 4 Hours, Sample A-12, (x200).....171
11	SEM Micrograph of Untreated Coke Activated for 4 Hours, Sample A-12, (x1000).....171
12	SEM Micrograph of Untreated Coke Activated for 6 Hours, Sample A-17, (x200).....173

PLATE	PAGE
13 SEM Micrograph of Untreated Coke Activated for 6 Hours, Sample A-17, (x1000).....	173
14 SEM Micrograph of Potassium Treated (4% KOH) Coke Activated for 2 Hours, Sample A-11, (x200).....	175
15 SEM Micrograph of Potassium Treated (4% KOH) Coke Activated for 2 Hours, Sample A-11, (x1000).....	175
16 SEM Micrograph of a Cross Section of Potassium Treated (4% KOH) Coke Activated for 2 Hours, Sample A-11, (x250).....	177
17 SEM Micrograph of Potassium Treated (4% KOH) Coke Activated for 4 Hours, Sample A-14, (x200).....	179
18 SEM Micrograph of Potassium Treated (4% KOH) Coke Activated for 4 Hours, Sample A-14, (x1000).....	179
19 SEM Micrograph of Potassium Treated (4% KOH) Coke Activated for 6 Hours, Sample A-18, (x200).....	180
20 SEM Micrograph of Potassium Treated (4% KOH) Coke Activated for 6 Hours, Sample A-18, (x1000).....	180
21 SEM Micrograph of a Cross Section of Potassium Treated (4% KOH) Coke Activated for 6 Hours, Sample A-18, (x445).....	182

1. INTRODUCTION

Activated carbons are predominately carbon compounds with the ability to adsorb molecules from an aqueous or gaseous stream. They are manufactured from carbonaceous materials such as plant matter, wood, coal, petroleum, plastics, petroleum wastes, etc. [1-25]. Activated carbons are characterized by a very large specific surface area with typical values of 100 - 1000 m² g⁻¹ [26] and a large specific pore volume ranging from 0.2 - 1.0 cm³ g⁻¹ [26]. The internal porosity is composed of different sizes of pores known as micropores, transitional pores (mesopores) and macropores. The size range of each pore classification is defined differently by various authors but is usually based on its adsorptive function. According to Dubinin [27], micropores have a diameter of less than 20 nm, transitional pores range from 20 to 500 nm, and macropores have a diameter of 500 nm to several thousand nanometers. The IUPAC [26] classification of pores gives the diameters for micropores as less than 2 nm, between 2 and 50 nm for transitional pores and over 50 nm for macropores.

The micropores, which can make up to 95% of the total surface area, represents the sites where the majority of the adsorption occurs. The transitional and macropores are important for providing access from the exterior of the activated carbon to its interior surfaces, thus providing a route for the adsorbate to migrate to an adsorption site.

Adsorbates such as non-ionic molecules and solids are adsorbed by pore filling [26] but ionic and/or polar molecules are adsorbed by physiochemical and chemical reactions on the surface of the activated carbon [29]. The chemical adsorption (chemisorption) binds the adsorbate to the carbon surface by forces approximating a chemical bond. The ease of adsorption of specific adsorbates is dependent on the surface chemistry of the activated carbon. The surface of activated carbon can consist of a wide variety of functional groups [30]. Depending on the types of functional groups, the activated carbons can be classified as acidic, basic or neutral [29].

The physical structure (porosity, surface area, pore distribution, etc.) and the surface chemistry combine to give activated carbons their adsorptive properties. Both the physical and chemical properties are a direct result of the type of raw material used and the manufacturing method. By varying the production methods and manufacturing variables, activated carbons can be tailored to have widely different adsorptive properties [31]. Some activated carbons are ideal for adsorbing gas molecules from a gaseous stream, such as removing toxic compounds from flue gases [32-40], separating oxygen or nitrogen from air [41-44], separating heavier hydrocarbons from natural gas and storing methane in activated carbons [45,46].

Activated carbons which are ideal for adsorption from a liquid phase have quite different properties from those for gas adsorption. The

mesopores and macropores have to be fully developed for transporting molecules to the adsorption sites, and the surface chemistry must be more reactive. There are different types of activated carbons suitable for different types of adsorbates present in wastewater. Typical uses of activated carbons are: purification in the food industry [26], water and wastewater treatment [28], and the recovery of precious metals from hydrometallurgical processes [47-49]. Activated carbons are also used in the food processing, pharmaceutical, chemical, petroleum, mining, nuclear, automobile, and vacuum manufacturing industries [30].

Although there are as many methods of producing activated carbons as there are raw materials [30], the manufacturing process must accomplish two basic things, carbonization and then activation.

Carbonization is where the elemental carbon content of the raw material is increased by pyrolysis, heating the raw material in an inert atmosphere to drive off moisture, volatiles and non-carbon elements. Carbonization also changes the molecular structure of the raw material; the carbons form aromatic rings which in turn form sheets of aromatic carbons. These carbon sheets in turn combine to form microcrystals. Thermal stresses then rupture and recombine these microcrystals into a slightly porous structure [26] suitable for further treatment. Nevertheless, the overall structure of the carbonized material still retains characteristics of its original structure [10,52]. Carbonization can also be carried out by chemical methods where strong acids and dehydrating agents are added to carbonize the raw

material [53-56]. These dehydrating agents may or may not be recovered and recycled.

The second step in the manufacturing process is activation, where the necessary porosity and pore structure is imparted on the carbonized material [57-62]. This is generally achieved by physical activation, where an activating gas is made to react with the carbon at a high temperature so that a selective etching occurs that causes pores to develop. Typical activating gases are steam (H_2O) and carbon dioxide (CO_2); less used gases are oxygen (O_2), hydrogen (H_2), and hydrogen sulphide (H_2S) [63,64]. The activation proceeds until the desired surface area, porosity, and surface chemistry is achieved. Maximum surface area generally occurs when 40 - 60% of the carbon has been removed by activation [30]. Catalysts are sometimes added to increase the activation rate or to modify the porosity being developed [65-72]. Activation can also be carried out chemically, which involves mixing a carbonized material with an activating agent and then calcining the mixture at a high temperature. This is usually sufficient to produce the desired results although some physical activation may be required [53-56].

There is presently a need for more efficient and less costly methods of pollution control in the petroleum industry. Activated carbons are currently gaining wide popularity for wastewater treatment because of their efficiency and ease of use [28]. In the near future, activated carbon

technology is expected to provide a 'superclean' technology that is ten times more efficient than the current best available technology for air and water treatment [73].

The two existing oil sands plants in northern Alberta produce 3000 tons of petroleum coke per day as a by-product of upgrading bitumen into synthetic crude oil [75]. Syncrude Canada Ltd. produces fluid petroleum coke which is presently discarded and Suncor Inc. produces delayed petroleum coke of which 10 - 20% is used as fuel with the rest discarded. Suncor is expected to switch to fluid coke technology in the near future under a modernization plan [75]. This waste coke is abundant and readily available as a feed stock to produce activated carbon for on-site air and water treatment. The process of converting coke into activated carbon is identical to the gasification methods used to produce synthetic fuel gas from coal [77]. The production of activated carbon from coke can be carried out separately or in conjunction with synthetic water-gas production.

The utilization of this waste coke will provide several advantages to the synthetic crude oil industry in Alberta by:

- a) utilizing a cheap and/or worthless and abundant by-product as a raw material for the production of a valuable and commercially saleable activated carbon for use in wastewater treatment facilities locally, nationally and internationally.

- b) disposing of a major by-product of serious environmental concern to the petroleum industry, and**
- c) enhancing the development of advanced environmental technology.**

Consequently the primary objectives of this thesis are:

- 1) To investigate the production of activated carbon from fluid petroleum coke using technology that would be available in the oil sands industry,**
- 2) To compare the activation of raw fluid coke with coke treated with a catalyst,**
- 3) To study the physical and chemical properties of the activated cokes produced including the gaseous by-products,**
- 4) To determine the adsorptive properties of the activated cokes with respect to wastewater treatment,**
- 5) To identify the mechanics of activated carbon formation, and**

6) To compare the adsorptive capacities of raw coke, activated cokes, and a commercially available activated carbon.

2. LITERATURE REVIEW

2.1 Petroleum Coke from Athabasca Oil Sands Bitumen

Three types of petroleum cokes can be produced from bitumen derived from the Athabasca oil sands in northeastern Alberta. They are delayed coke, fluid coke and flexicoke [75,76]. Delayed coke is presently being produced by Suncor Inc., while fluid coke is produced at Syncrude Ltd. Flexicoke has been produced in a prototype flexicoker [75]. Today, fluid and delayed coke are being produced at a rate of 3000 tons per day [74]. These cokes have been studied for use as a fuel source [76], for gasification [77], for metal recovery [78], and as a sorbent for recovering residual bitumen [79,80].

2.1.1 Delayed Petroleum Coke

Delayed petroleum coke is produced from the delayed coker process, where bitumen is heated to about 480°C, introduced into a coking drum, and left to degrade thermally. After distillation of the volatile materials, the involatile coke is broken up hydraulically and cleared from the coking drum [75]. The coke particles are irregularly shaped ranging in size from centimeters to microns.

The delayed coke particles display no visible porosity down to a range of 500 microns [75]. Delayed coke is amorphous in structure [87],

with 92% of the carbon in aromatic form with half of the carbon atoms bonded to hydrogen atoms [78]. Delayed petroleum coke [78] has a high ash content containing high concentrations of vanadium, nickel, and sulphur.

2.1.2 Fluid Petroleum Coke

Fluid petroleum coke is produced in a fluidized bed reactor operating at temperatures of 600 °C [75] to 1000 °C [76]. A thin film of bitumen is sprayed onto a fluidized bed consisting of hot coke particles. The volatile material is driven off to be upgraded into synthetic crude oil and the coke particles get coated with a layer of coke. Excess fluid coke is removed from the reactor to be discarded.

The coke consists of solid, spherical particles ranging in size from a few microns to 2 cm. The coke is very abrasive and can have a Hardgrove Index as low as 17. The spherical particles have an 'Onion skin' internal structure [75] consisting of 30 to 100 layers of coke [81]. Scanning electron microscopy reveals a smooth, non-porous surface [78].

The high temperature conditions produces a non-porous graphitized carbon as indicated by its low amenability to acid leaching. All the carbons are aromatic with 45% of the carbons bonded to hydrogen atoms [78].

Fractal analysis, using N_2 adsorption, indicates that the specific surface area varies from 1 to $15 \text{ m}^2 \text{ g}^{-1}$ with decreasing particle size [83]. Fractal analysis describes the fractal geometry of the surface, where increasing and similar detail is revealed with increased magnification, a phenomena known as scale-invariance [83]. The fractal dimension of a surface is a measure of the space-filling ability of the surface: a higher value of fractal dimension indicates a more irregular surface [84]. Particles smaller than 69 microns have a different fractal dimension than larger particles; the specific surface area does not increase with decreasing size under 69 microns, probably due to a different chemical structure than the larger particles [83].

2.1.2.1 Gasification of Fluid Petroleum Coke

Fluid petroleum is difficult to gasify; requiring long residence times and relatively high temperatures to achieve high carbon conversions [84]. High carbon conversions of over 80% by weight need temperatures in excess of 1000°C [77].

It is suggested that the coke gasification rate is affected by the inaccessibility of active sites. The coke gasification rate is dependent on two factors, the composition of the bitumen used and the coking conditions [75]. These two factors influence the nature and concentration of active sites, accessibility of active sites to reactive gas and catalysis by mineral

matter [85,86]. The rate of oxygen adsorption may be directly related to the accessibility of the active sites. The higher the rate of oxygen adsorption, the higher the rate of gasification. Oxygen adsorption was shown to increase with decreased temperature of coking, soak time and particle size [86].

2.1.3 Flexicoke

Flexicoke is produced by a modified fluid coking process where a gasification cycle is added to the fluid coking system. The coke leaving the coker is passed through a gasifier loop where it reacts with steam to produce a low calorific value fuel gas. The flexicoking tends to agglomerate the individual coke particles into large porous structures [75].

2.1.4 Adsorption Properties of Petroleum Coke

Delayed coke has been studied for use as a sorbent in the recovery of residual bitumen from aqueous tailings streams [79,80]. The coke displays oleophilic properties and readily agglomerates with bitumen when mixed vigorously with tailings pond sludge. A strong linear correlation exists between the amount of bitumen recovered and the BET surface area of the coke particles. The porosity and the medium pore size also correlate to bitumen recovery. One study by Kumar *et al* [79] indicates that the size of the coke particle is the most important variable in bitumen recovery. Another study by Hall *et al* [80] states that the external surface area and

not the total surface area is the most important variable in the sorption of bitumen. The bitumen adsorbed by the coke particles can be desorbed by high temperatures and the coke recycled for reuse. One study indicated a bitumen recovery of 40% by weight [80], while another indicated a recovery of 80 to 200% bitumen by weight [79]. These cokes were mildly activated with steam at a temperature of 870°C for two hours.

2.1.4.1 High Surface Area Activated Cokes

Only three studies have been found which actually looked at producing activated carbon from petroleum coke: one from fluid coke, one from delayed coke, and the last from an unidentified petroleum coke.

The study by O'Grady *et al* [88] used low ash petroleum cokes from unidentified sources to produce activated carbons with specific surface areas of over 2500 m² g⁻¹ and 'extraordinary' adsorptive properties. A direct chemical activation process was used for production of the activated carbon. Petroleum coke was mixed with 2 to 4 times its weight of potassium hydroxide (KOH). The mixture was calcined at 400 to 500°C, then pyrolyzed at 800 to 900°C. The potassium salts were removed by washing with water.

The study by Metraier [81] describes a patent where treated fluid coke in a fluid bed reactor is activated with air at 800°F for 11 hours to reach a burnoff of 35 wt%. Then steam is added at a rate of 9.0 ft³ per hour per pound of coke at 1650°F for 6 hours to achieve a burnoff of 70 wt%. The coke is reported to have good results in water purification.

The study by Tollefson [89] converted delayed coke from Suncor Inc. to an activated carbon with a specific surface area of 220 - 400 m² g⁻¹. The product had good wettability and abrasion resistance. The method of activation was not given.

2.2 Activated Carbon

The study of activated carbons covers a wide range of carbon types, manufacturing methods, applications, and regeneration techniques. Activated carbon is manufactured from carbonaceous material to produce a high carbon, high porosity, high surface area material with very good and universal adsorptive properties. The manufacturing process involves carbonization and activation. Carbonization increases the carbon content and activation develops the physical and chemical properties of the activated carbon. Carbonization and activation can be carried out either physically or chemically using dehydrating agents. Physical activation involves carbon gasification with an activating gas at high temperatures. The activated carbon can be manufactured as a granular activated carbon (GAC) or as a powdered activated carbon (PAC). Powdered activated

carbon is obtained by crushing activated carbon. Granular activated carbons can be produced from granular raw material or raw material can be bonded with a physical binder to form pellets. Granular activated carbons are usually characterized by large surface areas and small pores while PACs usually have larger pores and less surface area [29].

The specific physical properties of activated carbon determines its usefulness. It can be used in either gaseous or liquid environments for contaminant removal, or to separate and recover a specific component of a liquid or gaseous mixture. Some activated carbons can adsorb their own weight or more in adsorbate. Activated carbons were often used once and then discarded but recent technology makes it possible to regenerate activated carbons for reuse. Regeneration involves either thermal decomposition or chemical removal of the adsorbate.

There is a extensive body of experimental data on activated carbons, with many studies on types of raw materials used, carbonization and activation procedures, adsorption properties, rates of reaction, catalytic activity, use of catalysts, surface chemistry and physical properties. The type of raw material and the manufacturing method both determine the final properties of an activated carbon. Due to the variability of some raw materials, many results are not reproducible. No general theory exists which can predict the physical or chemical properties of an activated carbon using a uniform raw material and a specific manufacturing process.

Raw material is almost never uniform in composition and the variables used in manufacturing are numerous. Activated carbons are basically similar, but each individual type of activated carbon is unique and must be evaluated as such.

2.2.1 General Properties

Activated carbons are composed of carbon (80 - 97%) [26,30] with minor amounts of hydrogen, oxygen, sulphur and nitrogen. Mineral ash may range from 1 to 20% of the total mass. Usually ash is removed before or after manufacturing [54,55]. Generally the lower the ash content the better the adsorption properties of activated carbon. Some ash content is uneconomically or physically impossible to remove. In some cases the ash content beneficially influences the surface chemistry of the activated carbon by acting as a catalyst [109].

The ability of activated carbon to adsorb specific molecules from both a gas and liquid phase is a direct result of its porous nature and surface chemistry. Activated carbon may have a specific pore volume of $0.2 \text{ cm}^3 \text{ g}^{-1}$ to over $1.0 \text{ cm}^3 \text{ g}^{-1}$ [80], consisting of interconnected pores, cracks and fissures ranging in size from 0.1 to several thousand nanometers [26]. The high specific pore volume in turn leads to a high specific surface area which in some commercial activated carbons can range from 200 - 1000 $\text{m}^2 \text{ g}^{-1}$. The maximum surface area achieved is over 2500 $\text{m}^2 \text{ g}^{-1}$.

The surface chemistry of an activated carbon affects its adsorptive properties, as well as its catalytic, redox, electrochemical and hydrophilic or hydrophobic properties. The surface chemistry is ultimately determined by the type and quantity of heteroatoms attached to its surface, especially oxygen.

Adsorbates can be adsorbed either physically or chemically. Physical adsorption involves weak attractive forces and physical entrapment. In chemical adsorption, molecules react with the surface of the activated carbon in strong chemical reactions or strong 'physiochemical' [29] reactions, referred to as chemisorption.

2.2.1.1 Physical Structure

Crystalline Structure

The porosity and surface chemistry of activated carbon is related to its crystalline structure. The activated carbon structure is composed of microcrystals with a graphite like appearance. The crystals consist of parallel layers of aromatic sheets of carbon spaced 0.335 nanometers apart and orientated so that one half of the carbon atoms in one layer is placed exactly over or under the centers of the aromatic rings of the adjacent layer. A representation of how aromatic carbons align themselves in parallel layers is shown below in Figure I.

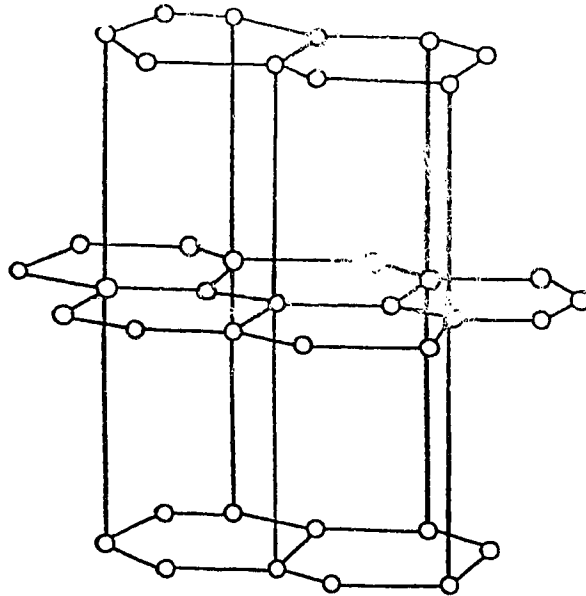


Figure I. Graphite crystal by Cookson [90].

Unlike graphite crystals, the presence of defects and heteroatoms causes disorder in the crystal lattice. The interlayer distances vary from 0.34 to 0.35 nm, and the orientation of the respective layers vary from each other. This disorderly structure is termed a turbostatic structure. A comparison of a three-dimensional crystal lattice of graphite (a) and a turbostatic structure of an activated carbon microcrystal (b), is shown below in Figure II.

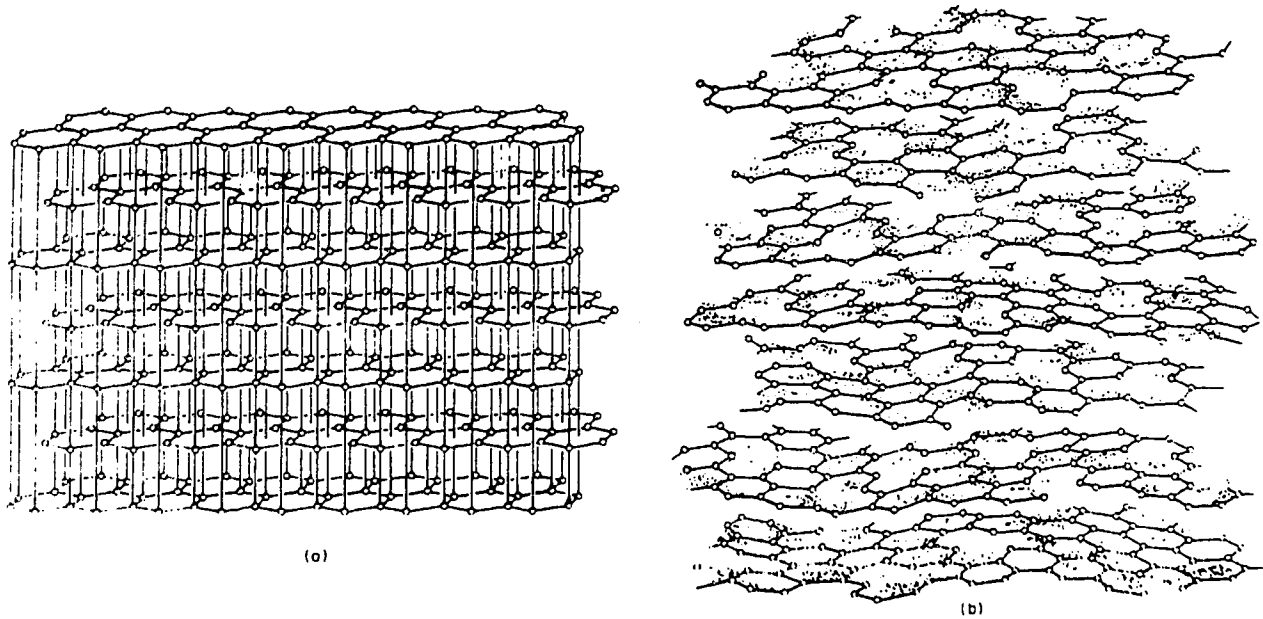


Figure II. Graphitic structure (a) vs turbostratic structure (b)
by Mattson *et al* [29].

The microcrystals have diameters of 1 to 10 nm and consist of 5 to 33 layers of aromatic sheets [26].

Cookson [90] doubts that the structure of the microcrystals is analogous to the structure of graphite. Instead, the microcrystals should be visualized as stacks of flat aromatic sheets cross linked in a random manner as illustrated below in Figure III.

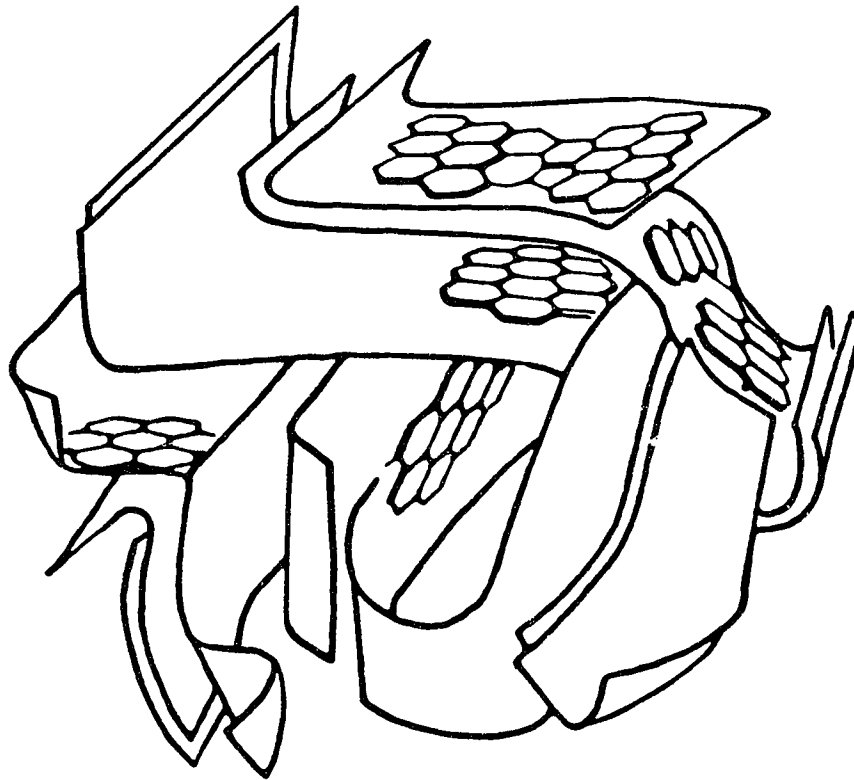


Figure III. Orientation of aromatic sheets in a microcrystal
from Bansal [30].

The size and orientation of the microcrystals are influenced mainly by the type of raw material used and by the production method. Carbons which are easily carbonized, graphitize easily and tend to align their microcrystals in parallel lines. Carbons which are hard to carbonize, do not graphitize easily and the microcrystals tend to produce a chaotic, irregular alignment of microcrystals. A comparison of an aligned and chaotic structure is shown below in Figure IV.

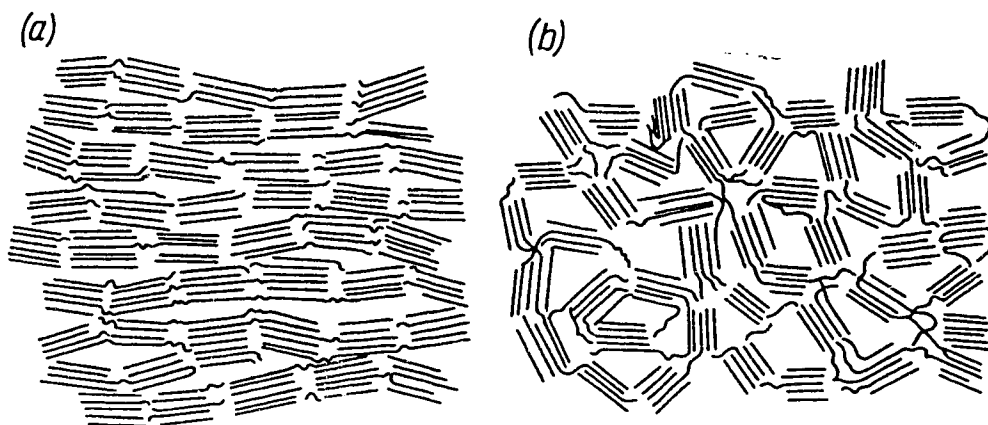


Figure IV. Aligned (a) vs chaotic (b) microcrystals
from Jankowska *et al* [26].

Carbons with a chaotic arrangement of microcrystals have a well developed pore structure, relatively high hardness due to strong cross-linking, and a low absolute density of $< 2 \text{ g cm}^{-3}$. Carbons which graphitize easily when carbonized form a regular structure, are weak, soft, have a poorly developed pore structure and a high absolute density of 2.26 g cm^{-3} .

Porosity

Activated carbons have a high porosity, consisting of interconnected pores of different shapes and sizes. The pore sizes are usually divided into arbitrary or specific categories. Dubinin [27] based his system on effective radii and their influence on the adsorption of gases. Dubinin proposed three types of pores, macro, meso and micropores.

Macropores, have a diameter greater than 500 nm. The surface area of the macropores is often less than 5% of the total surface area but these pores constitute up to 33 to 50% of the total pore volume [30]. These pores are not important for providing adsorption sites but they are important because they act as transport arteries for the adsorbate to migrate from the exterior fluid medium to the interior of the carbon particle.

Mesopores range in size from a diameter of 20 to 500 nm. These pores are transitional pores in that some adsorption takes place on their surfaces but they still act as transport arteries for adsorbate to migrate deeper into the activated carbon particle. The total volume of mesopores can vary from 20 to 35% [26] and the surface area can range from 5 to 25% [30].

Micropores have a diameter of less than 20 nm. They can make up to 20 to 40% of the total pore volume but up to 95% of the total surface area. The size of these pores is small enough to facilitate the adsorption of gas molecules. The energy of adsorption is higher in micropores than in the other two pores [23].

Activated carbons can be tailor made; by varying carbonization and activation parameters [111] only micropores of a certain size can be produced. A carbon with a large volume of micropores of a certain size is referred to as a molecular sieve can be used for gas separation [41-44]. The shape of the pores is also very important in facilitating the type of molecules that can be adsorbed. Bottle shaped pores can be produced [42] which have a smaller pore size at the surface than in the interior. These are suitable for gas separation. Regular pores with larger sizes at the surface are used for liquid adsorption purposes.

The relationship of the micro, meso and macropores to each other and how they form the pore structure is still under debate [26]. One theory states that macropores start at the surface of a carbon particle, and then branch into mesopores which in turn branch into micropores. An alternate theory states that all three sizes of pores intersect the surface and may not connect to each other and/or may connect to each other in no particular order.

Heteroatoms

Heteroatoms such as oxygen, hydrogen, sulphur and halogens are chemically combined with the carbon atoms especially at the edges and corners of the individual graphite sheets in the microcrystals. Oxygen is the most important heteroatom because it affects the reactivity and surface chemistry of the carbon. The next most important heteroatom is hydrogen. Oxygen is present either because it was present in the raw material or it becomes attached because of the activation process. Oxygen is easily attached to the carbon structure, especially at the edges and corners of the aromatic sheets due to unfilled valences in the individual carbon atoms. The oxygen content of an activated carbon can range from 1 to 25% by weight [26]. The amount of oxygen can be varied by changes in the activation parameters. Oxygen can be removed by pyrolysis at high temperatures or added by moderate pyrolysis in an oxygen rich atmosphere. Also aging of activated carbon causes some oxygen to chemically bond with the carbon.

Hydrogen is bonded more strongly to the carbon than oxygen and thus requires much higher temperatures to remove. Hydrogen exists either in aromatic form attached covalently to the edges of the aromatic sheets or in aliphatic form where it is attached to the edge of the aromatic carbons in aliphatic or alicyclic groups [26].

Mineral Matter

Mineral matter or ash originates from the mineral content of the raw material. Ash is important in the production of activated carbon and also influences the adsorptive capacity. During activation mineral matter can lower the rate of activation by blocking areas of the carbon from the activating gases [107] or it can increase the activation rate by catalyzing the carbon conversion reaction [107,108]. In activated carbons, ash is not chemically attached to the carbon crystals but occluded or trapped in the pores of the activated carbon [26]. Ash consists mainly of oxides, followed by sulphates, carbonates and minor amounts of other compounds of iron, aluminium, calcium, sodium, potassium, magnesium. Often large quantities of silicon are present.

Ash usually does not interfere in gaseous adsorption except for taking up volume which could be used for holding adsorbate. In liquid adsorption, the oxides and alkali salts in the ash can influence the chemistry of the adsorbate by changing the pH and/or reacting with some adsorbates such as polar molecules, making them less susceptible to adsorption. Ash can be removed by leaching with acids. Depending on the complexity and silicon content of the ash, hydrochloric and hydrofluoric acids are used [109]. Acid treatment tends to enlarge the mesopores [110] and increase the micropore volume by unblocking micropores [109,127]. Ash can be removed either before or after the manufacturing stage [29].

2.2.1.2 Surface Chemistry

The surface chemistry of activated carbons significantly influences its adsorptive capacity, as well as other properties such as its catalytic behavior, its electrochemical reaction, and its hydrophilic or hydrophobic nature. Surface chemistry is determined by the type and quantity of heteroatoms, especially oxygen. Most heteroatoms are attached to the flat surfaces of the microcrystals, but some are located at the corners, edges and intercrystalline spaces. Heteroatoms bonded on the surfaces form functional groups typical of aromatic compounds and react in a similar manner. Heteroatoms bound in the interior of the microcrystals are virtually inert. Often heteroatoms combine with each other, especially oxygen and hydrogen, to form surface functional groups such as phenols (-OH), or carboxyls (-COOH).

Surface Functional Groups

Surface functional groups can originate from raw material which has a high oxygen content such as wood or sugar, or they can originate from the activation process. Activated carbons generally have a significant amount of oxygen and hydrogen chemically bonded to the surface carbons. Oxygen containing functional groups can make up to 90% of the total functional groups [26].

The oxygen functional groups can be divided into two types, acidic

functional groups which can be neutralized with bases and basic functional groups, which can be neutralized with acids. Mattson *et al* [29], further classified activated carbons by relating the type of functional group to activation temperature. Carbons which are oxidized at a low temperature have acidic functional groups, are neutralized by bases and are known as **L** carbons. These carbons are hydrophilic and have a negative zeta potential. Carbons which are oxidized at high temperatures have basic functional groups, are neutralized by acids and are classified as **H** carbons. They display a positive zeta potential. The dividing line for this classification has been found to be activation temperatures of 500 to 600 °C. Carbons activated below 500 °C become acidic, those activated above 600 °C become basic. Oxygen functional groups formed at low temperatures are less stable than oxygen functional groups formed at higher temperatures. All functional groups can be found on activated carbons at any one time but one group, acid or basic, usually predominates.

The surface chemistry of activated carbons can be deliberately modified after manufacturing. The quantity of oxygen can be increased by oxidation, exposing the activated carbon to oxidizing agents, such as oxygen, ozone, air, water vapour, carbon dioxide and nitrogen oxides [26] at a suitably high enough temperature. The carbon can also be oxidized by treatment with nitric or sulphuric acids, hydrogen peroxides, chlorine water, etc., [30]. Oxygen functional groups can also be removed by heating the activated carbon under vacuum or in an inert atmosphere to a

temperature of 1000°C [29]. The functional groups thermally decompose into CO₂, CO, H₂O, and H₂. At extremely high heat treatments (> 3000°C), activated carbons can be made non-polar and still retain their adsorptive capacity [118].

Functional Groups

The principal functional groups usually found on activated carbons are phenols, lactones, carboxyls, aldehydes, ketones, quinones, hydroquinones anhydrides, carbonyls and cyclic peroxides [29,30]. Nearly all functional groups known in organic chemistry have been proposed to exist on activated carbons. A model of an oxidized sheet of carbon in a microcrystal with its functional groups is shown below in Figure V from Jankowska *et al* [26].

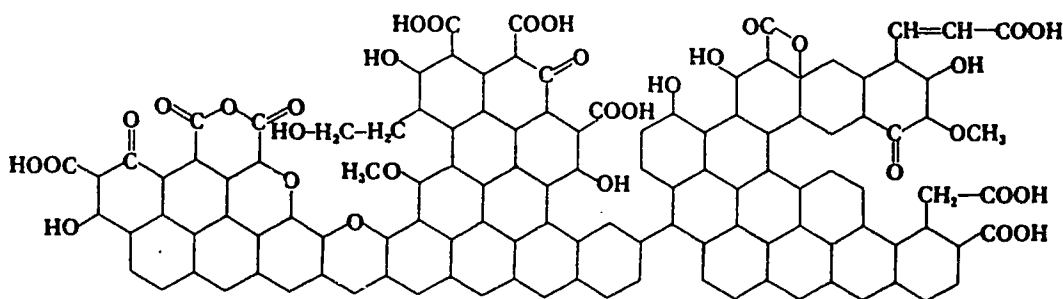


Figure V. Functional groups on activated carbon.

The carbonyls and lactones render the carbon surface polar in nature, which decreases the adsorption of non-polar compounds [29]. However the quinones and hydro-quinones enhances the adsorption of non-polar compounds through the formation of an electron donor complex. The basic oxides found on basic activated carbons are harder to identify. It has been suggested by Bansal *et al* [30] that the functional groups consist of chromene and pyrone-like structures.

The analytical methods used to determine the type and amount of surface functional groups include:

- 1) selective neutralization of surface functional groups with bases or acids of various strengths [29],
- 2) thermal decompositon and analysis of evolved gases [29],
- 3) polarography [26],
- 4) cyclic voltammetry [26], and
- 5) Infrared (IR) spectroscopy [30].

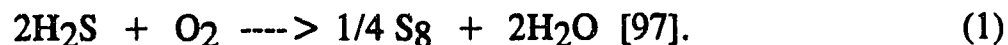
2.2.1.3 Catalytic Properties

Activated carbons have been found to be excellent catalysts for oxidation of hydrogen sulphides and the reduction of nitric oxides.

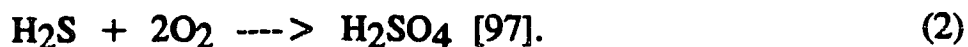
Hydrogen Sulphide Oxidation

Activated carbons can remove hydrogen sulphide (H₂S) from natural and synthetic gases. Hydrogen sulphide is normally adsorbed onto activated carbon, but in the presence of oxygen at 100 - 200 °C, hydrogen sulphide is converted into elemental sulphur by catalytic oxidation. Elemental sulphur is then adsorbed onto the activated carbon at loading rates approaching 120% by weight [97]. The sulphur can be recovered and the carbon regenerated by hot gas desorption at 450 °C or by the use of organic solvents.

The chemical reaction that occurs when hydrogen sulphide and oxygen adsorb onto activated carbon at temperatures of 100 - 250 °C is:



Other side reactions may produce sulphuric acid instead of elemental sulphur as by the reaction:



The production of sulphuric acid is influenced by reaction conditions and possibly a promotor. Promotors are usually metals which are impregnated onto the activated carbon to improve the catalytic activity. Some promotors used are iodine or metals like iron [97], chromium [98], and nickel, cobalt, molybdenum and vanadium [99].

Nitric Oxide Reduction

Activated carbon is a highly effective catalyst in the selective reduction of nitric oxides to nitrogen. Nitric oxides (NO_x) can be removed from waste gases in tandem with sulphur oxides (SO_x) [100-102]. Firstly, the main sulphur gas, sulphur dioxide (SO_2) is catalysed on activated carbon in the presence of oxygen and water by the reaction:



The sulphuric acid is removed and then the nitric oxide, usually in the form of NO is catalysed by the activated carbon in the presence of ammonia which acts as a reducing agent. In the absence of oxygen, the chemical reaction is:

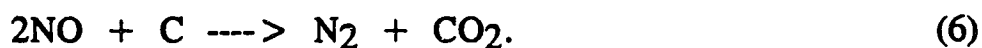


In the presence of excess oxygen the chemical reaction is:



These reactions can take place at temperatures as low as 150°C [102].

The use of specialized activated carbons such as activated Polycrylontrile (PAN) carbon fiber [103,104], makes it possible to reduce NO with carbon according to the following reaction:



Studies have been carried out to determine which properties of activated carbons are the most important in nitric oxide reduction. Illan-Gomez *et al* [105] determined that only the surface area of the activated carbon is important in the reduction, the greater the area the more NO reduced. Juntgen *et al* [128] argues that catalytic activity is influenced only to a small degree by surface area. They state that activation conditions such as carbonization temperatures, burnoff and the types of heteroatoms incorporated into the carbon structure are more important to catalytic activity.

Catalytic Support

Activated carbon can be used as a catalyst support for other catalysts because of its large surface area, and stability at high temperatures and pressures. There is a positive synergy that can occur between the catalysts and activated carbon support [106]. Chemical reactions can occur between the catalytically active phase and the support surface which enhances the overall chemical reactions. This property can be important in such reactions as the Fisher-Tropsch synthesis and the conversion of methanol [106].

2.2.1.4 Adsorption Models

The adsorption capacity of activated carbons depends on its physical structure, pore volume, specific surface area, and its surface chemistry. In the adsorption of gases, the physical structure is paramount, while the surface chemistry is of minor importance except for adsorbing polar molecules. In liquid adsorption, the surface chemistry is the most important factor but the physical structure also plays a major role.

2.2.1.4.1 Gas Adsorption

In gas adsorption, gas or vapour is concentrated on the surface of the activated carbon. The random ordering of the aromatic sheets in the

microcrystals causes variations in the arrangement of the electron clouds. This causes an attractive force to be projected outwards perpendicular to the aromatic sheets. In addition the exposed edges and corners of the aromatic sheets have unpaired electrons and vacant valencies which also impart an attractive force. Gas molecules are adsorbed by weak physical forces such as van der Waals and hydrogen bonding, until equilibrium of the attractive forces is established. The amount of gas molecules that are adsorbed is dependent on the gas pressure and temperature. The higher the pressure and the lower the temperature, the more gas adsorbed.

Heat of Adsorption

Adsorption is usually a spontaneous exothermic reaction. The heat of adsorption may be used to differentiate between physical and chemical adsorption on a solid adsorbent in some cases. In physical adsorption, the amount of energy released ranges from 4.0 to 80 kJ mol⁻¹ [26] while chemisorption ranges from 0 to 400 kJ mol⁻¹.

Langmuir Isotherm

Langmuir, 1918 [92], postulated an adsorption theory to explain how gas molecules are adsorbed. He assumed that gas molecules are adsorbed independently onto the surface of the activated carbon and that all adsorption sites are equal to each other. Thus an idealized monolayer of

gas covers the surface of the activated carbon. By measuring the amount of gas adsorbed and by knowing its physical dimensions, the surface area can then be determined. The limitations of this theory is that not all sites on the activated carbon are equal. The energy of adsorption varies depending on where the site is located on a microcrystal, on the flat of the aromatic sheet or on the edges. Also the energy of adsorption varies due to intermolecular interactions [26]. A gas molecule adsorbed onto a site which is surrounded by adsorbed gas molecules has a different energy of adsorption than if there were no adjacent adsorbed gas molecules. The main difficulty with the Langmuir isotherm is that it does not take into account multilayer adsorption.

BET Isotherm

In 1938, Brunauer, Emmett and Teller (BET) [93] developed a model of adsorption that did take into account multilayer adsorption. The model assumed that gases adsorbed onto existing layers of gases already adsorbed onto the activated carbon. The theory predicts that as the pressure of the gas increases more layers are adsorbed. By determining the amount of gas adsorbed at certain pressures, it is possible to determine the specific surface area. Pore size distribution is determined by Kelvin condensation.

Classical BET procedure measures the specific surface area of an adsorbent at 77 K using nitrogen assuming that a nitrogen molecule

covers 0.162 nm^2 . Brunauer *et al* [93] claim that there are five types of adsorption isotherms for gases. They are illustrated below in Figure VI. They measure the amount of adsorption (a) against pressure (P) over saturated vapour pressure (P_0).

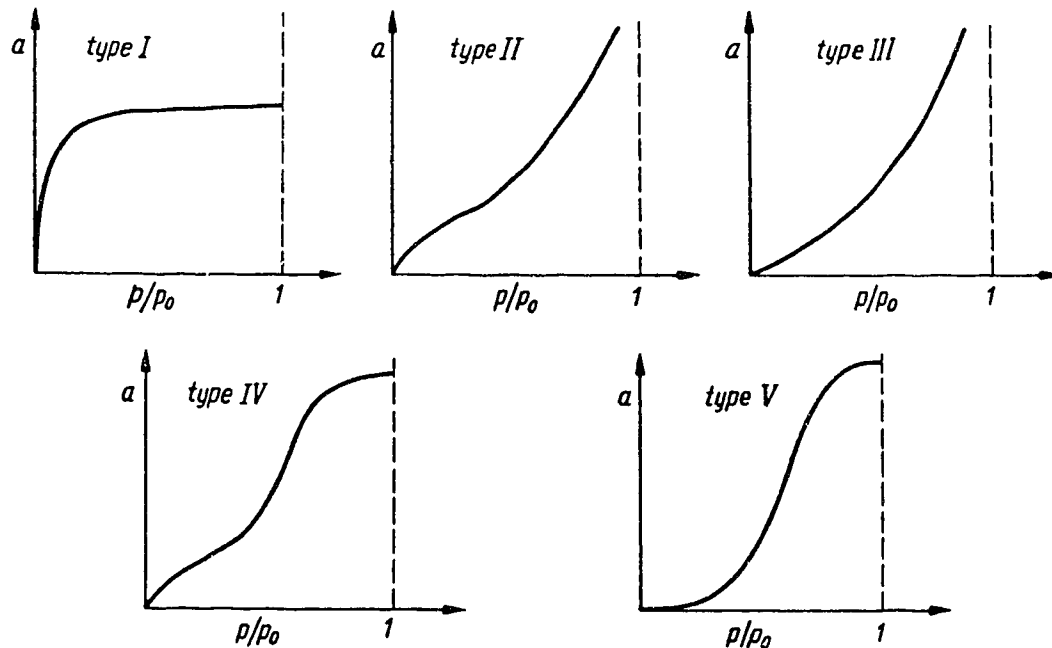


Figure VI. Adsorption isotherms by Brunauer *et al* [93].

- TYPE I** Langmuir Adsorption Isotherm - only one monolayer is adsorbed,
- TYPE II** Multilayer Adsorption Isotherm,
- TYPE III** Multilayer Adsorption Isotherm - where the heat of adsorption is less than the heat of condensation (rare isotherm), and

TYPE IV,V Multilayer Adsorption Isotherm - where a limited number of adsorption layers occur due to the width of some pores.

Micro, Meso and Macropore Adsorption

The presence of micropores substantially increases the adsorption of gases because in a micropore, the opposite walls are spaced close enough together so that the attractive forces in the walls overlap, thus the adsorption potential increases in micropores. Adsorption is greater in micropores than in mesopores and negligible in macropores.

Salas-Peregrine *et al* [121] have shown experimentally that micropore distribution is the most important criterion in gas adsorption. Activated carbons with a low pore volume but with a lot of very narrow pores have a greater adsorptive capacity than activated carbons with a larger pore volume and slightly larger micropores.

2.2.1.4.2 Liquid Adsorption

In liquid adsorption, the surface chemistry of activated carbons influences the type of adsorbate that will be adsorbed while the physical structure, such as pore size and volume, influences the amount of adsorbate adsorbed. The adsorption on activated carbon from a liquid phase has been studied less than adsorption from the gas phase. There is a great deal of literature on the practical aspects of adsorption from

dilute solutions but very little on the mechanics and theories of liquid adsorption. The adsorbate is adsorbed either physically or chemically. Physical adsorption can include trapping an adsorbate or a weak attraction due to opposite surface charges between the adsorbate and carbon. Chemical bonding (chemisorption) can include strong bonds such as covalent and ionic bonding.

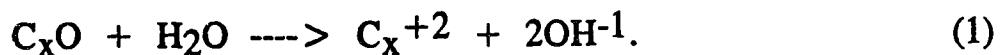
Electrical Double Layer

An activated carbon particle in a liquid medium develops a electrical double layer at the contact of the particle with the liquid or solvent. The electrical double layer consists of three parts: 1) solid phase, 2) inner layer and 3) outer or diffuse layer. The solid phase consists of the activated carbon surface which may have a net electrical charge as a result of an excess or deficiency of electrons. The net charge can be a result of chemical reactions that occurred during activation, exposure to oxygen, ionization of the surface functional groups, etc. The inner layer, also known as the compact, rigid, Helmholtz, or Stern layer [29], is made up of solvent molecules, neutral molecules and ions which are adsorbed onto the carbon surface. Ions which penetrate the inner layer to directly contact the solid carbon are referred to as specifically adsorbed. The diffuse layer is made up of molecules which are attached to the inner layer due to long range coulombic forces. These are referred to as non-specifically adsorbed molecules and are easily attached and detached from the inner layer

because the attractive forces are weaker than the adsorptive forces on the carbon surface. The adsorption of charged ions influences the structure and composition of the electrical double layer which in turn affects the overall charge of the activated carbon particle.

Adsorption of Electrolytes

The Frumkin Phenomena as described by Mattson *et al* [29] proposes an electrical theory of adsorption that states that the activated carbon acts as a gas-electrode when adsorbing an electrolyte. It proposes that the oxygen functional groups, described as C_xO and C_xO_2 , are strong enough to oxidize water molecules according to the equation:



The carbon surface acquires a positive charge and then non-specifically attracts anions onto the diffuse double layer. Dissolved gases in water, usually polar in nature bond to the activated carbon by van der Waals forces [122,123].

2.2.2. Production of Activated Carbon

The overall manufacture of activated carbon from a initial raw carbonaceous material includes two main steps, carbonization and activation. Carbonization increases the carbon content of the raw material by pyrolysis, heating in an inert atmosphere to drive off moisture and volatile matter from the raw material. Activation then forms the actual pores, fissures and cracks through selective treatment with activating gases such as steam, carbon dioxide, aerial oxygen, hydrogen, and hydrogen sulphide [26]. Activation can also be carried out chemically, using dehydrating agents such as $ZnCl_2$ and phosphoric acid. These are generally used on material with a low initial carbon content. Since activation is concerned with removing enough carbon to form pores, high temperatures are required to achieve a high enough reaction rate. Temperature for activation generally range from 800 to 1000°C.

In the manufacturing process, the properties of the activated carbon are influenced by the activation procedure, time, and activation parameters. However, the final properties are still dependent on the type of raw material used and how it reacts with the activation procedure [111].

2.2.2.1 Raw Material

The final properties of a individual activated carbon depends on the type of raw material used. Raw materials with a high volatile content and with a occurrence of initial macropores are susceptible to easy activation [26]. Material with low volatiles and porosity, such as graphite are difficult or sometimes impossible to activate.

The principal property for a raw material is a high carbon content followed by a suitable molecular structure. The most important raw materials used in commercial applications are wood, peat and coals. All types of coals are used ranging from lignites, brown coals, sub-bituminous, bituminous and anthracites [3-10,112]. Wood sources are usually waste products such as sawdust. Activated carbons produced from coconut shells are important in the recovery of gold in the milling industry [48,49], due to their high adsorption capacity, large volume of micropores and resistance to abrasion.

Activated carbons have been produced from fruit stones, biomass, fish, lignin (paper mill waste), bone, blood, asphalt, scrap tires, petroleum waste, PVC, kelp, sugar, molasses, plastics, petroleum, metal carbides, coal and wood tars, pitch, carbon blacks, and petroleum coke [1,2,11-25,119,120]. These materials only make up a small fraction of commercial activated carbons and are used for specialty purposes.

Coal is the most important raw material and comprises 60% of all activated carbons used in commercial applications. Coals are widely available, inexpensive and are easily activated due to their initial porous structure. All types of coal have been used for activated carbon but two distinct groups exist for activation purposes, soft and hard coals.

Soft coals, such as peat, lignite, brown coals and some sub-bituminous coals have the greatest volume of initial porosity including micro, meso and macropores. This is due to their low degree of metamorphism [26]. The main disadvantages of soft coals are their low carbon content, low tensile strength, and high ash and sulphur content. This is especially true in brown coals. Unless desulphurized before activation, sulphur is released as sulphur oxides during carbonization and activation. Ash can be removed by washing with acids. Due to these properties, soft coals are used to produce a cheap powdered activated carbon used only once and then discarded.

Hard coals have a higher mechanical strength but a lower initial porosity. They are used mainly for granular activated carbons due to their strength and abrasion resistance. The degree of metamorphism, and carbon content affects their ease of activation. Highly metamorphosed coals such as anthracite are more difficult to activate.

The production of activated carbon from coal usually follows the following procedure [42]:

- 1) grinding
- 2) pelletizing or briquetting (optional)
- 3) crushing briquettes (optional)
- 4) sizing
- 5) oxidation (if necessary)
- 6) carbonization
- 7) activation.

Oxidation is used to decrease the coking properties of some coals. Oxidation is also used to alter the properties of coal prior to carbonization/activation. Oxidized coals have a higher reaction rate and produce different adsorption properties [113-115].

Activated carbons have low bulk densities due to their high porosities. In some applications such as the storage of natural gas or methane for vehicle fuel where storage space is limited, the use of denser carbons is advantageous. Surfactants along with mechanical pressing can be used to increase the density without affecting adsorptive capacity [117]. The surfactants eliminates or minimizes the surface charge of the active carbon making it easier to physically compact.

2.2.2.2 Granulation

Granulation involves producing pellets or briquettes from a carbonaceous raw material with a binding agent. The raw material is pulverized, usually after carbonization and mixed with a binder to form a paste. The paste is either extruded or compressed to form pellets, cylindrical granules, briquettes, etc. using various machinery [94].

The properties required for a binder are:

- 1) the ability to bind the carbon material so it has enough strength to survive the carbonization and activation,**
- 2) during carbonization and activation, it should pyrolyze to produce good strength and abrasion resistance, and**
- 3) during carbonization, it should promote the formation of intergranular spaces which will lead to pores of the right size and shape during activation.**

Many materials have been used as binding agents but the best have been materials such as coal tar, wood pitch and tar, heavy oil, asphalt, etc. [26]. These materials have high carbon contents and behave in a similar manner to the raw material during carbonization and activation.

The tensile strength of a pellet or briquette depends on the particle size and weight percentage of binder [95]. A pellet's strength is controlled by the largest hairline fracture produced during production. The hairline crack derives from microfractures present in the particles. Binder added at a high hydrostatic pressure forces itself into microfractures. The less microfractures present, the less possibility for the formation of a larger hairline fracture thus the strength of a pellet is increased. The optimal percentage of binder varies in different cases but ranges from 4 to 12% [96].

2.2.2.3 Carbonization

The initial porous structure of activated carbon is first developed during carbonization. Activation then carries on developing the porosity along the same direction. Carbonization, is also known as pyrolysis or dehydration in the literature. Pyrolysis parameters which affect the properties of a carbonaceous material are: 1) maximum temperature, 2) time of heating, 3) rate of temperature increase and 4) pyrolysis atmosphere. Maximum temperature is the most important parameter and most carbonization occurs at temperatures of 500 to 800°C. Too high a temperature not only carbonizes the raw material but crystalizes the carbon into graphite which is very difficult to activate.

The carbonization induces two stages to the raw material, a softening stage followed by a hardening stage. Initially, the high temperatures

releases moisture and volatile matter from the interior of a particle resulting in a branched system of pores. Thermal decomposition of organic matter also produces gases which escape. The remaining material consists of large macromolecules mainly composed of carbon. High carbonization temperatures tend to split the weaker bonds of these macromolecules which leads to softening.

After the release and decomposition of the organic matter, the remaining carbon begins to change its structure, this is the hardening stage. The remaining carbon begins to condense and polymerize, becoming more orderly and turning into sheets of aromatic carbons. Shrinkage occurs which starts to decrease the innate porosity. These sheets of aromatic carbons tend to combine to form microcrystals similar to graphite. These microcrystals bond to each other with aliphatic type bonds and tend to orient themselves around the pores caused by the release of moisture and volatiles. The microcrystals form a spatial polymer and the spaces between the microcrystals form the primary porosity of the carbons. These pores are usually filled with tar and amorphous carbon from the thermal decomposition of the organic matter.

The length of pyrolysis affects the overall order of the carbon structure. With time, carbonized material can undergo a second softening after the hardening stage. The microcrystals tend to start packing and close up the existing pores. This results in a decrease in the volume of the pores and a more orderly carbon arrangement.

The rate of temperature change is also important to the final properties of activated carbon. A raw material is usually carbonized by raising the temperature at a certain rate and then soaking for a set period of time. A high rate of temperature increase causes the volatiles to be evolved and expelled quickly. This leads to the formation of larger pores than would have occurred at a slower heating rate. The microcrystals also start to form and orientate before all the volatiles are expelled leading to a less ordered final structure.

Thermal decomposition during carbonization leads to the formation of gases and vapours, especially carbon dioxide and water vapour. These can react chemically with the carbon structure unless they are quickly removed with a fast flow of inert gas such as nitrogen.

Pyrolysis generates an ordered structure of compact carbon with some porosity. The structure at the millimeter scale resembles the structure of the raw material. Char made from carbonized wood, for example, still retains the wood structure of capillaries, cell walls, etc. At the micro level, the structure is generally more ordered and orientated around pores formed during carbonization.

The presence of these initial micropores influences the rate of activation to follow. These pores facilitate the diffusion of activating gases into the carbon particle, increasing the surface area for the activation to occur thus increasing the overall activation rate. A more ordered structure with fewer

pores decreases the reaction rates of activation.

Pyrolysis is normally carried out in stationary, rotary or fluidized bed ovens. Nitrogen is normally used as the inert gas flow through the carbonized material. Fluidized bed reactors are becoming more common due to their energy efficiency and ease of temperature control.

Some raw material with a low carbon, high volatile and moisture content, such as biomass or fresh wood can be carbonized by chemical treatment. The raw material can be treated with large amounts of sulphuric and phosphoric acids. The carbonized material is then washed to remove the dehydrating agents before being sent for activation. Dehydrating agents such as zinc chloride ($ZnCl_2$) and magnesium chloride ($MgCl_2$) can be added to the raw material prior to heating to increase carbonization.

2.2.2.4 Activation

Activation is the most important process in the manufacturing of activated carbon, since this produces the porosity, high surface area and surface functional groups. The basic step is to treat a carbonized material with an activating gas such as steam, carbon dioxide, or oxygen at a high enough temperature so that the oxidizing gases reacts with just enough carbons to form pores. The oxidizing gases diffuse into existing pores,

react with carbon on the pore wall to form carbon oxide gases which then diffuse out. As carbon is removed the pore increases in width and length. At the end of the activation, a porous structure remains.

The carbonized structure consists of a matrix of microcrystals held together by aliphatic bonds. The spaces between the microcrystals make up the initial pore structure. These pores may be filled with tars and amorphous carbon deposits derived from the carbonization process. This tar and amorphous carbon is the first to react with the oxidizing gases because they are the most reactive types of carbons present. The next carbons to react are the edge and corner carbons, which make up 14% of all the carbons in the microcrystal. Oxidation proceeds along the pores widening them as it proceeds. At the microscopic scale, activation is often non-homogeneous and forms irregular pits and channels, usually occurring in the presence of catalytic active inorganic matter. Activation is carried out until the maximum surface area is achieved. The maximum surface area usually occurs when 50% of the carbon structure has been burned off [30]. Some types of raw materials require a burnoff of 40 to 60% before maximum surface area is achieved [26]. Beyond this point of activation, further oxidation starts to burn through the walls of the pores decreasing the total surface area. At high levels of oxidation, so much carbon can be removed from the carbon structure that it starts to collapse.

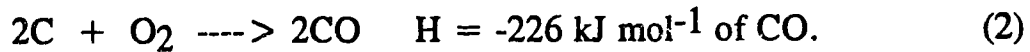
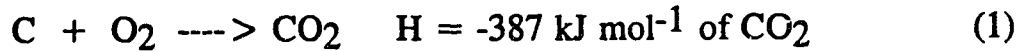
'Carbon oxidation is a complex heterogeneous process encompassing the transport of reagents to the surface of the particles, their diffusion into pores, chemisorption on the pore surface, reaction with carbon, desorption of the reaction products, and diffusion of these products to the particle surface' [26].

Temperature is the most important variable in activation. At too low a temperature, only the most reactive carbons are oxidized and the microcrystals may not be oxidized at all. Even if the microcrystals are oxidized, the rate of activation may be so slow that an inordinate amount of time is needed for complete activation. At too high a temperature, all the carbons react equally to the oxidizing agents, thus the first carbons to react are on the exterior of the carbon particle because the oxidizing agents do not have a chance to diffuse into the particle. The porosity is not developed and the carbon particle is quickly consumed.

Chemical Reactions

The rate of activation depends on the reactivity of the carbon with the oxidizing agent. The greater the reactivity, the lower the optimal temperature for uniform and maximum pore formation. Oxygen has the highest reactivity of the oxidizing gases followed by water vapour and then carbon dioxide.

Oxygen reacts with carbon in an exothermic reaction according to the following equations:



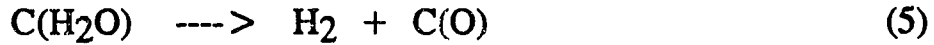
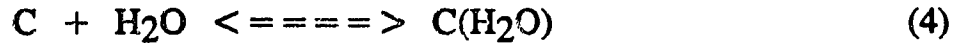
Both CO and CO₂ are formed independently of each other and the CO/CO₂ ratio is said to increase with temperature [26]. The use of oxygen presents many difficulties because the exothermic reactions makes accurate temperature control difficult and oxygen is so reactive, excessive burnoff can occur on the particle surface even under tight controls.

Water as super heated steam reacts with carbon endothermically. Steam is the major activating agent used for commercial activation followed by carbon dioxide. The basic carbon-water reaction is:



This reaction has been studied extensively because it is the basic reaction in coal gasification to produce synthetic water gas [124,125,129-144].

The mechanism of the water-carbon interaction can be described by the following equations [26]:



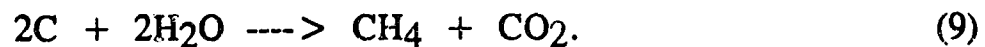
The presence of hydrogen has an inhibiting influence by its adsorption with carbon according to:



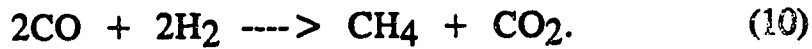
A secondary reaction produces carbon dioxide due to the catalytic nature of the carbon surface. The reaction is:



Gasification studies of coals using steam [124] have determined that methane is also produced on the carbon surface according to the thermally neutral reaction:



Methane can also be produced by secondary reactions composed of gases already produced but not yet removed from the high temperature environment. Such a reaction can occur between hydrogen and carbon monoxide as:



The composition of the gases produced from coal gasified with steam is a function of temperature. Figure VII below from Mattson *et al* [29] illustrates how the gas composition changes with different gasification temperatures.

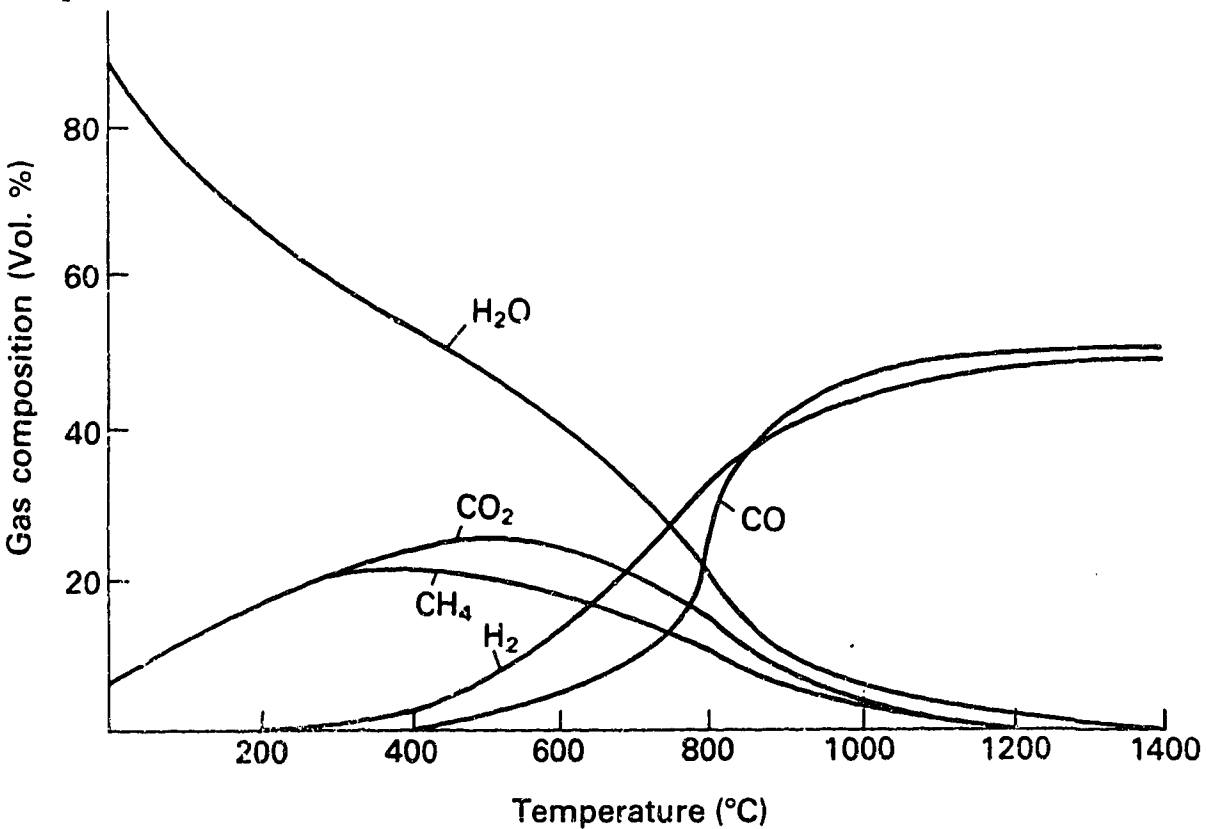


Figure VII. Composition of water-gas from coal gasification.

The mechanism of how carbon dioxide reacts with carbon can be given by two sets of reactions. The first set of reactions is:



The second set of reactions are:



The difference between the sets of equations is on the theorized but unproven inhibiting effect of carbon monoxide.

Chemical Activation

Chemical activation is often used with low carbon, high volatile materials such as peat and sawdust. The raw material is mixed with a dehydrating agent and heated to temperatures as high as 650°C where the oxygen and hydrogen in the raw material is selectively removed. Carbonization and activation takes place simultaneously.

The most commonly used dehydrating agents used in commercial applications are phosphoric acid, zinc chloride and potassium sulphide. Other agents that can be used for dehydration are sulphuric acid, metallic sodium or potassium, calcium oxide, calcium hydroxide, aluminum chloride, sulphur, nitric acid, chlorine, etc. [26].

The dehydrating agent is mixed in ratios of 0.4 to 5 parts of agent to 1 part of raw material. The ratio depends on the type of raw material and activating agent [94]. The mixture is usually dried at low temperatures, 80 - 150 °C before being heated or calcined at higher temperatures. After activation the dehydrating agent is recovered usually by washing. The advantages of chemical activation are faster activation times, high carbon yield and good adsorption properties. The major disadvantages are the extra manufacturing expense for the dehydrating agent and its recovery, and little control on influencing the final adsorptive properties.

Catalysts

The literature is extensive on the use of catalysts to increase the gasification rates of coals and petroleum cokes to produce syn-gas [124,125,129-144], and how they can increase the activation rate, pore development and surface chemistry of activated carbons [65-72,74]. Catalysts can be added to carbons prior to the carbonization or activation stage. The most common catalysts generally contain an alkali metal

such as potassium, calcium, magnesium or sodium. The alkalis can be added as metal, hydroxides, carbonates, etc.

The mechanism by which the alkali metal acts as a catalyst in carbon gasification is still in dispute [145-147] but it is thought that the alkali metal completely ionizes and then 'jumps' from one carbon to another acting as a site specific catalyst. Moulijn *et al* [148] argues that the alkali metal is not involved directly in the catalytic cycle but causes the catalytic activity with an oxygen transfer cycle. The type of catalyst affects the activation rates because certain catalyst penetrate deeper into the carbon than other catalysts [149].

Activation Equipment

Activation is carried out in multi-hearth furnances, rotary ovens and fluidized bed furnaces.

Multi-hearth furnances are energy efficient but uniformity in the final product is difficult to achieve because of non-uniform activation caused by uneven contact between the particles and activating gas.

Rotary ovens provide a better contact between the activating gas and carbon as well as a more uniform temperature distribution.

Fluidized bed ovens are becoming more common for activating carbons due to better temperature control, shorter activation times and a constant concentration of activating gas always in contact with the carbon particle.

2.2.2.5 Regeneration

The regeneration of spent activated carbons includes removing the adsorbate and restoring the adsorptive capacity. In metallurgical practice, regeneration is associated with the recovery of a valuable material, such as gold from a Carbon-In-Leach or Carbon-In-Pulp operation. The goal of regeneration is to restore the adsorptive properties so that an activated carbon can be reused many times over.

Regeneration entails dealing with two different types of adsorbates, those physically adsorbed and those chemisorbed. Physical adsorption is easily reversible because it involves weak attractive forces such as van der Waals and hydrogen bonding. Chemisorption usually involves much stronger bonds such as ionic and covalent bonds which are much harder to break.

Adsorbate held by physical adsorption can be easily removed by heating, lowering the air pressure or washing with a solvent [94]. In the case of chemisorbed substances, a great deal of energy is needed to overcome the chemical bonds. It becomes necessary to send the carbon through the activation process again. The carbon is usually reactivated

with steam at 700 to 900°C. The high temperatures are sufficient to remove most adsorbates, but the carbon structure can be damaged by extra burnoff, so tight regeneration controls are required.

3. EXPERIMENTAL

3.1 Materials

The fluid petroleum coke originated from Syncrude Canada Ltd. and was produced from their oil sands plant near Fort McMurray, Alberta. The sample was supplied from the Coal Research Branch of Energy, Mines and Resources Canada in Devon, Alberta. The sample was shipped in February, 1992 in a 5 gallon plastic pail and was stored in the same pail at a constant room temperature of 22 °C.

The sample contained a small percentage (< 1% by weight) of rusty iron, probably scale from the fluid bed coker. To simulate actual conditions, this iron was retained for all test samples.

The commercial activated carbon used for comparative purposes was 5-590-A Coconut Charcoal obtained from Fisher Scientific. This activated carbon is specifically produced for aqueous adsorption for laboratory purposes.

All chemicals and gases used in this study were of analytical grade. Only deionized water was used in the experiments.

3.2 Analysis

Coke samples were taken from the coke supply immediately before experimentation. Samples for size analysis, proximate analysis, ultimate analysis and carbonization were used directly as is. All other samples for the activation experiments were dried in batches of 100 - 200 g in a vacuum oven for 24 hours at a temperature of 110°C prior to use. Unused sample was kept under vacuum at room temperature until needed. Potassium treated coke was prepared by boiling 4% by weight of potassium hydroxide in relation to the weight of coke in a volume of deionized water. Coke was then added to the solution and the mixture gently heated to remove free water. The potassium coke was then dried under vacuum at 110°C for 24 hours. The sample was kept under vacuum at room temperature until needed.

Samples of 1 g were used in the pyrolysis experiments. The activation experiments employed samples of either 10 g or 50 g of coke. Activated cokes were stored in glass vials and plastic jars until needed for analysis. Samples that had to be pulverized before experimentation or analysis were crushed in a Brinkmann Centrifugal Grinding Mill to 95% passing 325 Tyler mesh (44 microns).

3.2.1 Size Analysis

Coke and activated coke samples were dry sieved using the American Tyler series of meshes ranging between 44 and 841 microns. The procedure followed the ASTM designation, D2862 - 92, 'Standard Test Method for Particle Size Distribution of Granular Activated Carbon'.

3.2.2 Proximate and Ultimate Analysis

Proximate analysis conformed to ASTM standards; moisture by ASTM D3173, volatile matter by ASTM D3175 and ash content by ASTM D3174. All testing was done inhouse.

The ultimate analyses were carried out by a commercial lab, C & G Labs of Edmonton, Alberta, according to ASTM standard D3176. The carbon, nitrogen, sulphur and hydrogen contents were determined directly and the oxygen content was inferred by difference.

3.2.3 Density Analysis

The bulk densities and absolute densities were determined for various coke samples. Bulk density is defined as the mass per unit volume of the coke samples in air including pores and interparticle voids.

Bulk densities were carried out according to ASTM D2854 but for this study were expressed as g cm^{-3} instead of tonnes m^{-3} .

Absolute density also known as 'nitrogen density' is defined as the mass per unit volume of the coke skeleton inaccessible to nitrogen gas, i.e. the density of the solid portion of the raw or activated coke. Absolute density does not take into account isolated internal pores which may affect the overall results. Absolute densities for raw coke were obtained using a Quantachrome Null Pycometer and nitrogen gas. Activated cokes tended to adsorb excess amounts of nitrogen making results uncertain. For activated cokes, the absolute densities were determined by immersion of a known sample of activated coke in varsol and calculating densities by displaced volume. The varsol was assumed to have penetrated all the pores equal to or greater in size than the smallest molecule in the varsol.

3.2.4 Scanning Electron Microscope Analysis

Samples of raw and activated cokes were prepared and viewed in an ISI - 60 Scanning Electron Microscope (SEM) operated at an energy of 20 Kev. The raw coke, and untreated activated coke were viewed without any surface treatment. The activated potassium coke samples were coated with carbon to prevent any potassium from fluorescing in the SEM.

3.2.5 BET Surface Area Analysis

The specific surface area and pore size distributions were determined by nitrogen gas adsorption at 77 Kelvin using the BET (Brunauer, Emmett, and Teller) equation [93]. Analysis was conducted with a Quantachrome automated adsorption apparatus, the Autosorb - 1, Model ASIT. Selected samples were compared with an Omnisorp (TM) 360, Version 10, automated adsorption apparatus also using nitrogen adsorption.

The surface areas were determined with a multi-point BET equation. The surface areas and total pore volumes were determined from the amount of vapour adsorbed at a relative pressure of 0.9994. The BET [93] and Langmuir [92] surface areas as well as the adsorption and desorption isotherms were generated from the data using the Autosorb's software.

3.2.6 Zeta Potential and pH Analysis

Relative Zeta Potentials were obtained using a Rank Brothers' Zeta Potential Meter. Activated coke samples were prepared by grinding to minus 38 microns and then adding 0.1 g of sample to 200 ml of deionized water. The pH of the samples were adjusted by the addition of hydrochloric acid (HCL) or sodium hydroxide (NaOH). The solutions were left to equilibrate for 30 minutes before testing.

The Zeta Potential (ζ) was calculated by the Smoluchowski [154] equation:

$$\zeta = \frac{300^2 4 \mu \pi V_e}{D E}$$

where:

ζ = zeta potential in volts

μ = viscosity in poise

V_e = electrophoretic velocity in cm sec^{-1}

D = dielectric constant of water, (80 g cm volt⁻² at 20°C)

E = voltage gradient, volt cm^{-1} .

The Zeta Potentials were then multiplied by 100 to obtain a Relative Zeta Potential for each sample.

The pH of the raw and activated cokes were determined using the ASTM D3838 - 80 standard titled, 'Standard Test Method of pH of Activated Carbon'.

3.2.7 Gas Chromatography

All gas samples were analyzed in a Hach, Carle, series 400 AGC, gas chromatograph (GC). The GC was calibrated for nitrogen, carbon monoxide, carbon dioxide, methane, and hydrogen sulphide.

3.2.8 Adsorption Analysis

The activated coke samples were tested for liquid-phase adsorption using methylene blue dye and iodine as adsorbates. The procedure followed was ASTM D3860 - 89a, 'Standard Practice for Determination of Adsorptive Capacity of Activated Carbon by Aqueous Phase Isotherm Technique'. All samples were pulverized to 95% passing 325 Tyler mesh (44 microns). Iodine and methylene blue dye were used for the adsorbates because of their ability to describe surface area [150], surface structure [151] and mineral content [152].

3.2.8.1 Methylene Blue Adsorption

A methylene blue solution was prepared by dissolving 800 mg L⁻¹ of dye into deionized water. The adsorption test was conducted at 22°C. The methylene blue concentrations in the tested samples were determined by spectrophotometry, using a Bausch and Lomb Spectronic 21 spectrophotometer. The wavelengths used for methylene blue concentration determination were 500 and 700 nm.

After the adsorption test, the procedure to determine the methylene blue concentration was to filter the solutions and activated cokes through Whatmann No. 4 paper filters to collect the solute. The solute was then centrifuged at 2000 rpm for 30 minutes to remove any microscopic coke particles which could affect the spectrophotometer reading. The solute was tested in the spectrophotometer at 500 nm using the 700 nm wavelength as a check. The residual methylene blue concentration was then calculated from a calibration chart.

3.2.8.2 Iodine Adsorption

Iodine solution was prepared by dissolving solid iodine in boiling water at a low pH of 1 to 2. The pH was achieved by adding sulphuric acid to deionized water and monitored by pH meter. The iodine concentration used was 100 mg L⁻¹.

After the adsorption test with the activated cokes, the solutions were filtered with No. 4 Whatmann Paper to obtain the solute. The residual iodine concentration was determined by titrating a known volume of solute with a solution of known concentration of sodium thiosulphate (Na₂S₂O₃). A starch indicator was used to determine the endpoint of the titration. Known concentrations of iodine were used to confirm the test method and sodium thiosulphate concentrations.

3.3 Pyrolysis and Activation

The pyrolysis analysis of the fluid petroleum coke was carried out separately from the activation tests, although the activation tests do include a pyrolysis phase. The pyrolysis entailed subjecting the samples directly to the experimental temperatures while the activation phase consisted of heating the samples at a specific heating rate.

3.3.1 Pyrolysis

The behaviour of fluid petroleum coke undergoing pyrolysis was studied by determining moisture and volatile loss of the coke versus temperature and time. Approximately 1 g of raw or pulverized raw coke was heated at a constant temperature for a specific length of time under a stream of nitrogen gas. The weighed samples were placed in ceramic boats and heated in a closed quartz tube which was itself placed in a horizontal tube furnace. The nitrogen flow was kept at a rate of $50 \text{ cm}^3 \text{ min}^{-1}$. Samples were heated for a specific length of time and then move to a non-heated section of the quartz tube, still under nitrogen, to cool. Samples cool enough not to react with the outside air were then placed in a dessicator until cool enough to weigh.

The carbon recovery (R) was calculated by dividing the weight after heating by the original weight, and expressed as a percentage. Conversely, the moisture and volatile loss, designated as burnoff (B) is $100\% - (R)$.

3.3.2 Activation

Activation and pyrolysis of the various coke samples were carried out in vertical stainless steel reactors. The activations were carried out in two series of runs. In series A, samples of 10 g were activated under various conditions. In series B, samples of 50 g were activated to obtain enough material for testing. The 10 g samples were activated in a 9.5 mm internal diameter (I.D.) reactor while the 50 g samples were activated in a 19.0 mm I.D. reactor. The reactor was placed vertically in a tube furnace with an accurate temperature controller.

The pyrolysis/activation procedure involved placing a measured amount of coke in the reactor and packing it with ceramic beads and heat resistant ceramic fiber (Fiberfrax). A metal clad thermocouple was inserted in the top of the reactor with its tip just above the coke sample. The reactor was then sealed and a gas flow was introduced from the top of the reactor and the exhaust exited at the bottom. Figure 1 below illustrates the schematic of the experimental setup. Nitrogen gas was used as a purge and steam was introduced as water from an inlet at the top of the reactor. Water was injected by syringe pump for accurate measurement. The exhaust gases were passed through a condenser and water trap to recover any unused steam. Exhaust gas samples were taken from the exhaust gas stream for gas analysis.

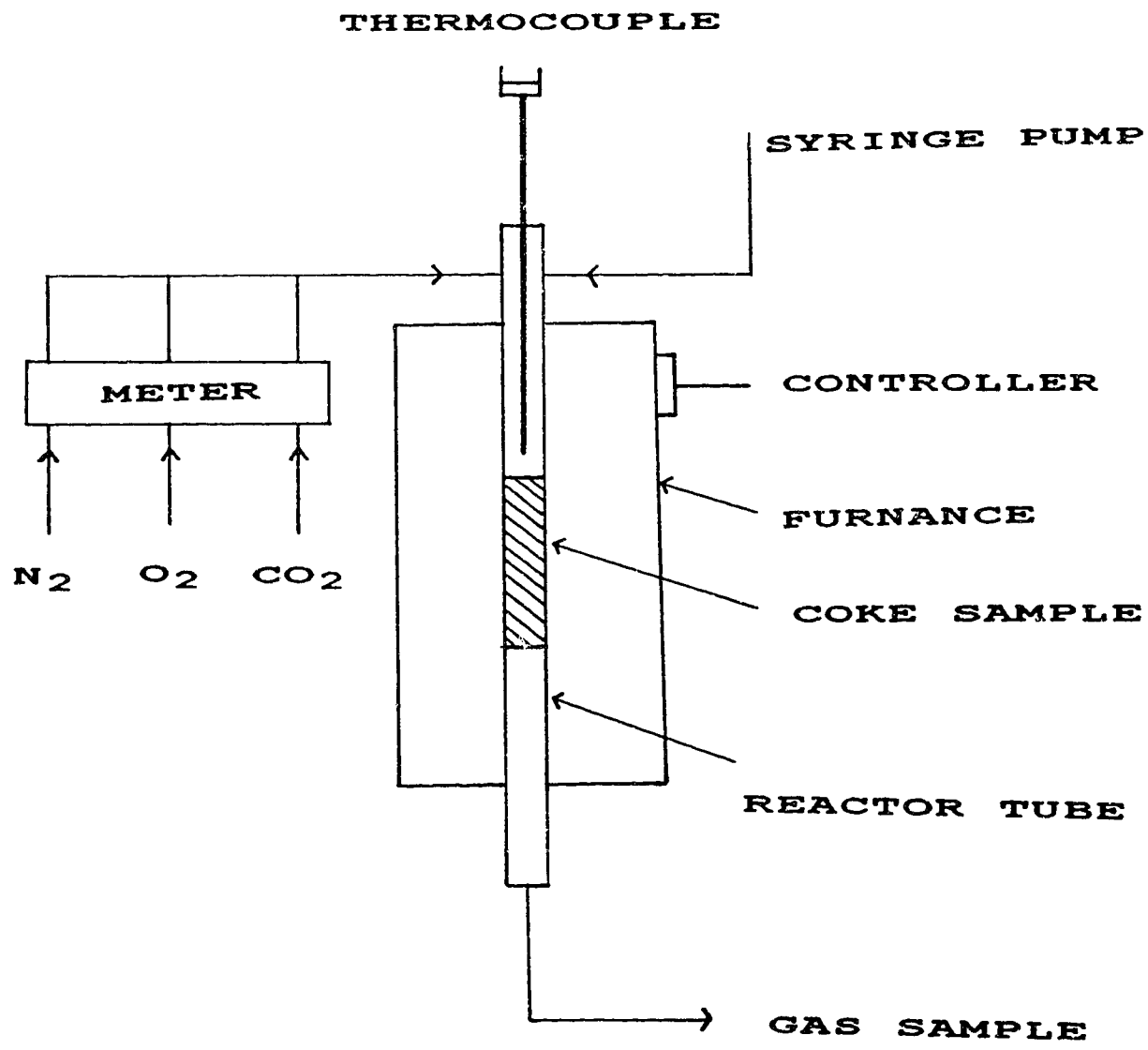


Figure 1. Schematic of the Pyrolysis/Activation
Reactor and Experimental Setup

The testing procedure is as follows: a sample is sealed in a test reactor and sealed. Nitrogen is used to purge the reactor at room temperature, 28 °C for a minimum of 12 hours. The gas flow is set at a rate of 7 cm³ min⁻¹ and 9 cm³ min⁻¹ for the 10 g and 50 g sample respectively. After purging the system, the pyrolysis stage occurs. The nitrogen gas rate is increased to 18 cm³ min⁻¹ and the temperature in the furnace is increased at a rate of 6.9 °C min⁻¹ and 5.5 °C min⁻¹ for the 10 g and 50 g samples respectively. The temperature is raised steadily until the reactor temperature reaches 850 °C. The 10 g sample reaches 850 °C in a time of 2 hours, the 50 g sample takes 2.5 hours to reach 850 °C. When 850 °C is reached, the activation phase is carried out. Water is introduced by syringe in specific amounts at specific times. The water was deoxygenated before use. The water was deoxygenated by boiling for a few minutes, cooling to room temperature and then was placed under vacuum for 24 hours.

Water was introduced at a rate of 5.0 g hr⁻¹ and 25g hr⁻¹ for the 10 g and 50 g samples respectively. For the 5.0 g hr⁻¹ rate, water was introduced by syringe in 0.5 ml increments every 6 mins. The 25 g hr⁻¹ rate of water was introduced in increments of 2.5 ml every 6 minutes. The sample was activated for the testing time required.

At the conclusion of activation, the power to the furnace was turned off and the reactor allowed to cool down overnight still under a flow of nitrogen. The reactor was then taken apart and the coke sample removed

and weighed. The sample was then stored in glass or plastic vials until needed for testing.

The recovery (R) is defined as the weight of the activated carbon divided by the original weight of sample multiplied by 100%. Conversely, the burnoff (B) is defined as $100\% - R$.

4. RESULTS AND DISCUSSION

4.1 Analysis

4.1.1 Pyrolysis of Fluid Petroleum Coke

Raw fluid petroleum coke was pyrolyzed at temperatures of 200 °C, 400 °C, 600 °C, and 800 °C. In addition, some coke was also pulverized and then pyrolyzed at 400 °C. The carbon recoveries versus pyrolysis time for raw coke are tabulated in Table 1 and graphed in Figure 2. The recoveries of the raw and pulverized coke pyrolyzed at 400 °C are tabulated in Table 2 and graphed in Figure 3.

Raw coke pyrolyzed in a nitrogen atmosphere exhibits mass loss at high temperatures. The mass loss can be explained by loss of moisture and volatile components from the coke. The main conclusions reached from this pyrolysis study are:

- 1) most of the mass loss occurs within the first 10 minutes of pyrolysis,
- 2) higher temperatures lead to higher moisture and volatile loss,
- 3) the maximum total moisture and volatile loss is

TABLE 1

Pyrolysis Analysis of Raw Fluid
 Petroleum Coke at 200°C, 400°C,
 600°C, and 800°C (As Received).

Pyrolysis Time (mins)	Recovery (wt %)			
	200°C	400°C	600°C	800°C
1	98.12	99.30	98.07	97.18
2	98.70	98.57	96.72	95.47
3		98.43	96.22	95.30
4	97.22	98.18	94.63	93.08
5	98.76	97.72	95.80	90.88 93.03
10	98.78	97.33	95.19	90.05 92.52
15	99.08	93.46	91.81 92.49	90.35
30	99.23	92.79	91.23 91.77	90.23
45		93.71	90.52	89.43
60	99.11	94.55	90.45	89.68
75		94.91	91.38 91.05	
90		93.85 92.53 95.08	90.20	89.64
105		96.00	90.65	
120		93.09 93.92	90.53	89.49
135			90.00	
150		94.84	90.31	89.84
165			89.77	
180		94.448	90.27	90.43

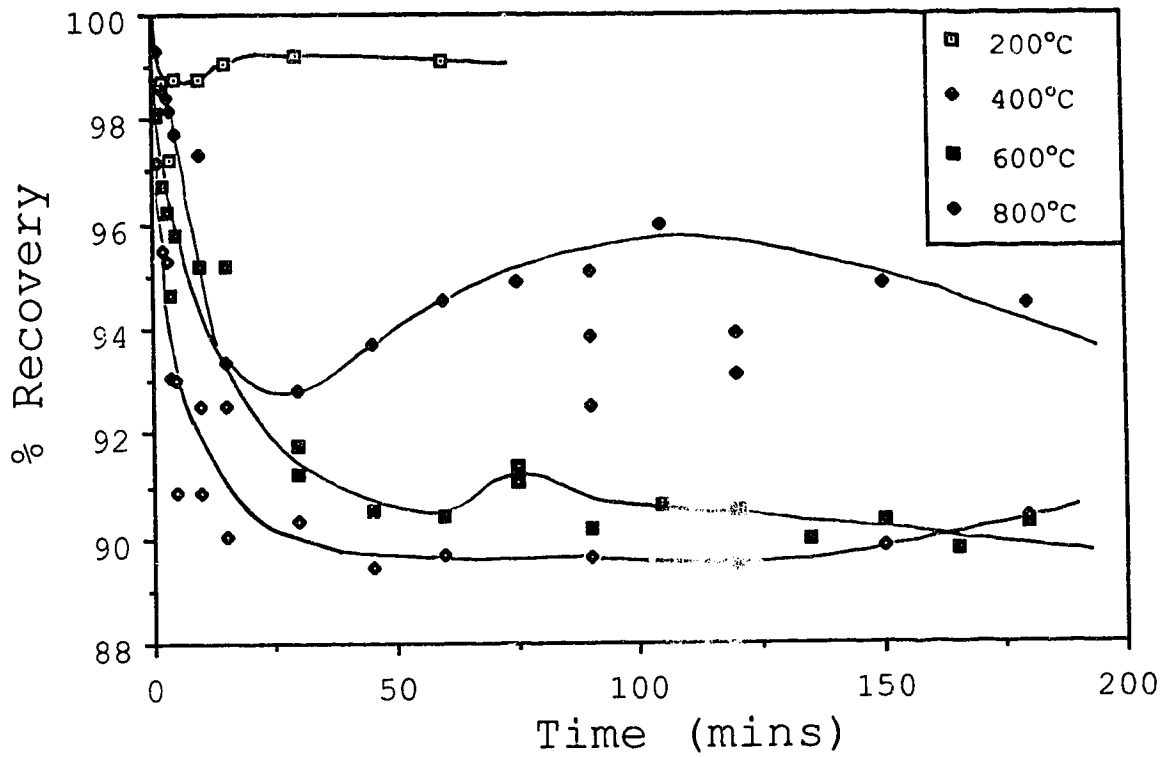


Figure 2. The Pyrolysis Recoveries of Raw Fluid Petroleum Coke at 200°C, 400°C, 600°C and 800°C.

TABLE 2

Pyrolysis Analysis of Raw Fluid
Petroleum Coke at 400°C,
(As Received and Crushed).

Pyrolysis Time (mins)	Recovery (wt %)	
	Uncrushed	Crushed (-200 mesh)
5		97.46, 97.41
10		96.93, 96.69
15	93.46	96.31, 96.60
30	92.79	96.57, 96.75
45	93.71	96.65, 96.32
60	94.55	96.74, 96.38
75	94.91	96.68, 95.39 96.69
90	93.85, 92.53 95.083	97.01, 96.92
105	96.00	
120	93.09, 93.92	96.87, 97.10
150	94.84	96.87, 96.98
180	94.45	96.38, 93.31

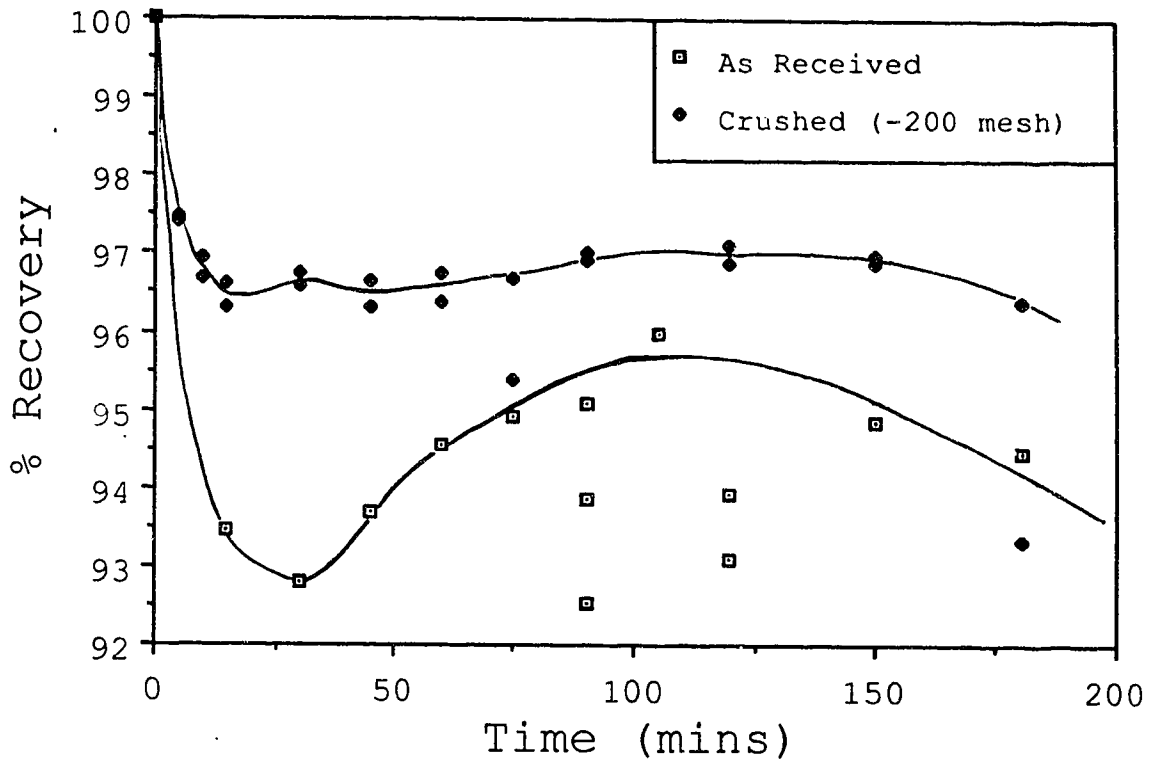


Figure 3. The Pyrolysis Recoveries of Crushed and Uncrushed Raw Fluid Petroleum Coke at 400°C.

approximately 10%, and

- 4) the coke displays some nitrogen adsorption at 400 °C after achieving a certain level of volatile and moisture loss. This nitrogen adsorption is observed as a gradual increase in the level of recovery between 50 and 120 minutes of pyrolysis at 400 °C.

The pyrolysis indicates that the majority of mass loss or burnoff occurs in the first few minutes of pyrolysis. The mass loss is initially rapid and then levels off. The amount of mass loss corresponds to pyrolysis temperature; the higher the temperature the greater the total mass loss. This suggests that the moisture and volatiles are not tightly bonded to the coke, hence the quick mass loss. Loss of mass at higher temperatures indicate that some moisture and volatiles are more tightly bonded or trapped in more inaccessible locations of the coke particle. At 200 °C the maximum burnoff is 2.8%, at 400 °C the maximum burnoff varies from 5 to 7.5%, at 600 °C the maximum burnoff is 9.5% and at 800 °C the maximum burnoff is 10%. From the graph, it appears that higher temperatures over 800 °C will not lead to significantly higher moisture and volatile loss.

Raw coke and pulverized raw coke were both pyrolyzed at 400 °C. The crushed coke had a maximum weight loss of 3% while the uncrushed coke had a weight loss of 5 to 7.5%. The discrepancy between the two

indicates that the act of pulverizing the coke released moisture and volatiles prior to pyrolysis. Since the moisture content is 1.8%, some of the weight loss must be attributed to volatile loss. Some volatiles may not be tightly bonded to the coke matrix and the energy of crushing may have freed them from the matrix. Another explanation is that the volatiles are trapped in pore and cracks and are released when the coke particle is crushed.

Both coke samples pyrolyzed at 400°C also show a unexpected gain in mass after a certain treatment time. The crushed coke sample increased in weight by 0.5% after 60 minutes of treatment, while the uncrushed sample showed a weight gain of approximately 2.5% after 30 minutes of pyrolysis. The weight gain appears very variable. The only source of mass for weight gain is from the nitrogen flowing over the sample. This phenomena may be explained by the presence of internal porosity in the coke particles consisting of micropores and/or microcracks. The weight gain can be attributed to nitrogen diffusing into the coke particle through microcracks and/or micropores recently vacated by the moisture (water molecules) and volatiles. Volatiles may be loosely bond to the coke matrix and when driven off, their absence may form micropores in the matrix. Another explanation is that volatiles are physically trapped and not bonded in the pores and cracks and heating drives them off freeing the pores for nitrogen diffusion.

There is no weight gain at temperatures of 600°C to 800°C. Since

volatiles are being released, no nitrogen is diffusing into the coke particle because these high temperatures may be deforming the coke structure. Fluid coke is produced at a temperature of 600 °C [75] so it is reasonable to expect deformation at higher temperatures. Deformation may close any pores or cracks after the moisture and volatiles are removed. Another possibility is that the coke particle is too hot or energetic for a nitrogen molecule to adsorb onto the surface either chemically or physically.

This pyrolysis study suggest an important property of fluid petroleum coke that may be useful in subsequent activation. Some porosity already exists in the coke particles and after removing the moisture and volatiles; this porosity can be used as a good starting point for activation to produce larger pores.

4.1.2 Activation of Fluid Petroleum Coke

The activation data was compiled from both the A and B-series of activations which consisted of untreated and potassium treated (4% KOH) cokes. The A-series consisted of six 10 g samples activated for times of 2, 4 and 6 hours. These samples were used for BET surface area evaluations. Series-B consisted of 12 samples of 50 g activated for times of 0, 1, 2, 3, 4, 5, and 6 hours. These samples were used for all other analytical tests. The mass recovery and burnoff were calculated for each activation. In addition to the recoveries, the amount of water that reacted was also calculated, and referred to as Water Efficiency. Water efficiency is defined as the mass of water which reacted with the coke sample over the mass of total water used in the activation. Unreacted water was recovered in the gas trap and measured as (W_i), and the total water used is (W_o). Water efficiency (W_{eff}) is defined as $((W_o - W_i) / W_o) * 100\%$.

Untreated Coke

The results of the activation of raw untreated coke are tabulated in Table 3 and the burnoff versus activation time is shown in Figure 4. The water efficiency versus activation time plot and water efficiency versus burnoff are plotted in Figures 5 and 6 respectively. Table 3 and Figure 4 also include samples B-3 and B-5, which were included for comparison. Sample B-3 consisted of only plus 177 micron coke particles; 177 microns

TABLE 3

Recovery, Burnoff and Water Efficiency for
Fluid Petroleum Coke Activated at 850°C.

Sample/ Activation Run	Initial Sample Weight (g)	Activation Time (h)	% Recovery	% Burnoff	% Water Efficiency
A-9	10.03	2	77.3	22.7	
A-12	10.09	4	46.2	53.8	
A-17	10.00	6	40.0	60.0	
B-1	50.00	6	31.5	68.5	
B-2	50.00	6	36.9	63.1	53.3
B-3*	50.00	6	43.8	56.2	33.3
B-4	50.00	6	32.5	67.5	40.0
B-5**	50.00	6	90.7	9.3	
B-10	50.01	2	72.7	27.3	46.0
B-11	50.01	4	54.3	45.7	47.0
B-12	50.01	1	84.2	15.8	28.0
B-13	50.04	0	91.7	8.3	
B-14	50.00	3	68.2	31.8	54.4
B-15	50.00	5	55.4	44.6	40.8
B-16	50.005	5	48.6	51.4	46.7

* Only + 177 micron coke particles activated

** No steam activation

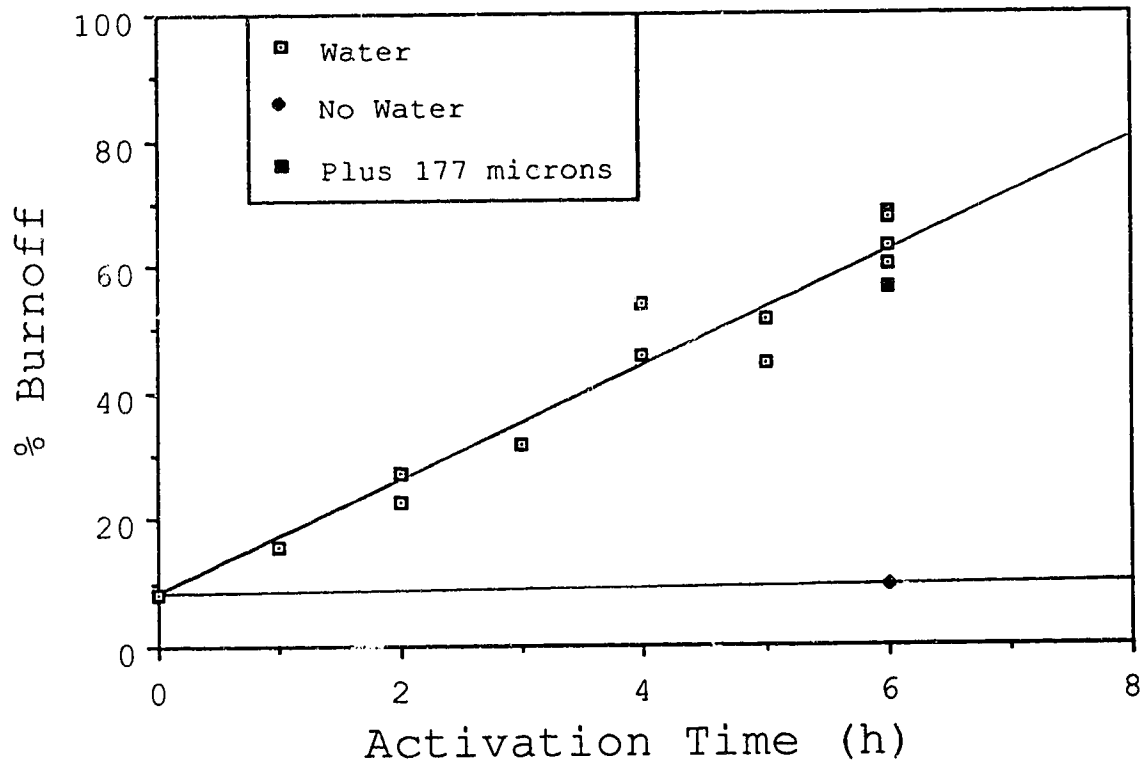


Figure 4. The Burnoff of Untreated Activated Coke as a Function of Activation Time.

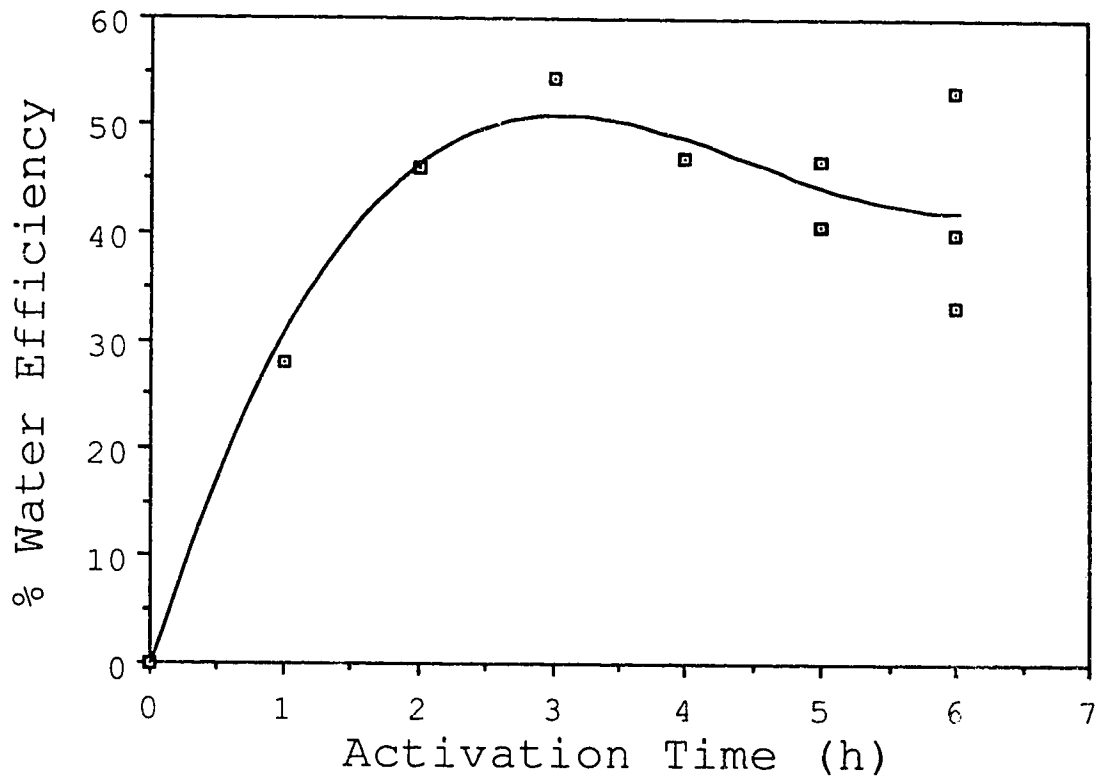


Figure 5. The Water Efficiency of the Activation of Untreated Coke as a Function of Activation Time.

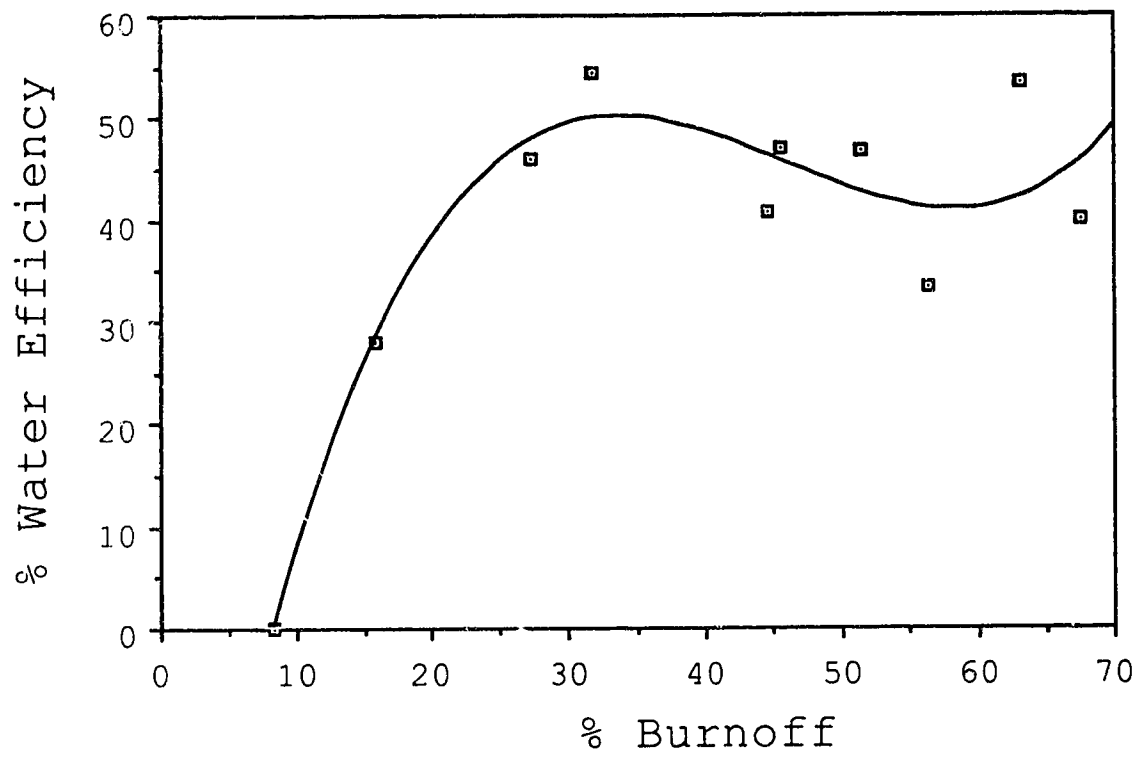


Figure 6. The Water Efficiency of the Activation of Untreated Coke as a Function of Burnoff.

corresponds to the d₅₀ of the raw coke sample. Sample B-5 was soaked for 6 hours without any steam activation.

The steam activation of coke as illustrated in Figure 4, indicates that the burnoff is constant over time. The rate of burnoff is 9.4% of the original mass per hour.

The burnoff at 0 hours of activation is 8.3%, as a result of the prior pyrolysis. With no steam activation, the burnoff is 9.3% after 6 hours of soak time. With steam activation, the burnoff averages 65% after 6 hours. As a comparison, the plus 177 micron sample had a burnoff of 56.2% after 6 hours. This shows that most of the burnoff occurs as a result of the coke reacting with steam during activation.

Steam activation removes carbon and other elements from the coke particle by chemical reaction at specific active surface sites. This activation exposes more surface area by creating and enlarging pores. The lower burnoff of the plus 177 micron sample can be explained by the fact that at the start of activation, it had less total surface area than a sample with minus 177 micron sizes. Thus less reaction sites lead to less reactions at the start of activation. With a constant burnoff rate, the total burnoff would be slightly less.

The water efficiency versus activation time as shown by Figure 5, indicates that the water efficiency starts low, rises quickly to a maximum

and then declines slowly. There is a steady rise in the first 3 hours of activation going from 0 to a maximum of 54.4% at three hours of activation. The water efficiency then declines slowly to approximately 40% at 6 hours of activation. This occurs with the rate of water introduced for activation remaining constant.

At the start of activation, the coke particles have a low surface area, therefore there are few surface sites for a carbon-water reaction to occur. As the activation proceeds, more surface area is exposed, thus more active sites for reactions to occur, and a higher reaction rate means a higher water efficiency. After reaching a maximum, the water efficiency drops due to less active sites occurring on the coke particles. At 6 hours of activation, 65% of the coke particle has been removed. Even with a high specific surface area, the loss of mass means that the total area starts to decrease, thus less sites for reactions are generated. In Figure 6, which shows water efficiency versus burnoff, a similar trend is noticeable. The water efficiency starts low, then rises quickly to a maximum at around 30% burnoff, then the efficiency starts to decline slowly.

The water for steam activation is introduced at a rate of 0.5 g H₂O/g Coke (initial wt). With a constant burnoff of 9.4%/h for the coke, and a maximum water efficiency of 54.4%, it can be calculated that at the point of maximum reaction (max W_{eff}), 0.4 g of water reacts with every 1.0 g of coke burned off.

Potassium Treated Coke

The results of the activation of potassium treated coke which includes recovery, burnoff and water efficiency are tabulated in Table 4. The burnoff versus activation time is illustrated in Figure 7, and the water efficiencies versus activation time and burnoff are graphed in Figures 8 and 9 respectively.

The burnoff rate for potassium coke is constant and as determined from Figure 7, the rate of burnoff is 12.6% of the original mass per hour. At 0 hours of activation, the burnoff due to prior pyrolysis is 9.7% and after 6 hours, the burnoff is 85.1%.

The water efficiency versus activation time presented in Figure 8, shows a similar trend as the untreated coke's water efficiency, but here the maximum efficiency occurs after two hours of activation, rather than three hours. The maximum water efficiency at two hours of activation is 54.0%, nearly identical to the untreated coke. After the maximum efficiency is reached, the efficiencies tend to remain level or slightly increase. There is a noticeable drop at three hours but the overall trend is level or slightly increasing. At 4 hours of activation the water efficiency is 57.0%, up 3.0% from after two hours of activation. The water efficiency versus burnoff as shown in Figure 9 shows a similar result as the untreated coke; the maximum water efficiency occurs at 30% burnoff.

TABLE 4

Recovery, Burnoff and Water Efficiency of
Activated Potassium (4% KOH) Fluid Coke.

Sample/ Activation Run	Initial Sample Weight (g)	Activation Time (h)	% Recovery	% Burnoff	% Water Efficiency
A-11	10.42	2	54.7	45.3	
A-14	10.46	4	40.0	60.0	
A-18	10.41	6	14.9	85.1	
B-6	52.00	4	42.6	57.4	56.0
B-7	52.01	4	46.3	53.7	58.0
B-8	52.01	4	44.0	56.0	
E-9	52.05	2	66.8	33.2	54.0
B-17	52.01	3	50.9	49.1	46.7
B-18	52.01	0	90.3	9.7	

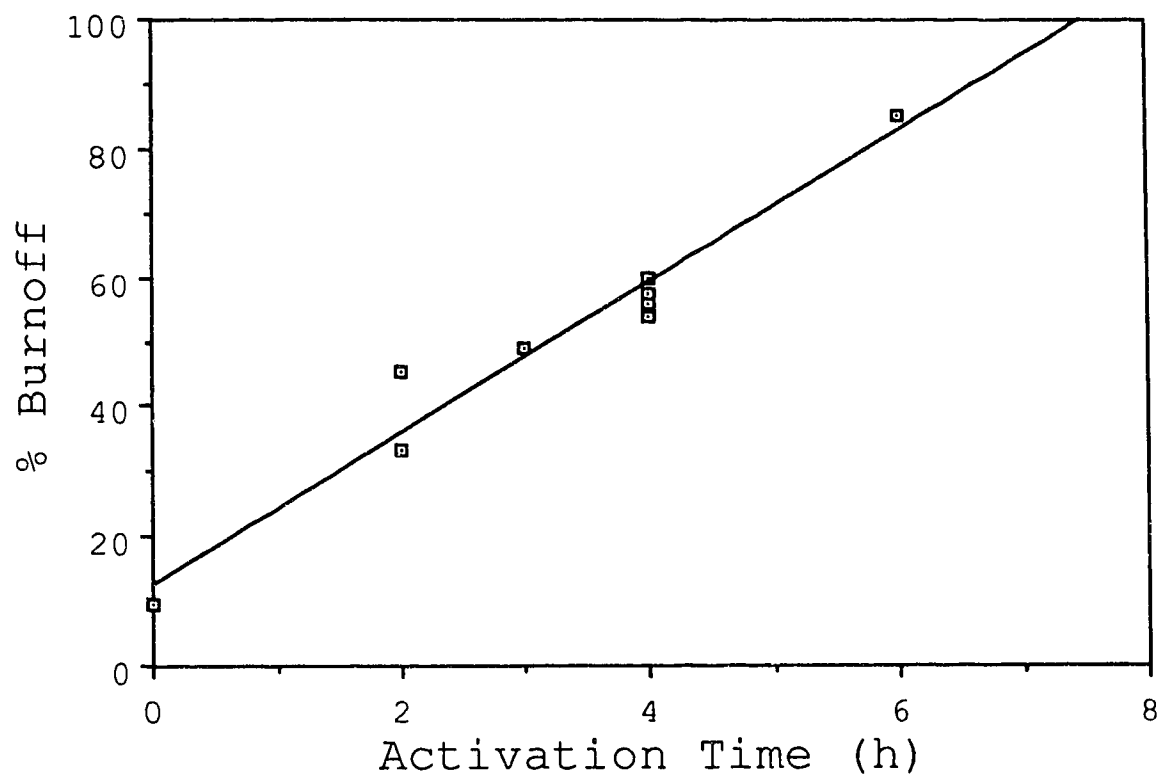


Figure 7. The Burnoff of Potassium Treated (4% KOH) Activated Coke as a Function of Activation Time.

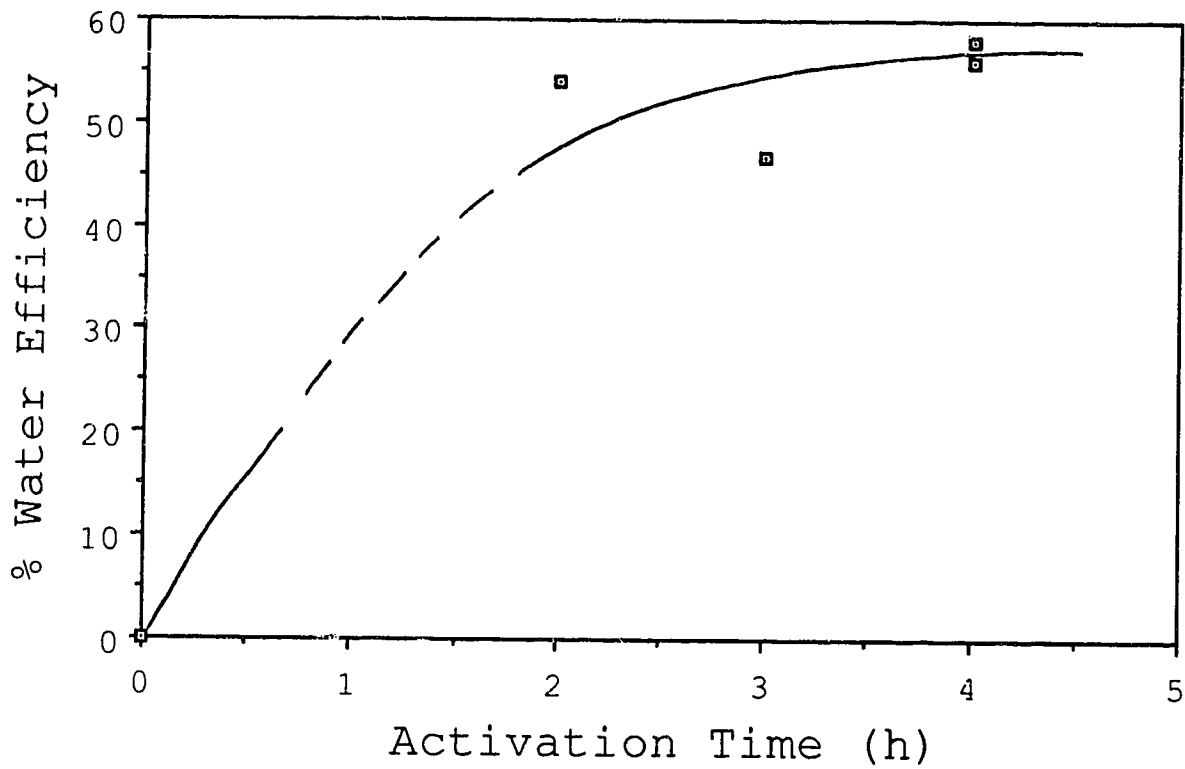


Figure 8. The Water Efficiency of the Activation of Potassium Treated (4% KOH) ~~Coke~~ as a Function of Activation Time.

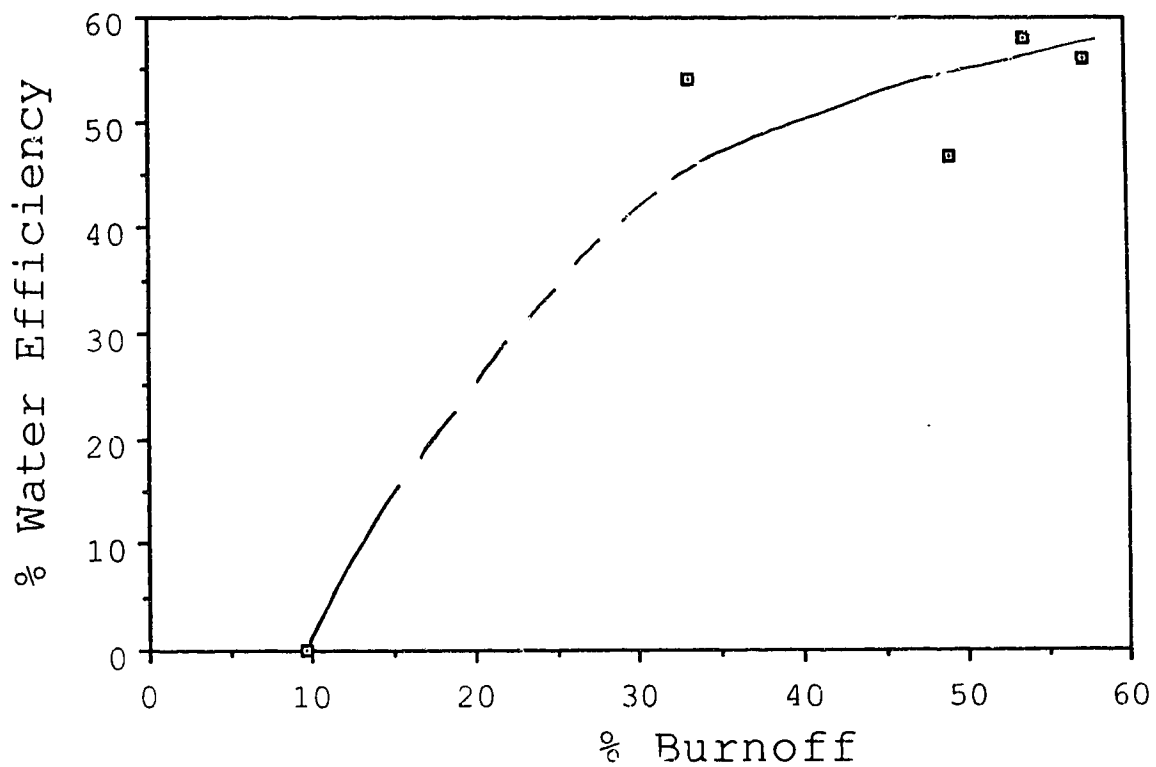


Figure 9. The Water Efficiency of the Activation of Potassium Treated (4% KOH) Coke as a Function of Burnoff.

Untreated versus Potassium Coke

Figure 10 compares the burnoffs of untreated and potassium cokes. As mentioned, untreated coke has a burnoff rate of 9.4% versus 12.6% for potassium coke. At 0 hours of activation, untreated coke has a pyrolysis burnoff of 8.3% and potassium coke has a burnoff of 9.7%. The maximum water efficiencies are nearly equal for each type of coke, but potassium coke reaches maximum water efficiency, or the maximum rate of chemical reaction one hour earlier.

The addition of potassium to coke does increase its burnoff rate by 3.2% compared to untreated coke. The potassium acts as a catalyst and increases the rate of burnoff without increasing the maximum rate of the water/coke chemical reactions. The addition of potassium seems to speed up the chemical reactions so the maximum rate of reaction is achieved earlier.

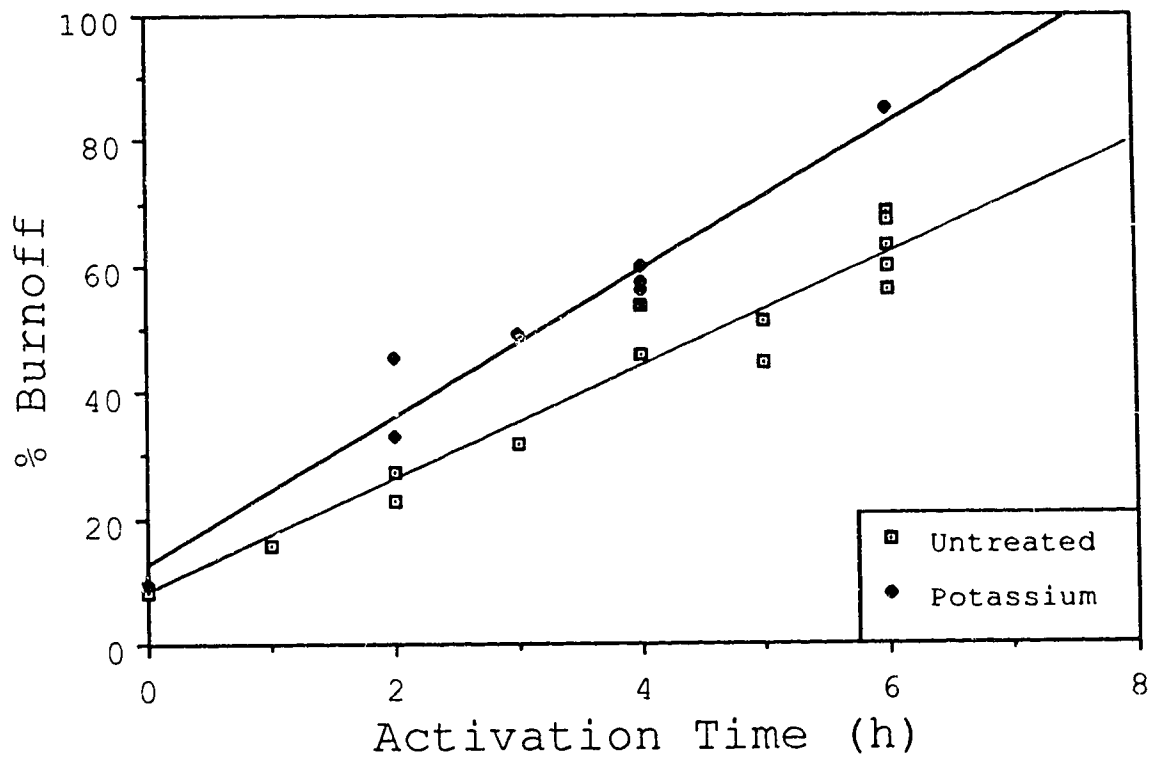


Figure 10. Comparison of the Burnoffs of Untreated Activated Coke and Potassium Treated (4% KOH) Coke as a Function of Activation Time.

4.1.3 Proximate and Ultimate Analysis

The proximate analysis of raw fluid coke and the ultimate analyses of raw coke, activated coke and activated potassium coke are tabulated in Table 5. All percentages are calculated as weight percent as received for the raw coke and weight percent for the activated cokes. Oxygen content was calculated by difference.

The activated cokes analyzed were those with the highest specific surface area. Activated coke is represented by sample B-1, and activated potassium coke by sample B-7. Sample B-1 has a specific surface of 318 $\text{m}^2 \text{g}^{-1}$ and a burnoff of 68.5%. Sample B-7 has a specific surface of 167.4 $\text{m}^2 \text{g}^{-1}$ and a burnoff of 53.7%. Sample B-7 was washed with 250 ml of boiling water to remove the potassium salts, then vacuum dried for 24 hours at 110°C before being sent for ultimate analysis.

Raw Coke

The proximate and ultimate analysis of raw coke is similar to those reported by other investigators of Syncrude coke [75-78]. A multi-element and ash analysis content was not determined in this study but is reported in other studies [75,76].

The moisture content determined by the proximate analysis is 1.8%, while the ultimate analysis indicates a moisture content of 4.0%. Other

TABLE 5

Proximate and Ultimate Analysis of Raw Coke, Untreated Activated Coke (B-1), and Potassium Treated (4% KOH) Activated Coke (B-7).

Proximate Analysis (wt% as recieved)

	Raw Coke
Moisture	1.8
Volatile Matter	7.1
Fixed Carbon	88.1
Ash	3.0

Ultimate Analysis (wt%)

	Raw Coke	Sample B-1	Sample B-7
Moisture	4.0	0.17	0.03
Carbon	77.4	79.20	79.55
Hydrogen	2.0	0.17	0.20
Nitrogen	1.7	0.94	1.14
Sulfur	6.5	4.80	4.50
Ash	5.8	12.90	15.00
Oxygen *	2.6	1.80	0.00

* By Difference

studies [77] give a proximate moisture content of 3.7%. Otherwise the ultimate and proximate analysis is similar to other studies except that the ash content is slightly lower in the sample used for this study. Ash content has been recorded as high as 8.0% by ultimate analysis [75,77,78] but this study indicates an ash content of 5.8%. It is evident that fluid coke from Syncrude can vary from study to study.

Activated Untreated Coke

The ultimate analysis data shows a sharp decrease in the moisture content from 4.0% for the raw coke to 0.17% for sample B-1. The low moisture content for the activated samples is a result of the high pyrolysis/activation temperatures.

The ash content increases from 5.8% to 12.9% between the raw and activated cokes. The activated coke had a burnoff of 68.5%, which corresponds to a recovery of 31.5%. If only the moisture, sulphur, heteroatoms and carbon were burned off during activation, the ash content of the activated sample with a 31.5% recovery would be expected to be 19.2%. This would indicate that some portion of the mineral content of raw coke is not inert.

The carbon content increases slightly from 77.4% in the raw coke to 79.2% in the activated coke.

The heteroatom content shows the most change between the raw and activated coke samples. The hydrogen content decreases by a factor of ten from 2.0% to 0.17%. Nitrogen displays a slight drop from 1.7% to 0.94% and sulphur drops from 6.5% to 4.8%. Oxygen drops by a factor of 2 from 2.6% to 1.8%. The large decrease in hydrogen can be explained by the increased aromatization of the carbon. As the carbon atoms form aromatic rings and sheets, hydrogen and oxygen are expelled. The functional groups containing nitrogen and sulphur also decompose leading to heteroatom loss.

A visual examination of the activated coke particles revealed a shiny black surface texture with no evidence of ash particles or ashing.

Activated Potassium Coke

The moisture content for the activated potassium coke is 0.03%. This water content is a result of the washing of the sample to remove the potassium salts and subsequent vacuum drying and is not a result of the activation process.

The ash content is 15.0%, higher than the activated cokes 12.9% even though the burnoff is only 53.7%. This burnoff should correspond to an ash content of 13.0%. The greater than expected ash content can be explained by the presence of residual potassium salts which are not washed out of the sample. The wash water was tested for dissolved solids

by evaporation and it was found that only 50% of the KOH or other potassium salts were recovered. It has been reported by Bruno *et al* [153] that potassium catalysts can react with mineral matter during the steam gasification of coals to form water-insoluble compounds. Some potassium probably combined with oxygen and other elements to form potassium aluminosilicates (KAlSiO_4) [153]. This extra ash skews the ultimate analysis in favour of ash over oxygen, thus the oxygen content of 0.0%. The carbon content is slightly higher at 79.55% than the 77.4% of the raw coke.

Hydrogen again shows a ten fold decrease from 2.0% to 0.2%, probably due to the aromatization of the carbon. Nitrogen decreases from 1.7% to 1.14%, a decrease of 32.9%. Sulphur decreases from 6.5% to 4.5%, a decrease of 30.1%

A visual examination of the coke particles reveals a dull, slightly grey appearance, likely caused by a thin coating of ash.

4.1.4 Size Analysis

Raw Coke

The particle size analysis of raw fluid coke is shown in Table 6, and plotted on Figure 11. A plot of the cumulative undersize data versus sieve size on a semi-log graph gives a d_{25} (25% wt passing size d) of 107 microns, a d_{50} of 177 microns and a d_{75} of 265 microns.

Activated Untreated Coke

The coke analyzed was sample B-2, which was activated for 6 hours, has a burnoff of 63.1%, and a specific surface area of around $300 \text{ m}^2 \text{ g}^{-1}$. The particle size analysis is shown in Table 7, and plotted on Figure 11. A semi-log plot gives a d_{25} of 120 microns, a d_{50} of 192 microns and a d_{75} of 275 microns. The data indicates that the activated coke particles are slightly larger in diameter than the raw coke particles. At d_{25} , the size increase is 12.1%, at d_{50} , it's 8.5% and at d_{75} , the increase is 3.8%, for an average of 8.1% overall.

Activated Potassium Coke

Sample B-8, was analyzed for particle size distribution and tabulated in Table 8 and graphed in Figure 11. Sample B-8 was activated for

TABLE 6

Particle Size Analysis of Raw Fluid

Petroleum Coke.

Sieve Size Range (microns)	Weight (g)	% Weight	Cumulative % Oversize	Cumulative % Undersize
+ 841	4.7727	4.38	4.38	95.62
- 841 + 589	1.4332	1.32	5.70	94.30
- 589 + 425	3.7427	3.44	9.14	90.86
- 425 + 297	8.6810	7.97	17.11	82.89
- 297 + 250	14.9762	13.75	30.86	69.14
- 250 + 212	11.3436	10.42	41.28	58.72
- 212 + 177	9.1093	8.37	49.65	50.35
- 177 + 150	13.6711	12.55	62.20	37.80
- 150 + 106	18.9540	17.41	79.61	20.39
- 106 + 75	14.2934	13.13	92.74	7.26
- 75 + 53	6.4249	5.90	98.64	1.36
- 53 + 45	0.8756	0.80	99.44	0.56
- 45 + 38	0.1511	0.14	99.58	0.42
- 38	0.4693	0.43		

TABLE 7

Particle Size Analysis of Activated
Fluid Petroleum Coke (Sample B-2).

Sieve Size Range (microns)	Weight (g)	% Weight	Cumulative % Oversize	Cumulative % Undersize
+ 841	0.6686	3.64	3.64	96.36
- 841 + 589	0.3064	1.67	5.31	94.69
- 589 + 425	0.6779	3.70	9.01	90.99
- 425 + 297	2.1869	11.92	20.93	79.07
- 297 + 250	1.9027	10.51	31.44	68.56
- 250 + 212	2.1524	11.73	43.17	56.83
- 212 + 177	2.3298	12.70	55.87	44.13
- 177 + 150	1.6813	9.16	65.03	34.97
- 150 + 106	3.0388	16.56	81.59	18.41
- 106 + 75	2.2805	12.43	94.09	5.91
- 75 + 53	0.7166	3.91	97.93	2.07
- 53 + 45	0.2093	1.14	99.07	0.93
- 45 + 38	0.0557	0.30	99.37	0.63
- 38	0.1130	0.63		

TABLE 8

Particle Size Analysis of Potassium

Treated (4% KOH) Fluid Coke (Sample B-8).

Sieve Size Range (microns)	Weight (g)	% Weight	Cumulative % Oversize	Cumulative % Undersize
+ 841	1.2690	5.63	5.63	94.37
- 841 + 589	0.3517	1.56	7.19	92.81
- 589 + 425	0.8789	3.90	11.09	88.91
- 425 + 297	2.3837	10.57	21.66	78.34
- 297 + 250	1.9533	8.66	30.32	69.68
- 250 + 212	2.3903	10.60	40.92	59.08
- 212 + 177	2.4894	11.04	51.96	48.04
- 177 + 150	1.9967	8.85	60.81	39.19
- 150 + 106	3.8968	17.28	78.09	21.91
- 106 + 75	3.3475	14.84	92.93	7.07
- 75 + 53	1.1497	5.10	98.03	1.97
- 53 + 45	0.2884	1.28	99.31	0.69
- 45 + 38	0.0348	0.15	99.46	0.54
- 38	0.1270	0.56		

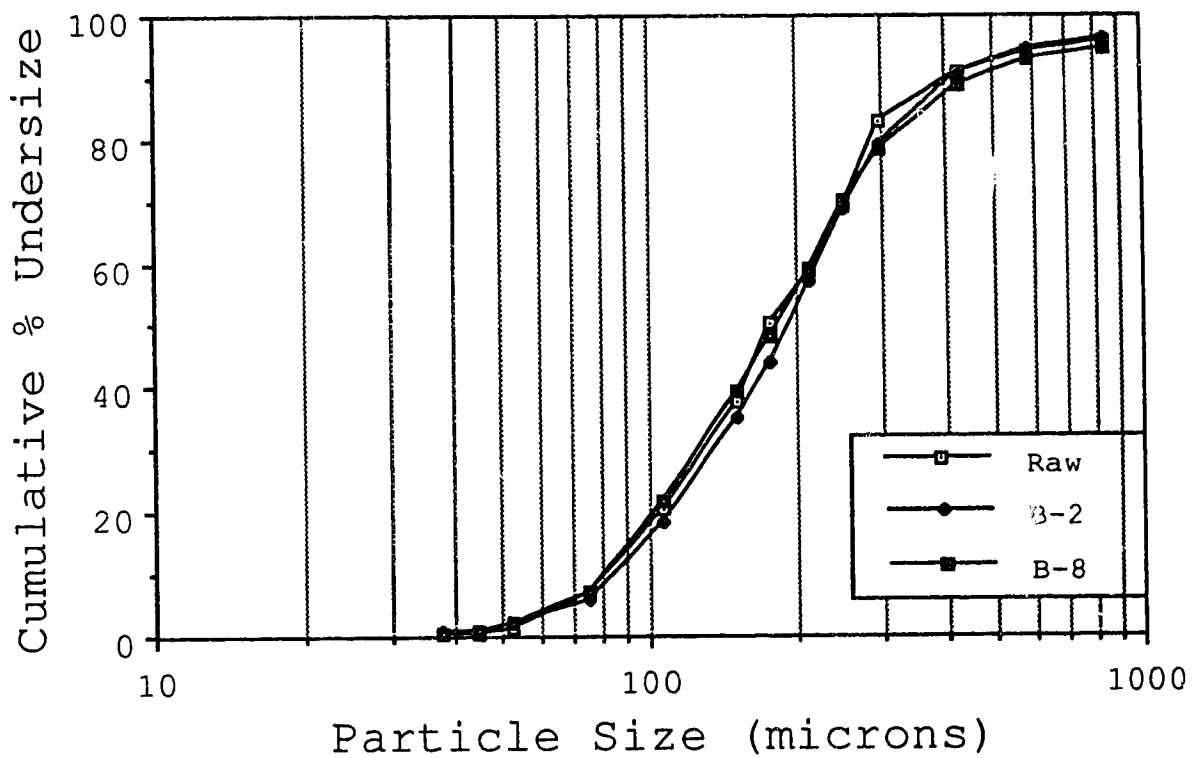


Figure 11. The Particle Size Analysis of Raw Coke, Activated Coke (Sample B-2), and Potassium Treated (4% KOH) Activated Coke (Sample B-8).

4 hours, and had a burnoff of 56.0% which corresponds to a specific surface area of around $165 \text{ m}^2 \text{ g}^{-1}$. A semi-log plot gives a d_{25} of 111 microns, a d_{50} of 185 microns and a d_{75} of 275 microns. The size increases at d_{25} , d_{50} , and d_{75} are 3.7%, 4.5% and 3.8% respectively, for an average diameter increase of 4% overall.

4.1.5 Density Analysis

4.1.5.1 Bulk Density

The bulk density of raw fluid petroleum coke was determined to be 1.0415 g cm^{-3} . The bulk density decreases to 1.0283 g cm^{-3} after vacuum drying at 110°C for 24 hours. The decrease is due to the loss of moisture.

The bulk densities of activated untreated cokes are tabulated in Table 9. Bulk densities versus activation times and burnoff are graphed in Figures 12 and 13, respectively.

At 0 hours of activation the bulk density of the coke is 1.1723 g cm^{-3} . As a result of the pyrolysis, the bulk density increases from 1.0415 g cm^{-3} for the raw coke to 1.1723 g cm^{-3} for the pyrolyzed coke. Since the size analysis of the pyrolyzed coke indicated that the change in the size particles is insignificant, the higher bulk density can be explained by carbonization and the loss of volatiles. In contrast to the pyrolysis, as activation progresses the bulk density decreases at a constant rate of 0.057 g cm^{-3} per hour as shown in Figure 12.

The particle size analysis of the activated coke samples indicates that the overall size distribution does not change significantly for the coke particles, therefore the decrease in bulk density can be explained by the development of pores in the coke particles. Sample B-3, which

TABLE 9

Bulk Densities of Raw Coke and
Activated Fluid Petroleum Coke

Sample\ Activation Run	Activation Time (h)	% Burnoff	Bulk Density (g cm ⁻³)
Raw			1.0415
Raw (dried)			1.0283
A-9	2	22.7	1.0604
A-12	4	53.8	0.9608
A-17	6	60.0	0.8678
B-1	6	68.5	0.7884
B-2	6	63.1	0.8495
B-3*	6	56.2	0.8095
B-4	6	67.5	0.8361
B-10	2	27.3	1.0786
B-11	4	45.7	0.9431
B-12	1	15.8	1.1256
B-13	0	8.3	1.1723
B-14	3	31.8	1.0048
B-15	5	44.6	0.9514
B-16	5	51.4	0.8939
Coconut Char			0.3700

* Only +177 micron coke particles activated.

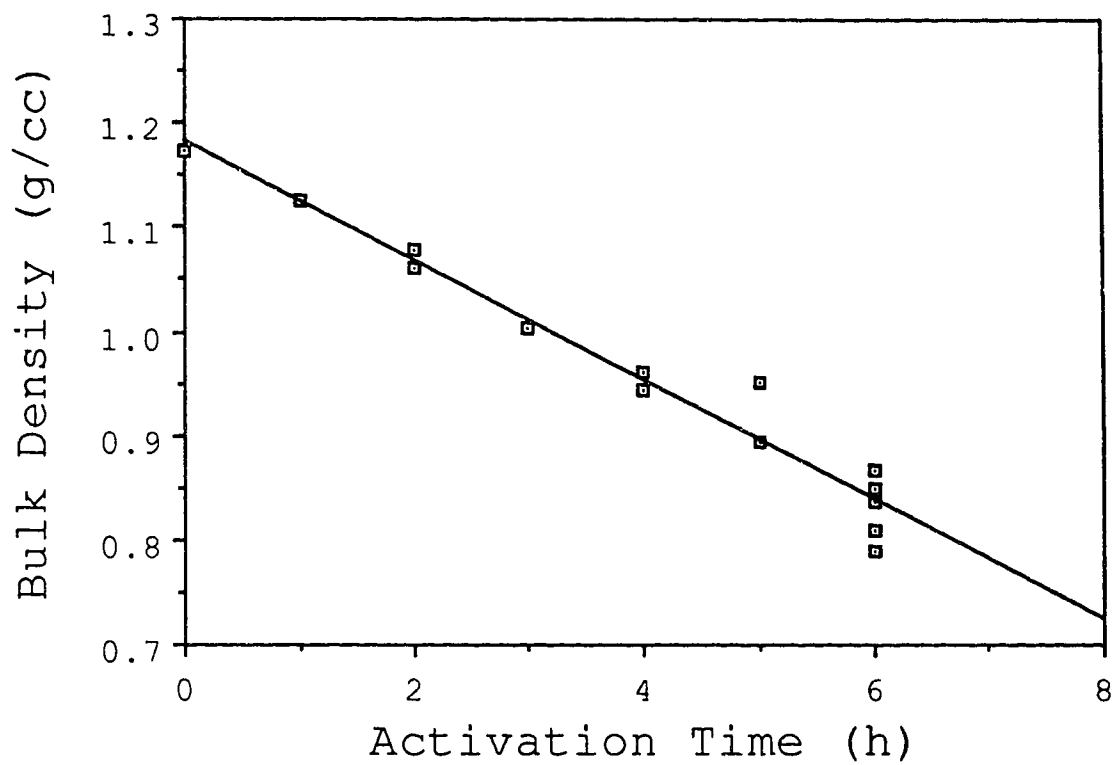


Figure 12. The Bulk Densities of Untreated Activated Coke as a Function of Activation Time.

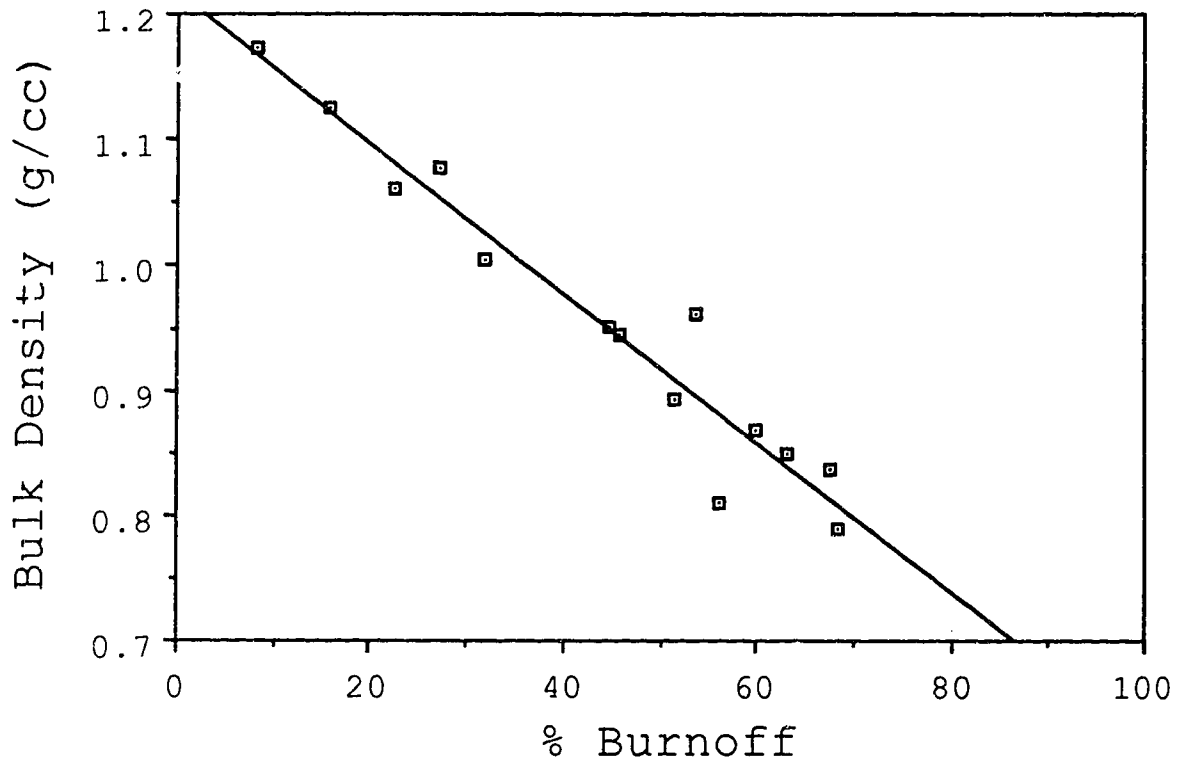


Figure 13. The Bulk Densities of Untreated Activated Coke as a Function of Burnoff.

consists of the larger plus 177 micron coke particles lies off the general trend of the other data points. At the same burnoff of 56.2%, sample A-3 has a bulk density of 0.8095 g cm^{-3} . From the main trend, at a burnoff of 56.2% the bulk density should be around 0.9 g cm^{-3} . This indicates that the larger sized coke particles are more prone to porosity development.

Bulk densities for potassium treated coke versus activation times and burnoff are tabulated in Table 10, and graphed in Figures 14 and 15 respectively.

Initial pyrolysis of potassium coke increased the bulk density to 1.1750 g cm^{-3} , similar to the untreated coke. With activation, the bulk density starts to decrease at a rate of 0.075 g cm^{-3} . As with the untreated coke, bulk density decrease is due to porosity development in the interior of the coke particle while the exterior dimensions of the coke particle remain relatively constant.

Both untreated and potassium activated coke bulk densities versus activation times and burnoff are compared in Figures 16 and 17, respectively. The rates of change of bulk density versus activation time differ from the untreated and potassium cokes. The rates of change for untreated coke is -0.057 g cm^{-3} per hour and -0.075 g cm^{-3} per hour for potassium coke. The rates of change for bulk density versus burnoff are similar for both types of coke at $-0.0058 \text{ g cm}^{-3}$ per % of burnoff.

TABLE 10

Bulk Densities of Activated
Potassium (4% KOH) Fluid Petroleum
Coke and Coconut Charcoal.

Sample/ Activation Run	Activation Time (h)	% Burnoff	Bulk Density (g cm ⁻³)
Coconut Char			0.3700
A-11	2	45.3	0.9993
A-14	4	60.0	0.9660
A-18	6	85.1	0.7278
B-6	4	57.4	0.8678
B-7	4	53.7	0.9330
B-8	4	56.0	0.9028
B-9	2	33.2	1.0228
B-17	3	49.1	0.9077
B-18	0	9.7	1.1750

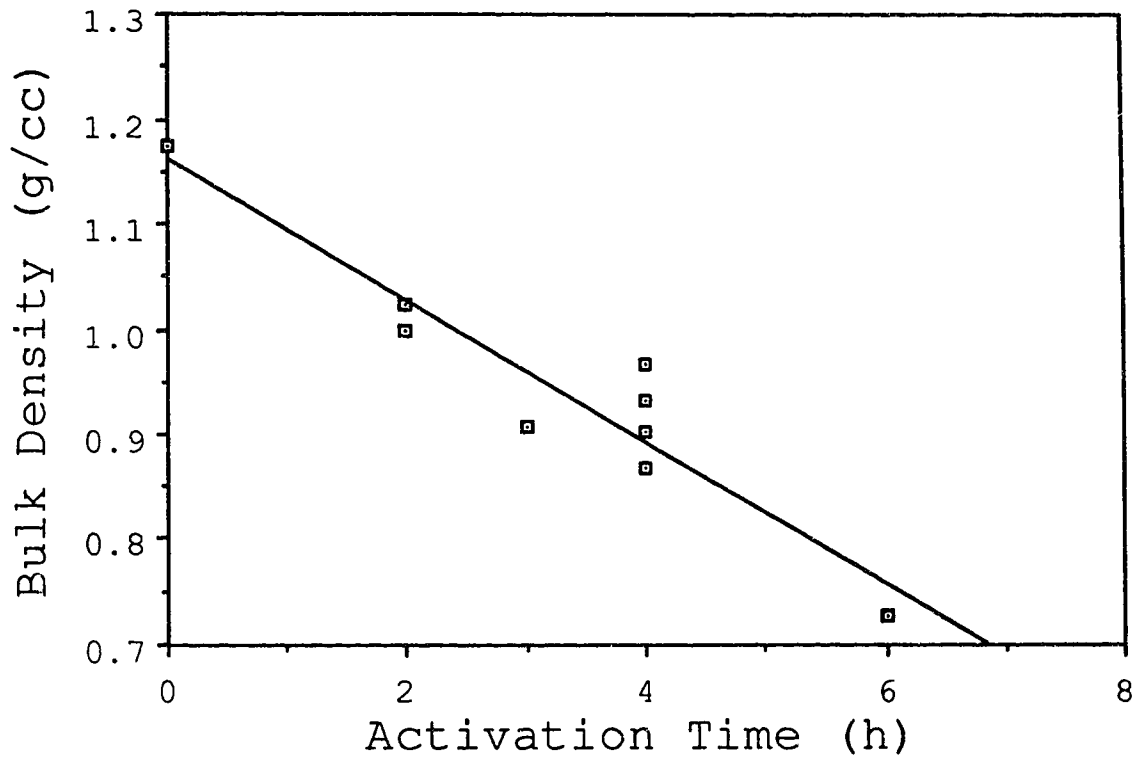


Figure 14. The Bulk Densities of Potassium Treated (4% KOH) Activated Coke as a Function of Activation Time.

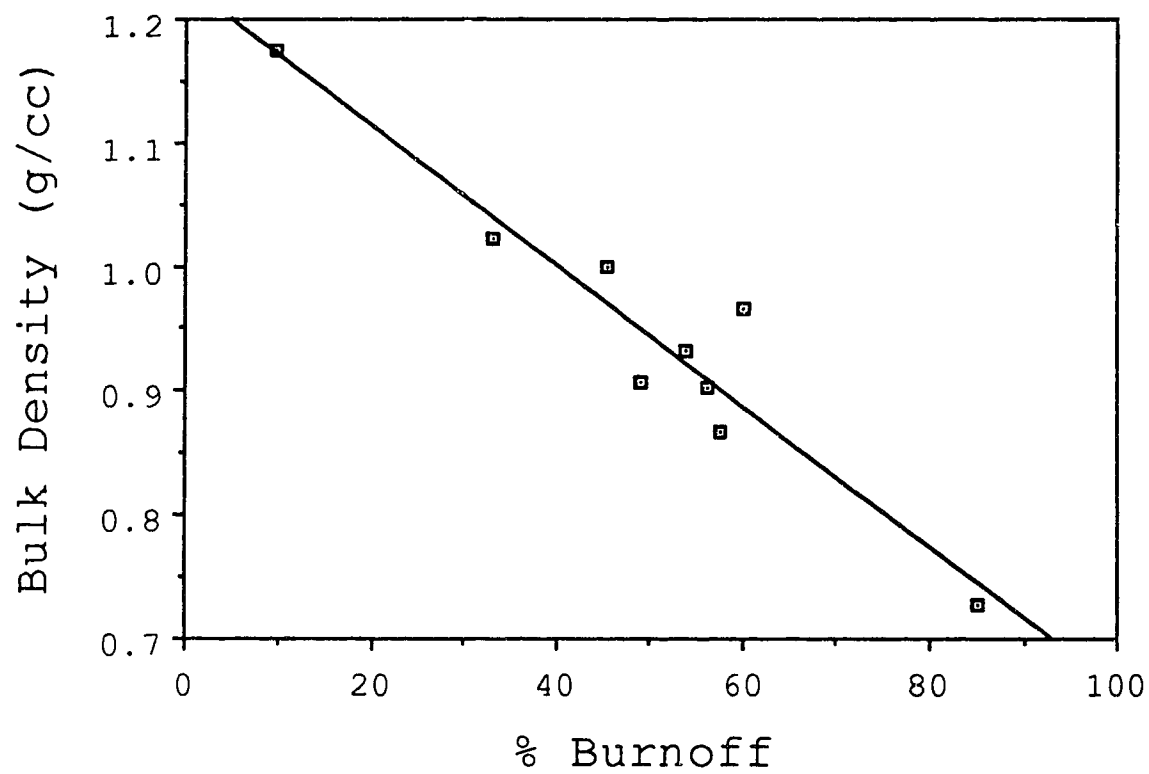


Figure 15. The Bulk Densities of Potassium Treated (4% KOH) Activated Coke as a Function of Burnoff.

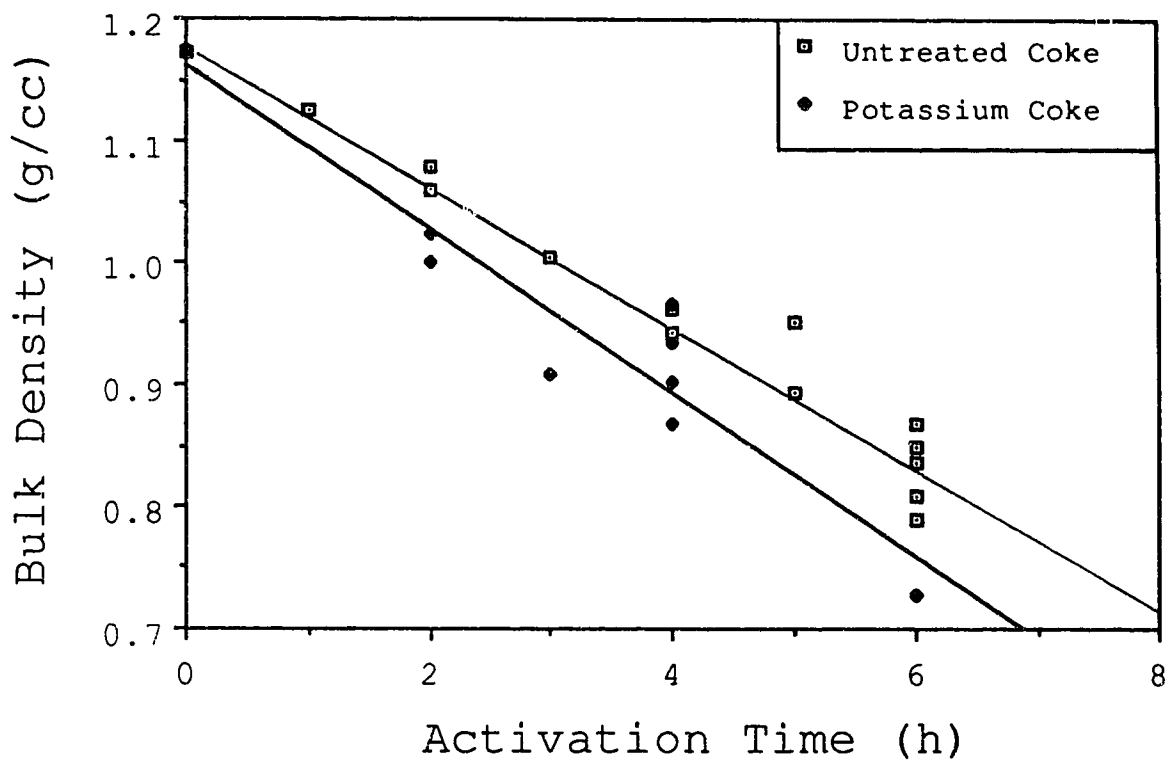


Figure 16. Comparison of the Bulk Densities of Untreated Activated Coke and Potassium Treated (4% KOH) Activated Coke as a Function of Activation Time.

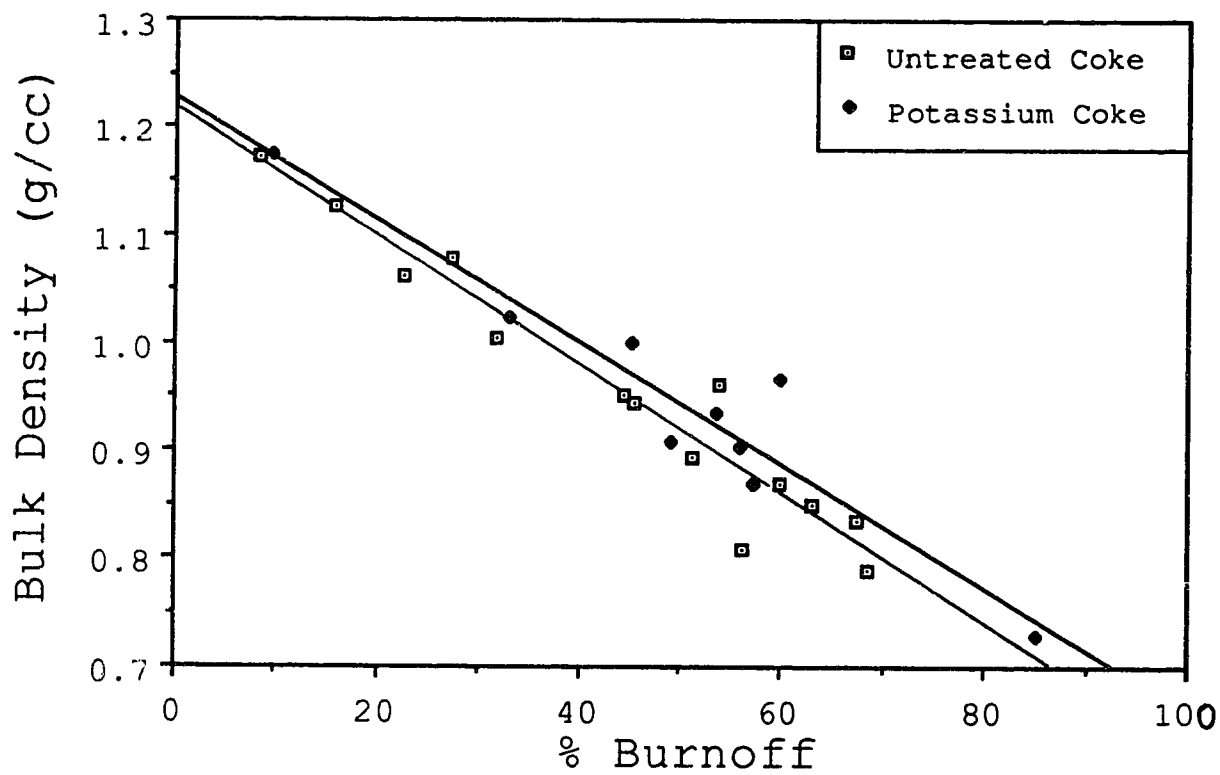


Figure 17. Comparison of the Bulk Densities of Untreated Activated Coke and Potassium Treated (4% KOH) Activated Coke as a Function of Burnoff.

The bulk density for coconut charcoal is 0.3700 g cm^{-3} , significantly lower than any of the fluid coke samples.

4.1.5.2 Absolute Density

The absolute densities for raw and vacuum dried fluid petroleum coke are given in Table 11. The density of raw coke averages 1.6475 g cm^{-3} , while for vacuumed dried (24 h, 110°C), the absolute density decreases to an average of 1.5867 g cm^{-3} , due to the loss of moisture. This result is unexpected because water has a specific density of 1.0 g cm^{-3} , much lower than the specific densities of carbon, 2.26 g cm^{-3} , or sulphur, 2.07 g cm^{-3} . A loss of water should lead to a higher absolute density because of the denser remaining elements.

The absolute density of Fisher Coconut Charcoal is 1.8309 g cm^{-3} . The absolute density seems quite high and may indicate that the charcoal was significantly carbonized with increasing levels of crystallinity. Some of the carbon may be in graphite crystal form. The bulk density is quite low at 0.3700 g cm^{-3} as expected.

The absolute densities of untreated activated coke versus activation times and burnoff are tabulated in Table 11, and graphed in Figures 18 and 19. Figure 18 shows that absolute density increases linearly in the first three hours of activation due to the loss of volatiles, such as light hydrocarbons and the densification of the carbon skeleton. Initial pyrolysis raises the absolute density from 1.5867 g cm^{-3} to 1.7829 g cm^{-3} . From 0 to 3 hours of activation the absolute density increases from 1.7829 g cm^{-3} to an average of 1.8850 g cm^{-3} . This rise in density is much lower

TABLE 11

Absolute Densities of Raw Coke,
Activated Untreated Coke
and Coconut Charcoal.

Sample/ Activation Run	Activation Time (h)	% Burnoff	Absolute Density (g cm ⁻¹)
Raw		0.0	1.6602
Raw		0.0	1.6347
Raw (dried)		3.7	1.5877
Raw (dried)		3.7	1.5857
B-13	0	8.3	1.7850
B-13	0	8.3	1.7818
B-12	1	15.8	1.7848
B-12	1	15.8	1.8159
B-12	1	15.8	1.7904
B-10	2	27.3	1.8458
B-10	2	27.3	1.8483
B-14	3	31.8	1.9235
B-14	3	31.8	1.8465
B-11	4	45.7	1.7828
B-11	4	45.7	1.8465
B-16	5	51.4	1.8628
B-16	5	51.4	1.9034
B-2	6	63.1	2.0200
Coconut Char	(6)*		1.8309

* Assumed Activation Time for Coconut Charcoal for Comparison.

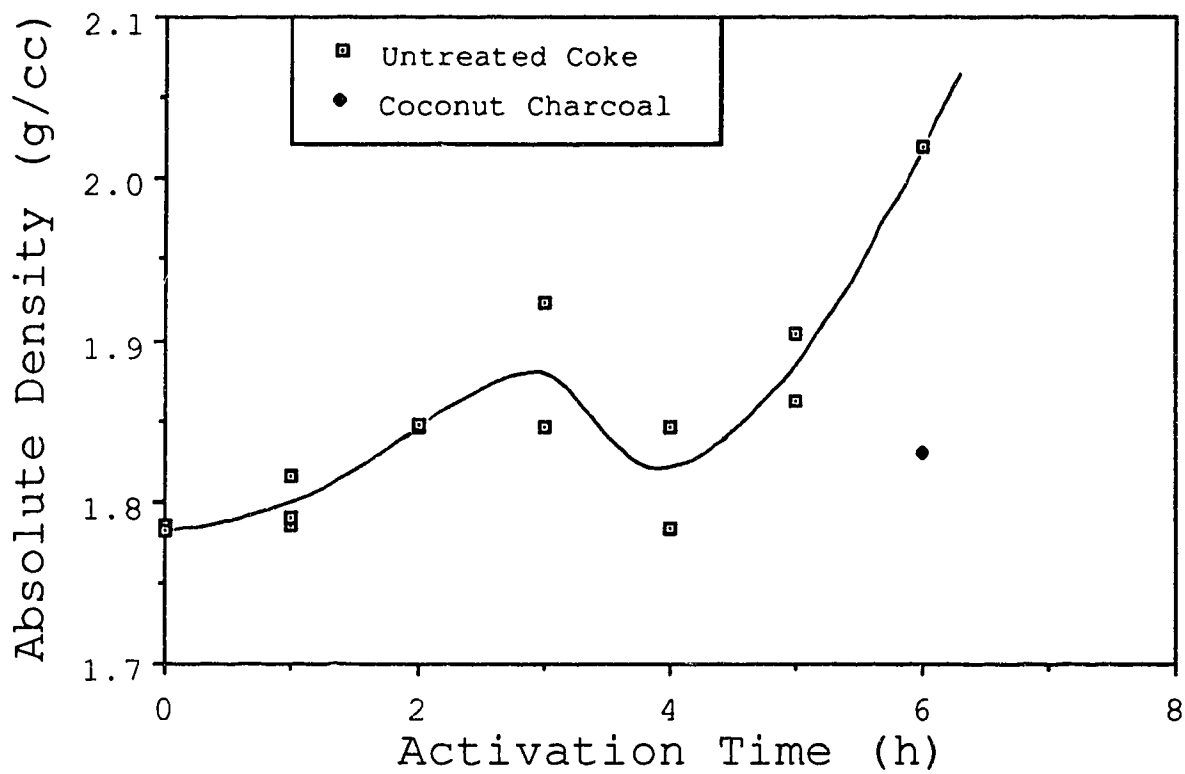


Figure 18. The Absolute Density of Untreated Activated Coke as a Function of Activation Time.

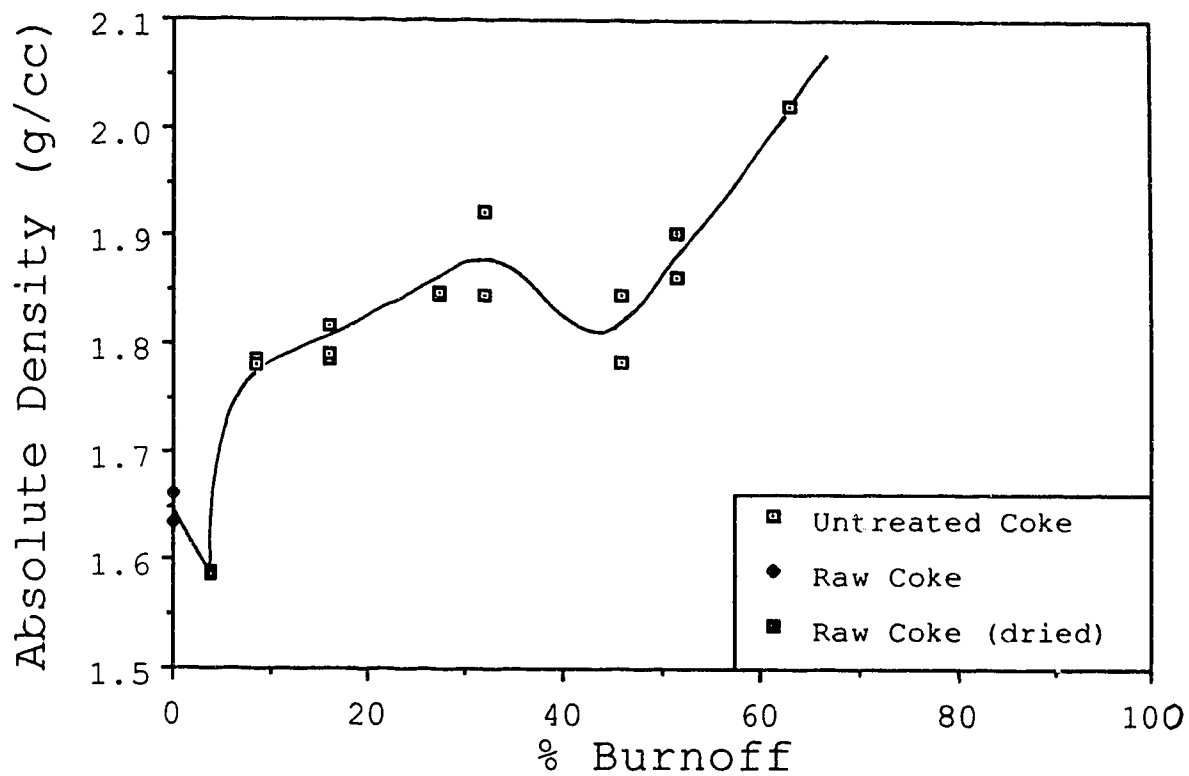


Figure 19. The Absolute Density of Untreated Activated Coke as a Function of Burnoff.

than in the pyrolysis phase because carbon is being burned off along with some sulphur and heteroatoms. The ash content is thus concentrated and the absolute density increases. Between 3 and 4 hours of activation, there is a distinct drop in absolute density, after which it rises again at a much faster rate as shown in Figure 18. Two regimes of specific density increases can be identified, one from 0 to 3 hours and the other from 4 to 6 hours. The rate of specific density increase or densification in the second regime is significantly faster than that in the first regime. This is an indication that the carbon structure differs between the two regimes. The sudden drop in absolute density between 3 and 4 hours of activation suggests a change in the overall carbon structure possibly due to the aromatic sheets of carbon rupturing and deforming into a less denser configuration. The resultant carbon structure exhibits a higher rate of densification. This phenomenon is also indicated in Figure 19 where a sudden drop in absolute density occurs between burnoffs of 30% and 40%, followed by a higher absolute density increase with increased burnoff.

4.1 6 BET Surface Area and Porosity Analysis

4.1.6.1 Surface Area

The multi-point BET analysis using the Autosorb - 1 indicated a specific surface area ranging from 4.6 to 5.5 m² g⁻¹ for raw fluid coke. The Omnisorp was used as a comparison and the specific surface area was determined to be 9.7 m² g⁻¹ as shown in Table 12. Both apparatuses employed nitrogen adsorption at 77 K. The complete Autosorb computer analyses for the raw coke samples are located in Appendix A.

Three samples of untreated activated coke were analyzed using multi-point BET nitrogen adsorption. They are activations/samples A-9, A-12 and A-17, which corresponds to steam activation times of 2, 4 and 6 hours respectively. The Autosorb - 1 and Omnisorp N₂ BET areas are tabulated in Table 12 and the nitrogen BET area versus activation time and burnoff are shown in Figure 20 and 21. Sample A-12 was tested twice using the Omnisorp as a check against the Autosorb apparatus. The Autosorb area of 172.3 m² g⁻¹ corresponds to Omnisorp areas of 190.1 and 201.9 m² g⁻¹. The complete Autosorb computer analyses of these samples are located in Appendix A.

Figure 20 illustrates that the specific surface area of untreated coke increases with activation time. The N₂ surface areas are 118.8,

TABLE 12

Specific Surface Area of Raw Coke, Untreated
 Activated Coke, Potassium Treated (4% KOH)
 Activated Coke and Coconut Charcoal.

Sample/ Activation Run	Activation Time (h)	% Burnoff	AUTOSORB N ₂ BET Area (m ² g ⁻¹)	OMNISORB N ₂ BET Area (m ² g ⁻¹)
Raw Coke				
(1)			4.6	
(2)			5.5	
(3)				9.7
Untreated				
A-9	2	22.7	118.8	
A-12	4	53.8	172.3	190.1 201.9
A-17	6	60.0	318.6	
Potassium				
A-11	2	45.3	87.5	
A-14	4	60.0	167.4	196.5
A-18	6	85.4	176.3	
Coconut Char			1237.0	

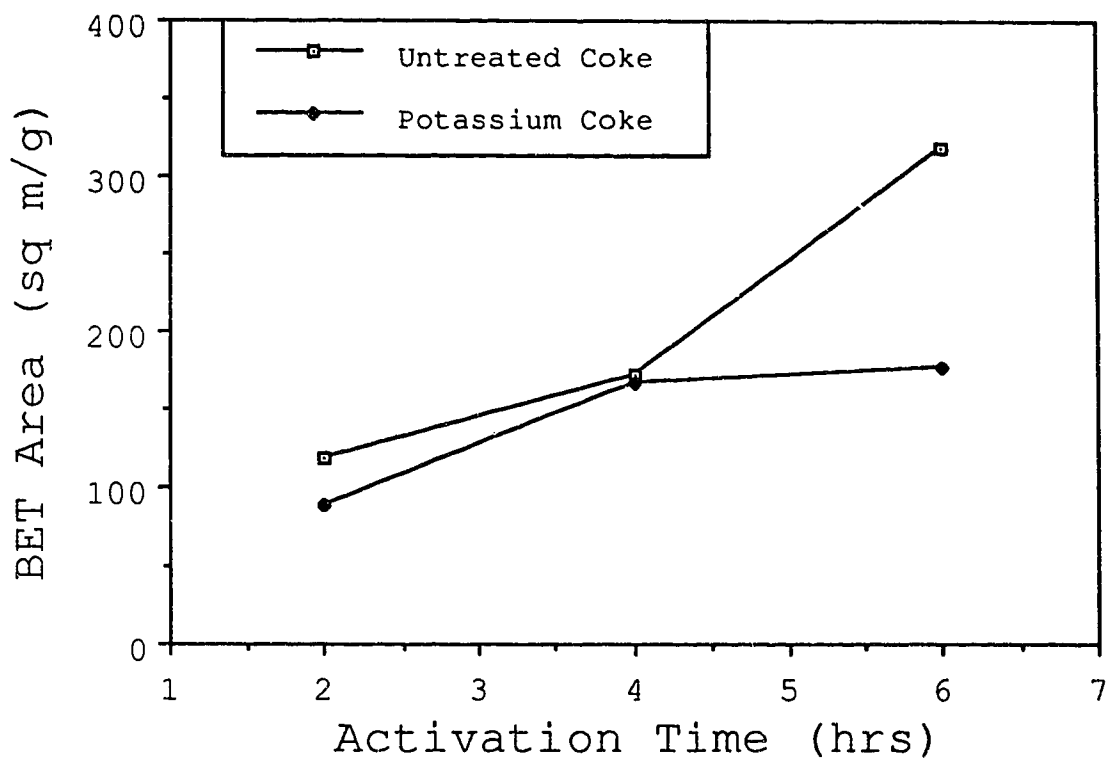


Figure 20. The BET Surface Areas of Untreated and Potassium Treated (4% KOH) Cokes as a Function of Activation Time.

172.3 and 318.6 $\text{m}^2 \text{g}^{-1}$ at 2, 4 and 6 hours of activation. There is an increase of 64 times of the specific surface area from raw coke to the coke activated for 6 hours. The trend of the graph is generally linear and indicates that greater surface area may be achieved beyond 6 hours of activation. At 6 hours of activation, the burnoff is already 60% and any more burnoff could cause the specific surface area to drop [29].

Figure 21 shows how the surface area of the untreated coke increases with burnoff. The trend indicates that there is a large increase in surface area, nearly a doubling of surface area, from 172.3 to 318.6 $\text{m}^2 \text{g}^{-1}$, between the burnoffs of 53.8% and 60.0%. These burnoffs correspond to activation times of 4 and 6 hours respectively. This indicates that while the burnoff between 4 and 6 hours is small, roughly 10%, the surface area increases by a factor of two. The absolute density data, Figures 18 and 19, shows that there is also overall change in the carbon structure at 4 hours of activation and this level of burnoff. The dramatic increase in surface area is possibly a combination of burnoff which forms pores and a structural change in the carbon skeleton which exposes more surface area.

Three samples of potassium treated (4% KOH) coke were analyzed with the multi-point nitrogen adsorption. They are activations/samples A-11, A-14 and A-18 representing 2, 4, and 6 hours of activation respectively. In addition, sample A-14 was analyzed by the Omnisorp for comparison. The specific surface areas versus activation time and burnoff are tabulated in

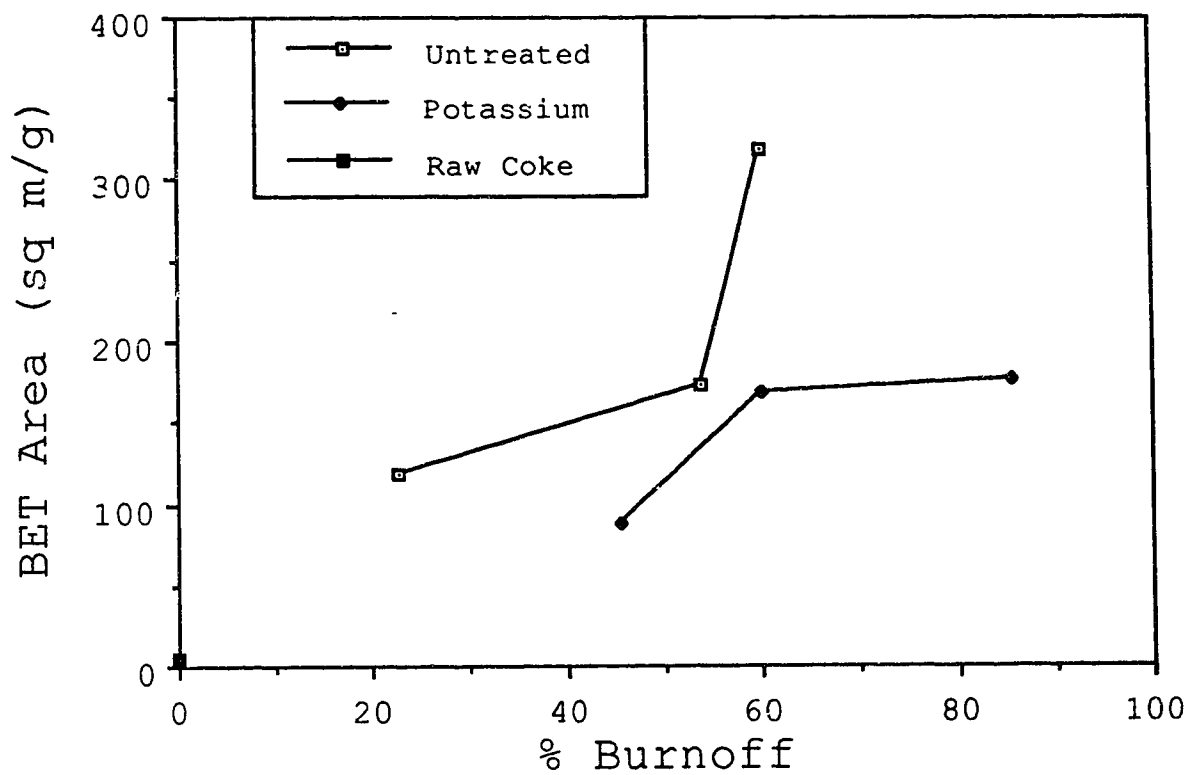


Figure 21. The BET Surface areas of Untreated and Potassium Treated (4% KOH) Cokes as a Function of Burnoff.

Table 12 and illustrated in Figures 20 and 21. All Autosorb computer analyses are located in Appendix A.

In Figure 20 and 21, surface area increases until 4 hours of activation or 60% burnoff is reached, then the rate of increase in the surface area decreases dramatically and nearly levels off with respect to activation time or burnoff. The specific surface areas for samples A-11, A-14, and A-18 are 87.5, 167.4 and 176.3 $\text{m}^2 \text{g}^{-1}$ respectively. Sample A-14 was analyzed by the Omnisorb and had a specific surface area of 196.5 $\text{m}^2 \text{g}^{-1}$. Beyond 4 hours of activation or 60% burnoff, the specific surface area increases by only 9 $\text{m}^2 \text{g}^{-1}$ in 2 hours of activation and 25% burnoff, thus the maximum surface area can be considered to have occurred at 4 hours of activation and 60% burnoff.

The specific surface area for Fisher coconut charcoal determined by multi-point BET analysis using nitrogen adsorption is 1237.0 $\text{m}^2 \text{g}^{-1}$. The complete Autosorb computer analysis is located in Appendix A.

4.1.6.2 Surface Area and Porosity Distribution

The Autosorb BET analyses were used to determine the distribution of the specific pore volumes of the coke samples. The Autosorb program arbitrarily chose an average pore radius of 12 angstroms for the coke samples. The micropore volume and surface area is defined as the total pore volume and surface area that occurs in pores of less than

12 angstroms. Conversely, mesopore volume and area is defined as the total pore volume and surface area occurring in pores of greater than 12 angstroms. This method is arbitrary and only used here for comparison.

The two raw coke samples have specific surface areas of 4.6 and 5.5 $\text{m}^2 \text{g}^{-1}$. The micropore surface areas are 3.5 and 4.3 $\text{m}^2 \text{g}^{-1}$ while the mesopore surface areas are 1.1 and 1.2 $\text{m}^2 \text{g}^{-1}$ respectively. This corresponds to 76.1% and 78.2% of the total area located in the micropores while 23.9% and 21.8% of the total area is located in the mesopores. The specific surface areas are tabulated in Table 13, while the percentages are listed in Table 14. A graphical representation of the percentages are illustrated in Figure 22. The two samples of raw cokes have specific volumes of 0.004 $\text{cm}^3 \text{g}^{-1}$. The specific micropore volumes are 0.0018 and 0.0023 $\text{cm}^3 \text{g}^{-1}$ respectively which corresponds to 45.0% and 57.5% of the total pore volume, while the specific mesopore volumes are 0.0022 and 0.0017 $\text{cm}^3 \text{g}^{-1}$ which correspond to 55.0 and 42.5% of the total pore volume respectively. The specific volumes are tabulated in Table 13, while the percentages of the pore volumes are tabulated in Table 14 and illustrated in Figure 23.

The specific surface area and specific pore volume distributions for the three samples of activated untreated coke are listed in Table 13 while the percentage distribution are listed in Table 14. The surface area distributions are illustrated in Figure 22 while the pore volume

TABLE 13

Surface Area and Porosity Characteristics of Raw Coke, Untreated Activated Coke, Potassium Treated (4% KOH) Activated Coke and Coconut Charcoal.

Sample/ Activation Run	Specific Surface Area (m ² g ⁻¹)			Specific Pore Volume (cm ³ g ⁻¹)		
	Micro- Pore	Meso- Pore	Total	Micro- Pore	Meso- Pore	Total
Raw						
(1)	3.5	1.1	4.6	0.0018	0.0022	0.004
(2)	4.3	1.2	5.5	0.0023	0.0017	0.004
Untreated						
A-9	91.7	27.1	118.8	0.048	0.031	0.079
A-12	103.0	69.3	172.3	0.053	0.089	0.142
A-17	190.4	128.2	318.6	0.097	0.147	0.244
Potassium						
A-11	61.7	25.8	87.5	0.032	0.037	0.069
A-14	123.9	43.6	167.4	0.064	0.066	0.130
A-18	108.5	67.8	176.3	0.055	0.109	0.164
Coconut	850.5	386.5	1237.0	0.4164	0.3514	0.7678

TABLE 14

Surface Area and Porosity Distribution
of Untreated and Potassium Treated
(4% KOH) Activated Fluid Petroleum Coke.

Sample/ Activation Run	Specific Surface Area		Specific Pore Volume	
	% Micro- Pore	% Meso- Pore	% Micro- Pore	% Meso- Pore
Raw Coke				
(1)	76.1	23.9	45.0	55.0
(2)	78.2	21.8	57.5	42.5
Untreated				
A-9	77.2	22.8	60.8	39.2
A-12	59.8	40.2	37.3	62.7
A-17	59.8	40.2	39.7	60.3
Potassium				
B-11	70.5	29.5	46.4	53.6
B-14	74.0	26.0	49.2	50.8
B-18	61.5	38.5	33.5	66.5
Coconut	68.8	31.2	54.2	45.8

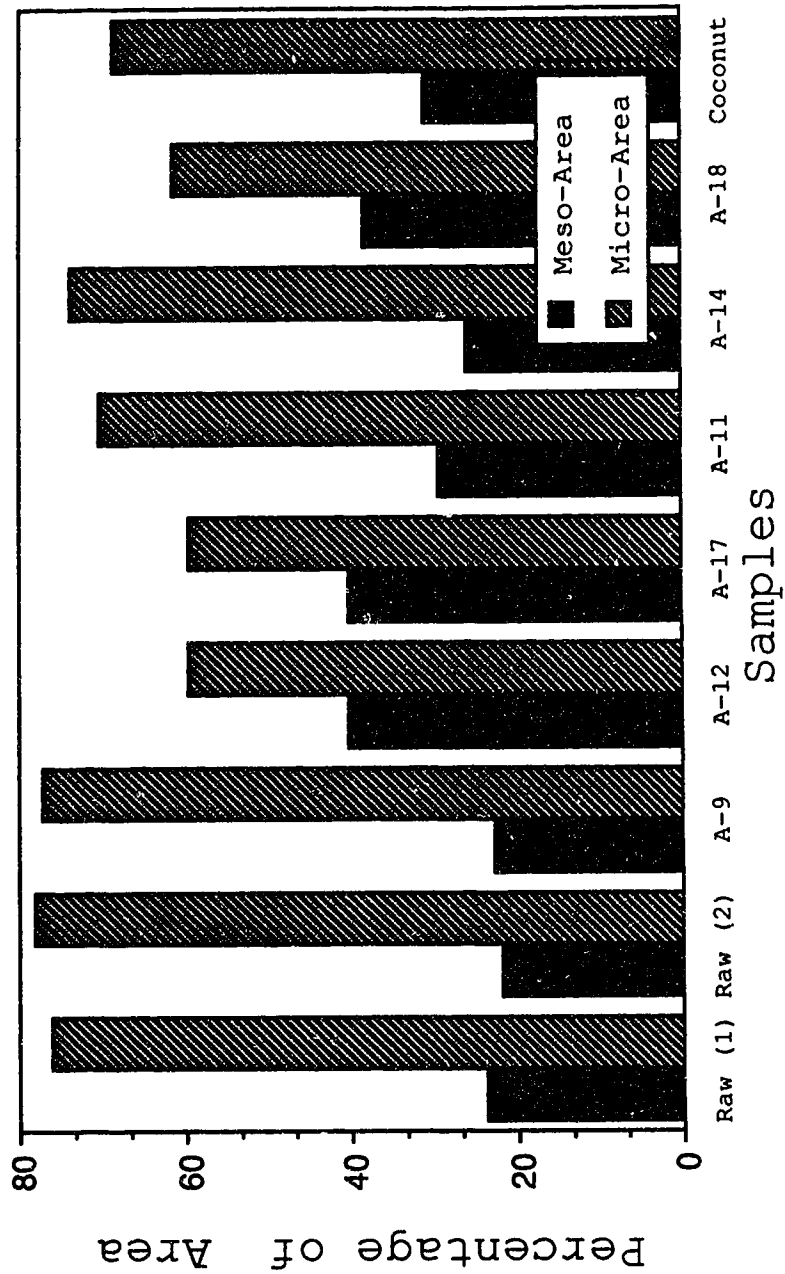


Figure 22. The Specific Surface Area Distribution Between Micro and Mesopores For Raw Coke, Untreated Coke, Potassium Treated (4% KOH) Coke and Fisher Coconut Charcoal.

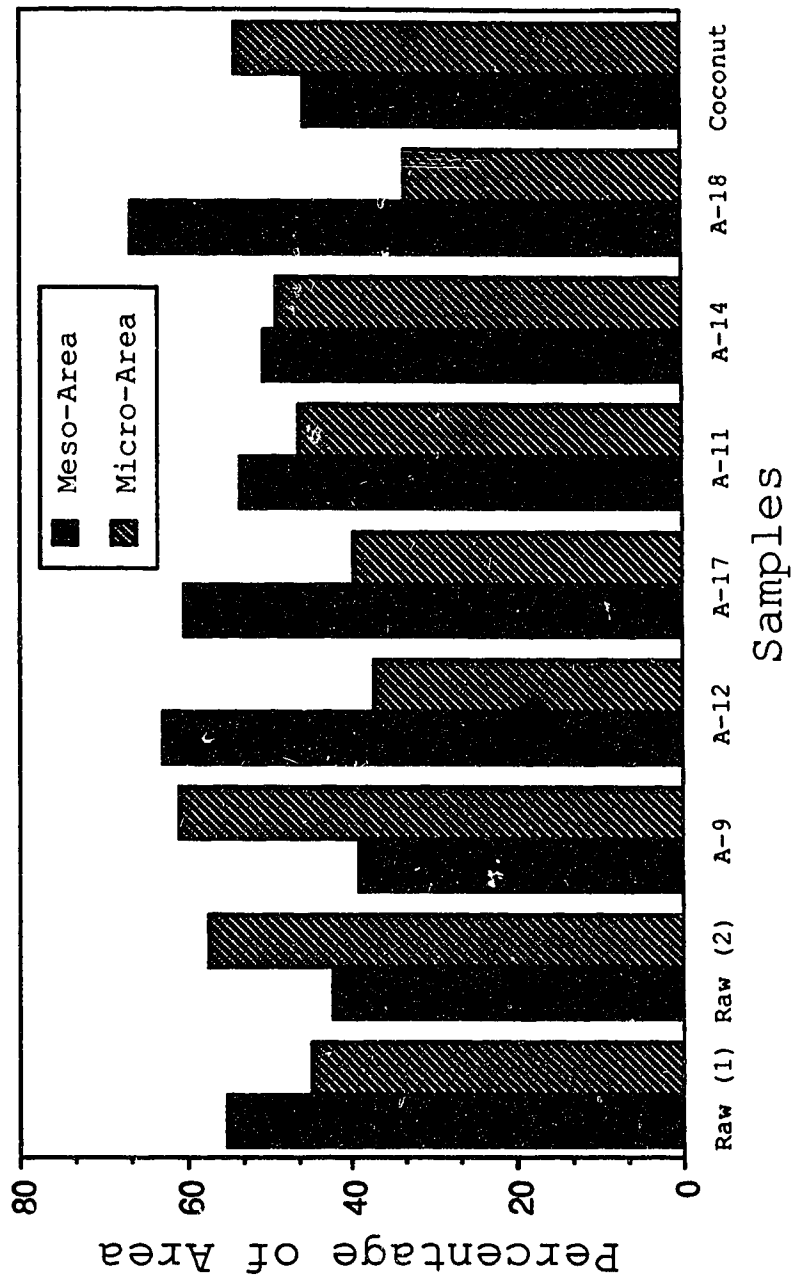


Figure 23. The Specific Pore Volume Distribution Between Micro and Mesopores for Raw Coke, Untreated Activated Coke, Potassium Treated Coke and Fisher Coconut Charcoal.

distribution are illustrated in Figure 23. The three samples, A-9, A-12 and A-17 which correspond to activation times of 2, 4 and 6 hours of activation have specific surface areas of 118.8, 172.3 and 318.6 m² g⁻¹ respectively. The micropore specific surface areas are 91.7, 103.0 and 190.4 m² g⁻¹ and the mesopore specific surface areas are 27.1, 69.3 and 128.2 m² g⁻¹ respectively. This corresponds to a breakdown of 77.2, 59.8 and 59.8% for the micropore areas and 22.8, 40.2 and 40.2% for the mesopore area respectively.

The untreated activated cokes samples A-9, A-12 and A-17 have total specific pore volumes of 0.0079, 0.142 and 0.244 cm³ g⁻¹ respectively. The micropore volumes are 0.048, 0.053 and 0.097 cm³ g⁻¹ and the mesopore volumes are 0.031, 0.089 and 0.147 cm³ g⁻¹ respectively. This corresponds to a breakdown of 60.8, 37.3 and 39.7% for the micropores and 39.2, 62.7 and 60.3% for the mesopores respectively.

The specific surface area and specific pore volume distribution for the three potassium treated (4% KOH) activated coke samples A-11, A-14 and A-18 are listed in Tables 13 and 14, and are illustrated in Figures 22 and 23. The total specific surface areas are 87.5, 167.4 and 176.3 m² g⁻¹ respectively, the micropore surface areas are 61.7, 123.9 and 108.5 m² g⁻¹ respectively and the mesopore areas are 25.8, 43.6 and 67.8 m² g⁻¹ respectively. This corresponds to a breakdown of 70.7, 74.0 and 61.5% for the micropore volumes and 29.5, 26.0 and 38.5% for the mesopores respectively.

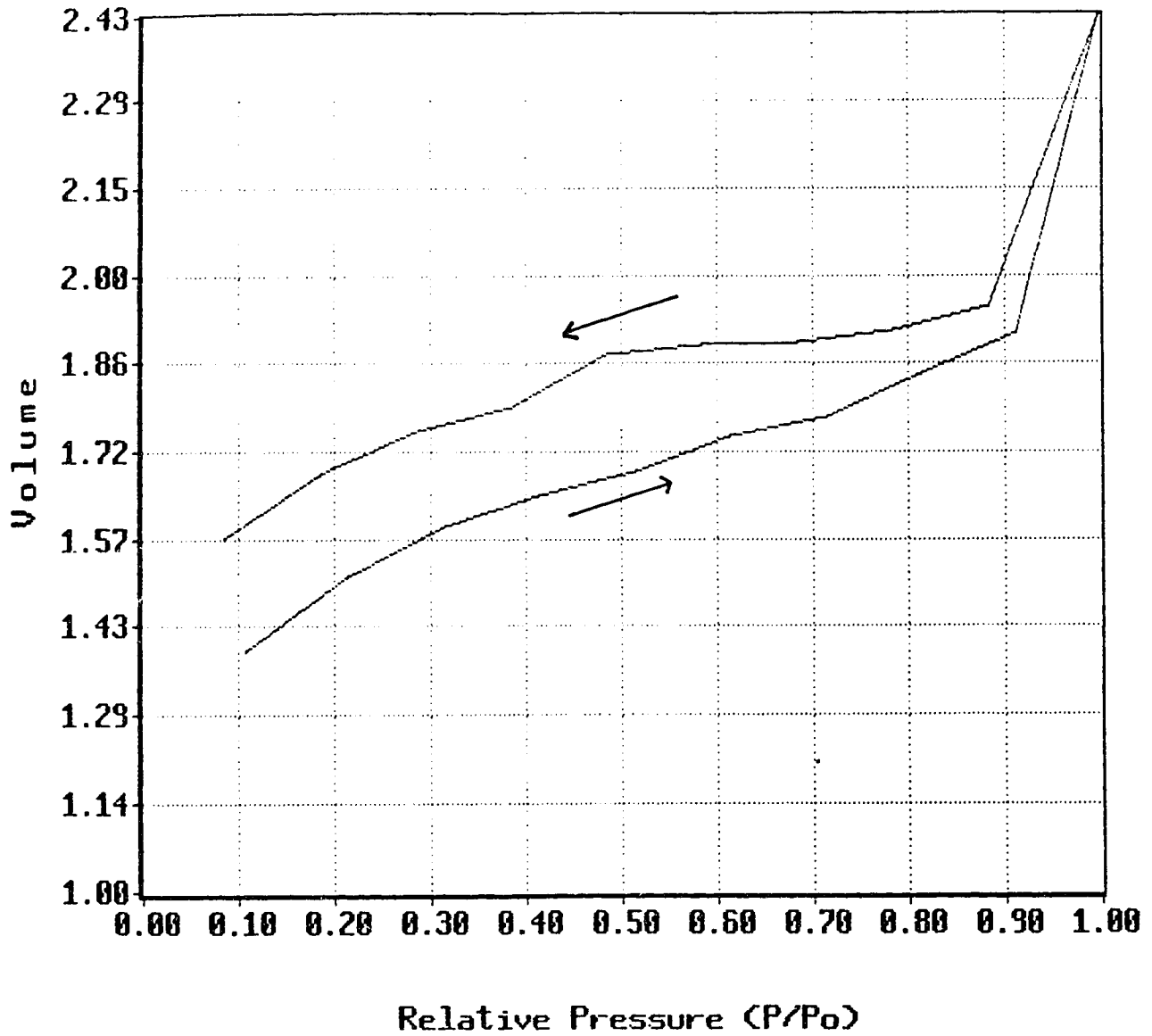
The total specific pore volumes for samples A-11, A-14 and A-18 are 0.069, 0.130 and 0.164 cm³ g⁻¹ respectively. The micropore volumes are 0.031, 0.064 and 0.055 cm³ g⁻¹ and the mesopore volumes are 0.037, 0.066 and 0.109 cm³ g⁻¹ respectively for the three samples. This breaks down into 46.4, 49.2 and 33.5% for the micropore volumes and 53.6, 50.8 and 66.5% for the mesopores respectively.

The total specific surface area for Fisher coconut charcoal is 1237.0 m² g⁻¹ with 850.5 m² g⁻¹ in the micropores while 386.5 m² g⁻¹ in the mesopores. Percentage wise, 68.8% of the total surface exists in the micropores while 31.2% of the total area lies in the mesopores. The total specific pore volume is 0.7678 cm³ g⁻¹ with 0.4164 cm³ g⁻¹ consisting of micropores and 0.3514 cm³ g⁻¹ of mesopores. This breaks down into 54.2% of the total pore volume consisting of micropores and 45.8% consists of mesopores. The specific area and pore distribution data are found in Tables 13 and 14, and illustrated in Figures 22 and 23.

4.1.6.3 Adsorption Isotherms

The nitrogen adsorption and desorption isotherms for the two raw coke samples are illustrated in Figures 24 and 25. The configurations of the adsorption isotherms appear to resemble either a Type IV or Type V isotherm [93]. Type IV and V isotherms correspond to multilayer adsorption where a limited number of adsorption layers occur due to the width of some pores [93].

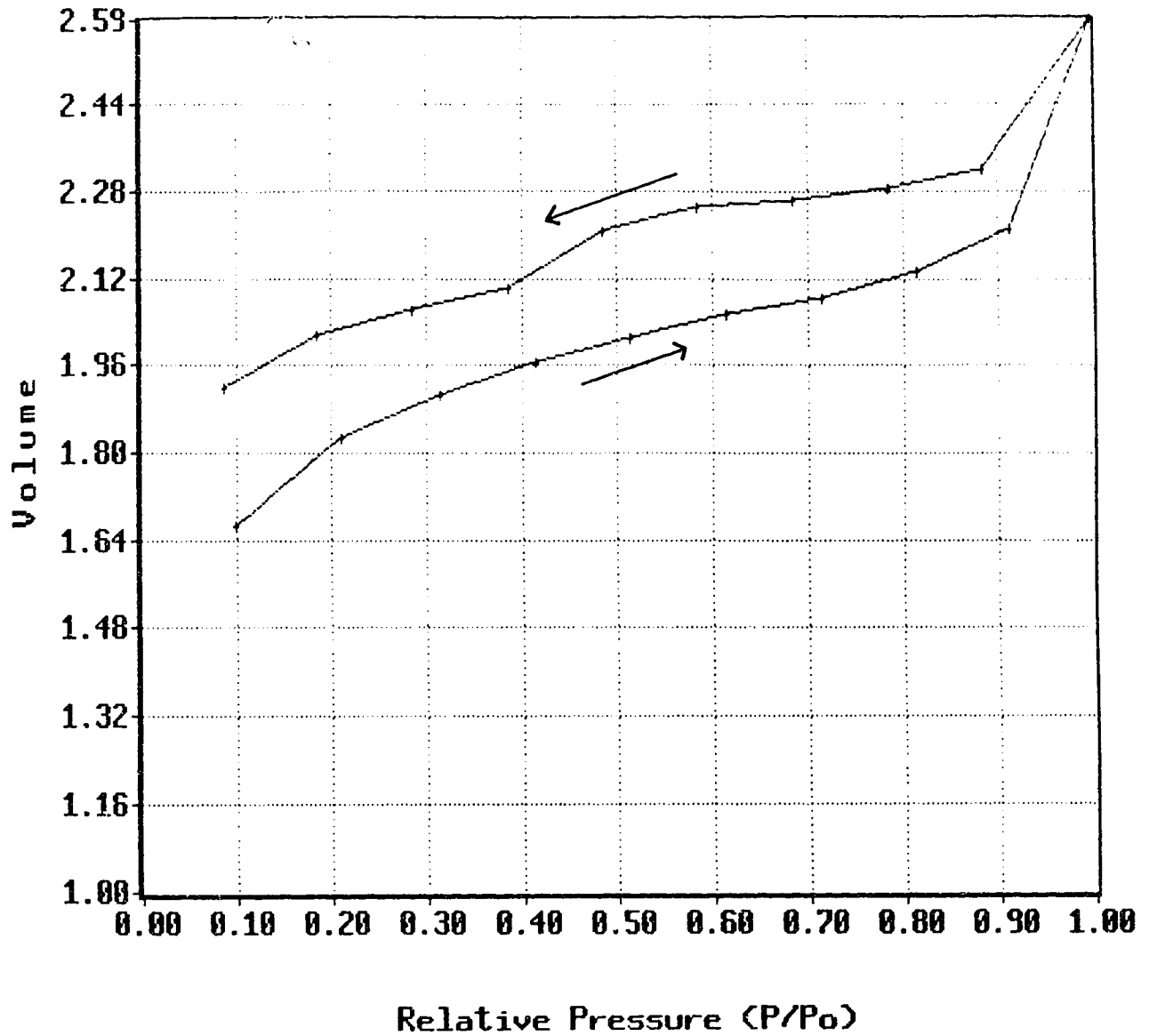
Isotherm



X-AXIS SCALE UNIT.....
Y-AXIS SCALE UNIT..... cc/g x 1E0

Figure 24. Adsorption and Desorption Isotherms for Raw Petroleum Coke (Sample C-1).

Isotherm



X-AXIS SCALE UNIT.....
Y-AXIS SCALE UNIT..... cc/g x 1E0

Figure 25. Adsorption and Desorption Isotherms for Raw Petroleum Coke (Sample C-2).

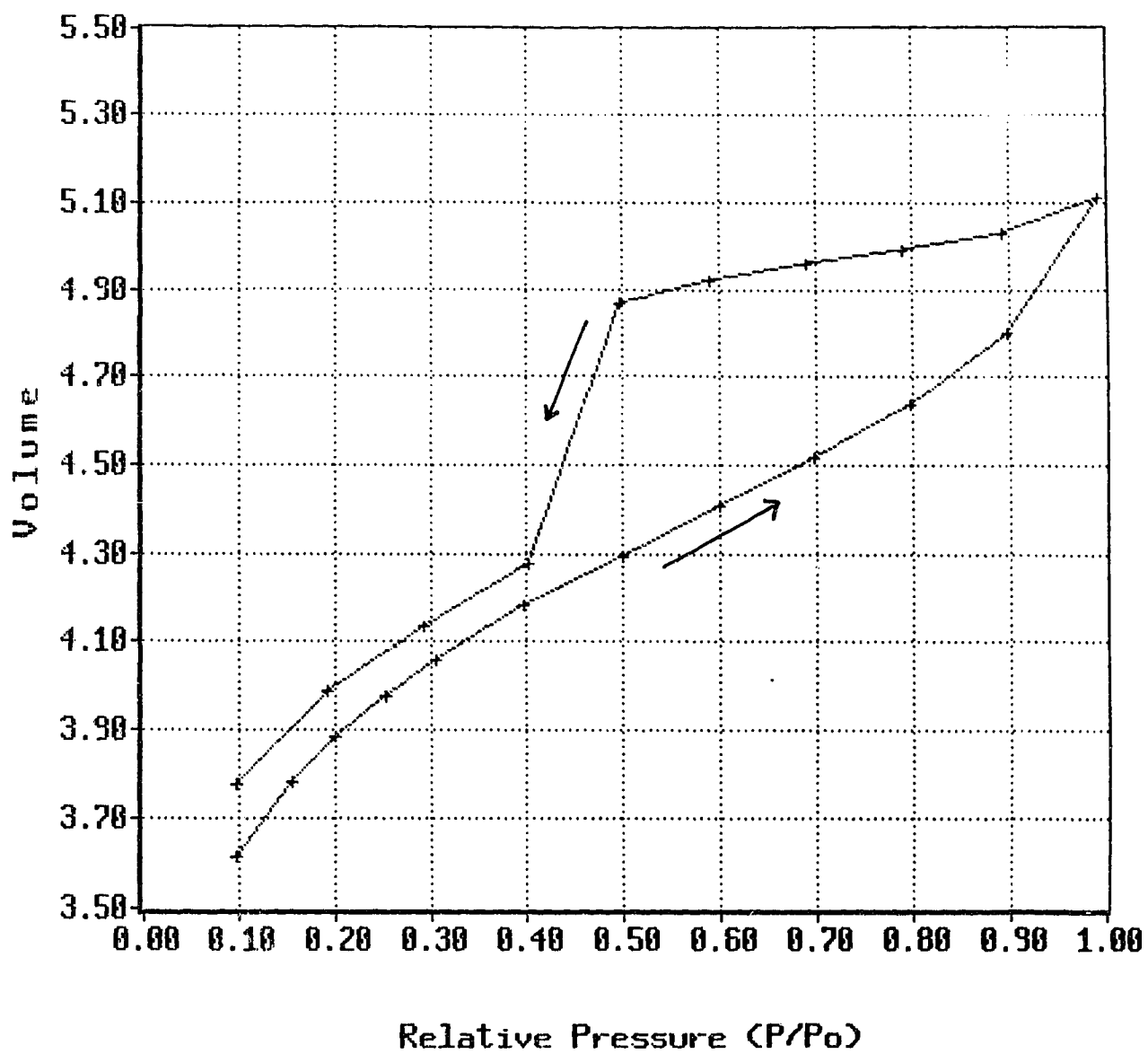
The adsorption and desorption isotherms for untreated activated coke, samples A-9, A-12 and A-17, are illustrated in Figures 26, 27 and 28. These samples correspond to 2, 4 and 6 hours of activation respectively. The shapes of the adsorption curves indicate either a Type IV or V isotherm indicating multilayer adsorption for all the samples.

The desorption curves of the isotherms display a hysteresis loop. According to Gregg *et al*[91], the hysteresis loop is caused by the shape of some pores. 'Ink bottle' pores have a smaller diameter entrance than the interior of the pores. Nitrogen condenses normally but can only evaporate when the pressure drops past a certain point because of the surface tension of the meniscus. Pores with wide entrances and smaller interiors, also known as V - shaped pores, fill and empty reversibly.

The adsorption and desorption isotherms for samples A-11, A-14 and A-18, potassium treated activated coke, are illustrated in Figures 29, 30 and 31. These samples correspond to 2, 4 and 6 hours of activation respectively. The adsorption isotherms either indicate Type IV or V adsorption, limited multilayer adsorption for the potassium coke samples.

The adsorption and desorption isotherms for Fisher Coconut charcoal is illustrated in Figure 32. The shape of the adsorption isotherm corresponds to a Type IV, limited multilayer adsorption isotherm. Area-volume-pore size summaries and isotherm data for each sample tested using the Quantachrome Autosorb are located in Appendix A.

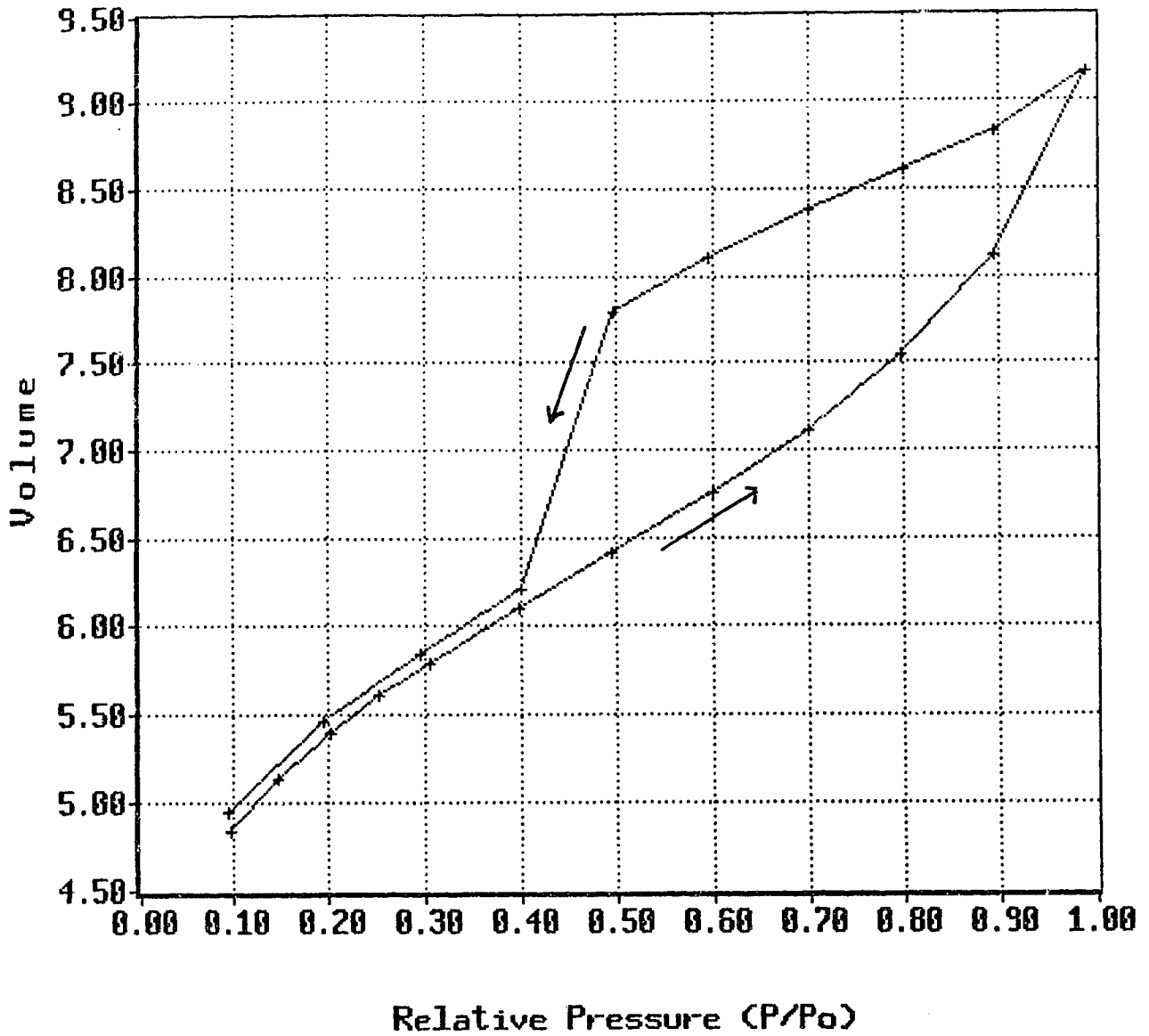
Isotherm



X-AXIS SCALE UNIT.....
Y-AXIS SCALE UNIT..... cc/g x 1E1

**Figure 26. Adsorption and Desorption Isotherms for
Untreated Activated Coke, (Sample A-9).**

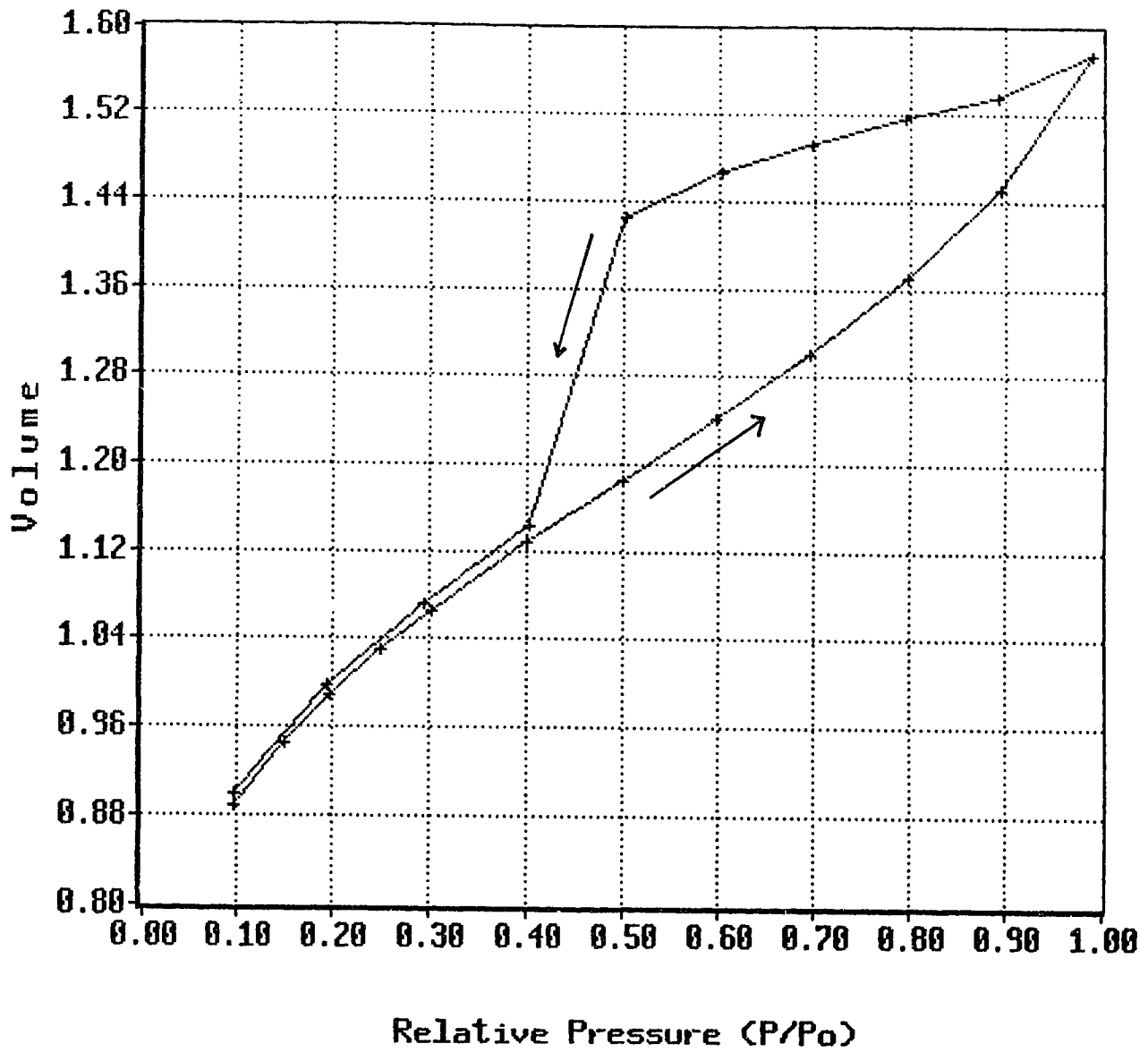
Isotherm



X-AXIS SCALE UNIT.....
Y-AXIS SCALE UNIT..... cc/g x 1E1

**Figure 27. Adsorption and Desorption Isotherms for
Untreated Activated Coke, (Sample A-12).**

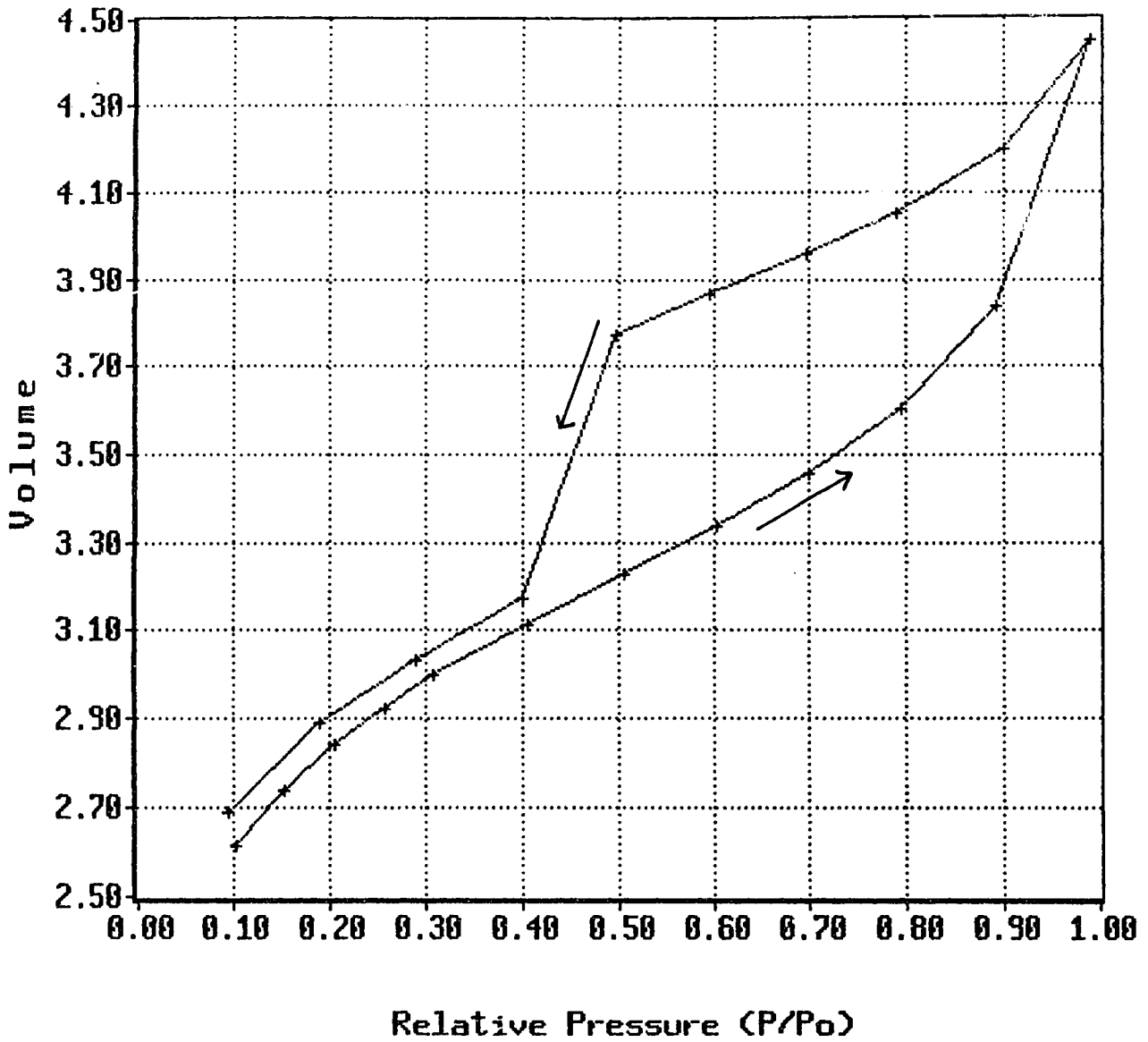
Isotherm



X-AXIS SCALE UNIT.....
Y-AXIS SCALE UNIT..... cc/g x 1E2

**Figure 28. Adsorption and Desorption Isotherms for
Untreated Activated Coke, (Sample A-17).**

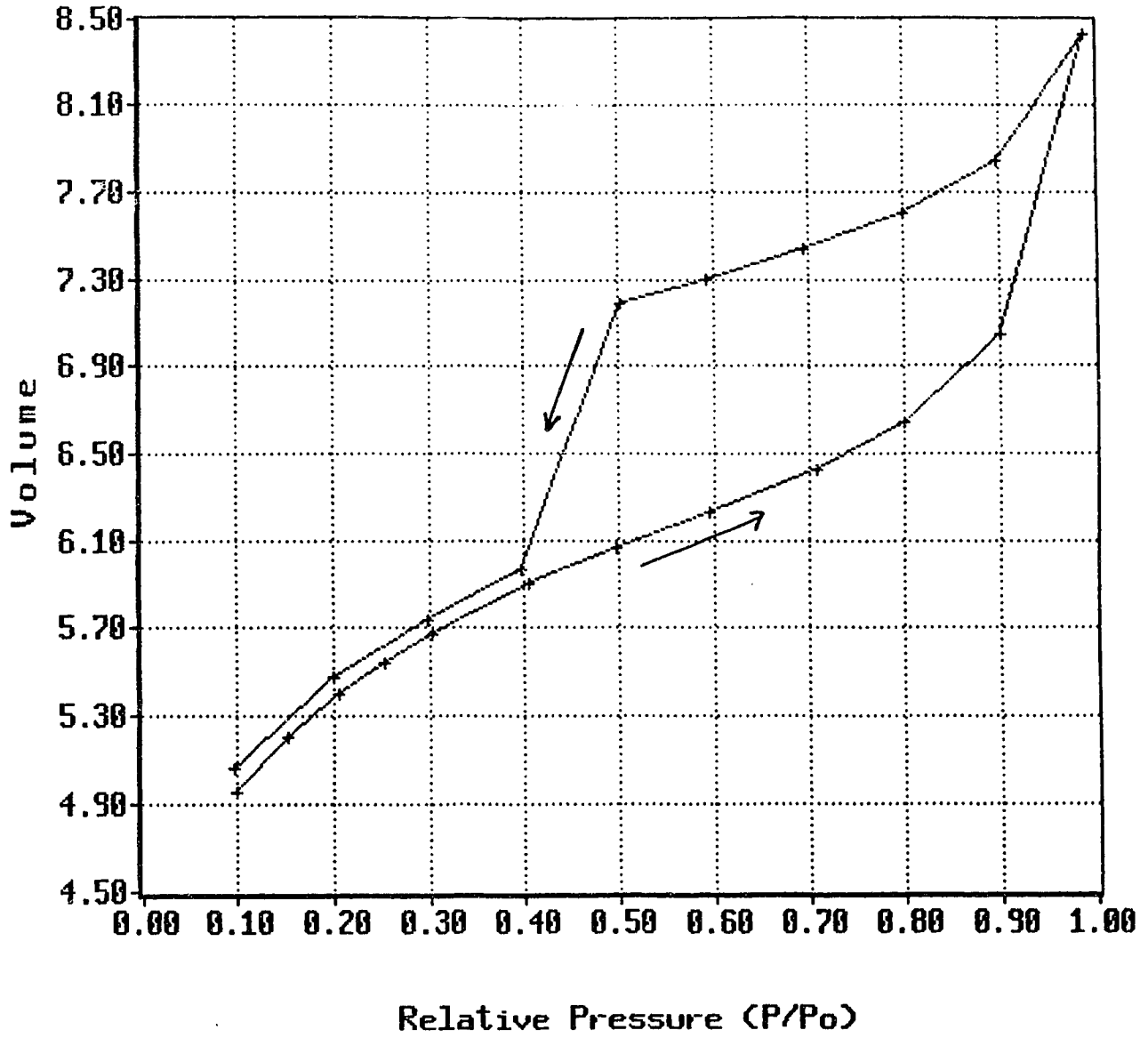
Isotherm



X-AXIS SCALE UNIT.....
Y-AXIS SCALE UNIT..... cc/g x 1E1

Figure 29. Adsorption and Desorption Isotherms for
Potassium Treated (4% KOH) Coke,
(Sample A-11)

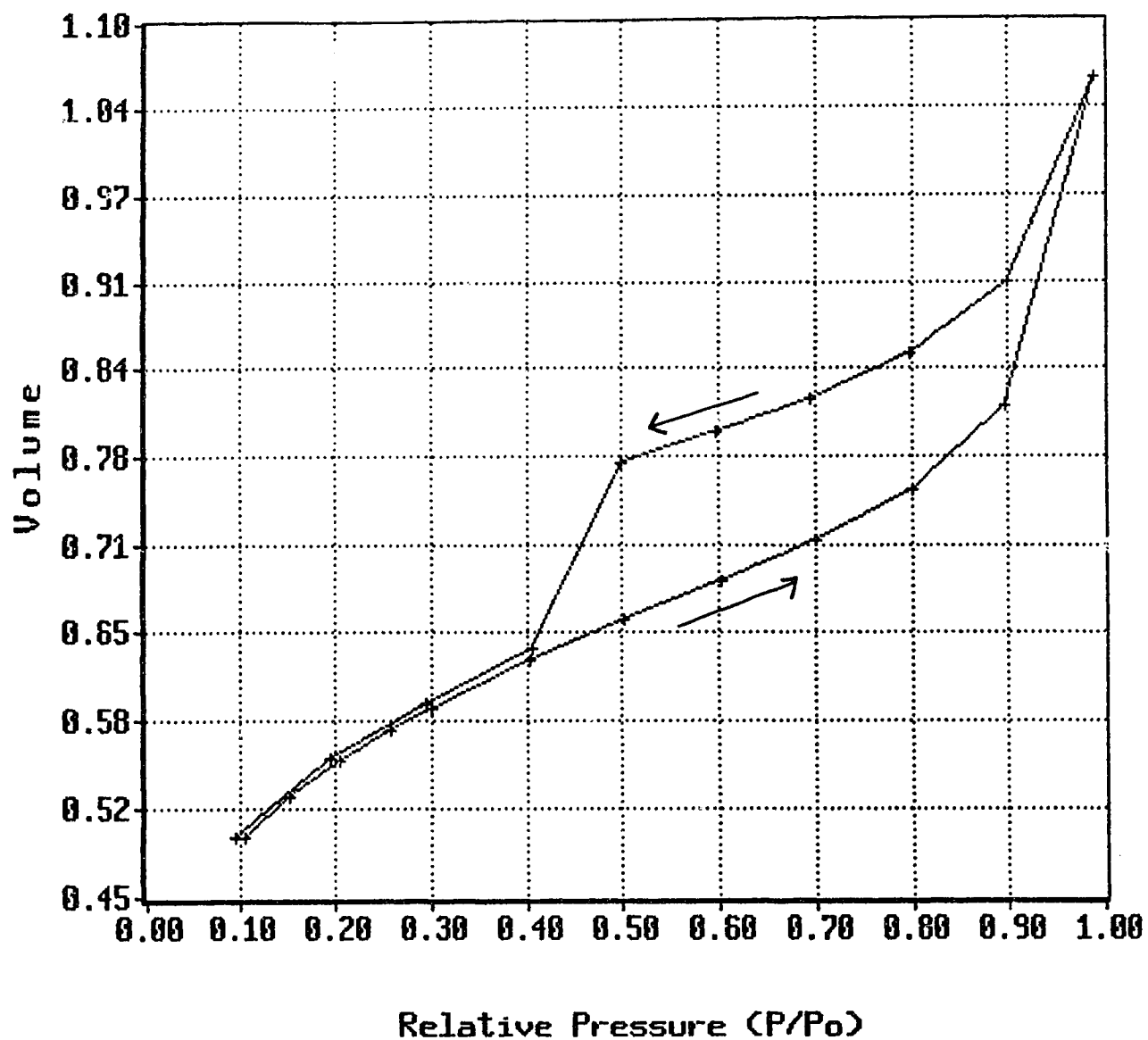
Isotherm



X-AXIS SCALE UNIT.....
Y-AXIS SCALE UNIT..... cc/g x 1E1

Figure 30. Adsorption and Desorption Isotherms for
Potassium Treated (4% KOH) Coke,
(Sample A-14).

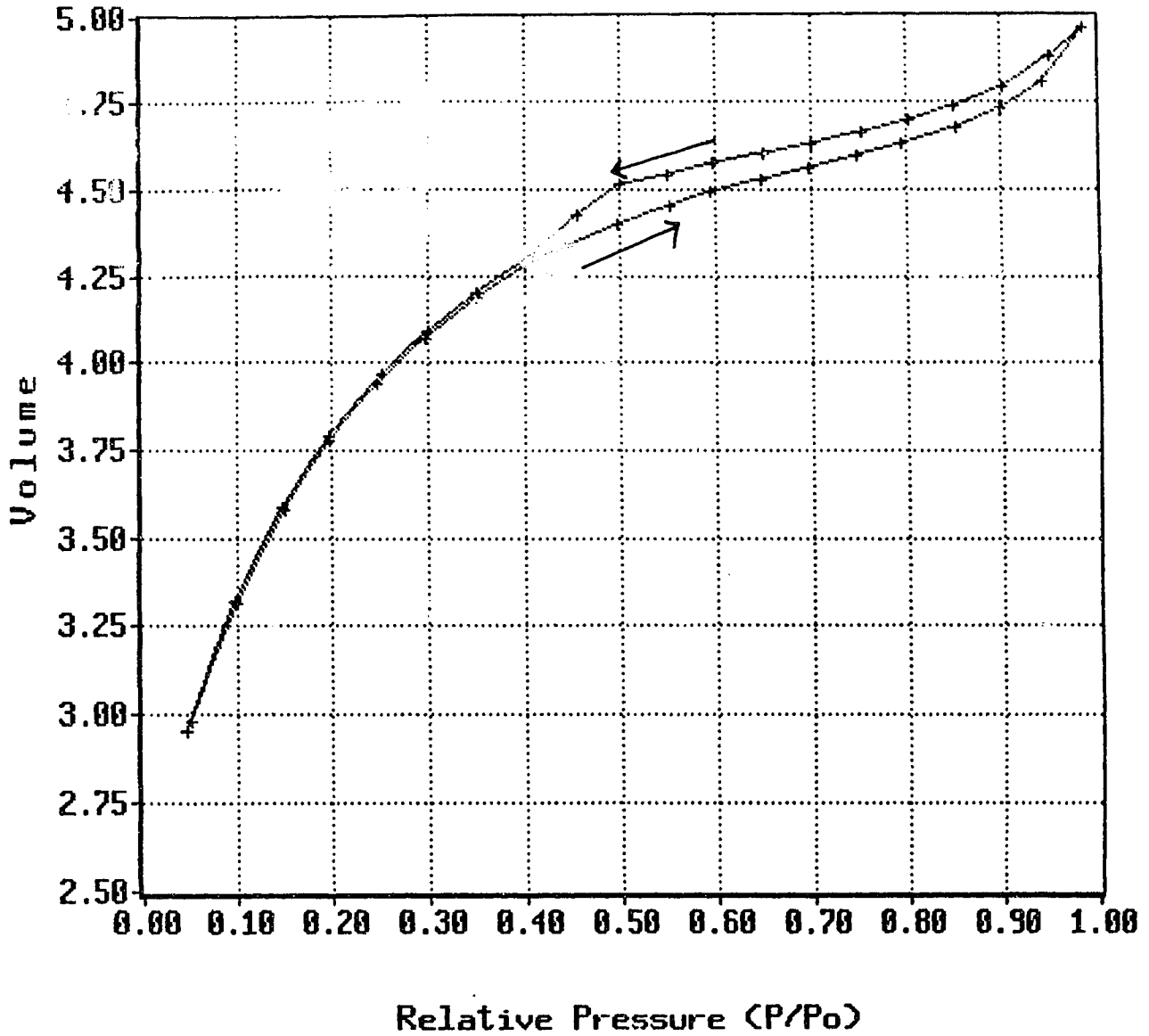
Isotherm



X-AXIS SCALE UNIT.....
Y-AXIS SCALE UNIT..... cc/g x 1E2

Figure 31. Adsorption and Desorption Isotherms for
Potassium Treated (4% KOH) Coke,
(Sample A-18).

Isotherm



X-AXIS SCALE UNIT.....
Y-AXIS SCALE UNIT..... cc/g x 1E2

Figure 32. Adsorption and Desorption Isotherms for Fisher Coconut Charcoal.

4.1.7 pH and Zeta Potential

4.1.7.1 pH

The pH's of raw coke, untreated activated coke, potassium treated activated coke and Fisher coconut charcoal were determined and compared. The untreated activated coke sample tested was B-1, which was activated for 6 hours, and corresponds to the maximum surface area obtained. The potassium coke sample tested was B-8, which was activated for 4 hours and nearly corresponds to the maximum surface area for potassium coke. This sample was washed to recover any potassium salts before testing. The pH's are tabulated as follows:

Sample	pH
Raw Coke	7.71
B-1 (Untreated)	8.33
B-8 (4% KOH)	6.16
Coconut Charcoal	9.13

The raw coke, untreated coke and coconut charcoal can be classified as H₁ carbons [29], carbons which 'adsorb' acids. The surface of this type of carbon contains basic functional groups which impart a positive surface potential. The high activation temperature (850 °C) 'fixed' oxygen and hydrogen to the carbon surface in the form of basic functional groups [29].

The potassium coke can be classified as a **L** carbon [29], which contains acidic functional groups causing a negative surface potential and primarily adsorbs basic ions. This sample was activated under the same activation conditions as the untreated coke sample B-1. According to Mattson *et al* [29], carbons activated below 600 °C are expected to form **H** carbons. The presence of the potassium hydroxide may have affected the formation of surface functional groups but more likely the washing altered the surface functional groups. Washing may have altered the surface chemistry by aiding oxygen adsorption which formed acidic functional groups. This in turn increased the **L** carbon characteristics (acidic, negative zeta potential, hydrophilic) of the carbon.

4.1.7.2 Zeta Potential

The relative Zeta Potentials of untreated activated coke, potassium treated activated coke and Fisher coconut charcoal were determined and compared. The untreated coke consisted of the sample from activation B-4 (6 h activation) which corresponds to the maximum surface area formed. The potassium treated coke sample was from activation B-7 (4 h activation), which nearly corresponds to the maximum surface area formed. Sample B-7 was washed to remove any soluble potassium salts. The Zeta Potentials are tabulated in Tables 15, 16, and 17 and illustrated in Figures 33, 34, and 35.

TABLE 15

Zeta Potential of Untreated Activated
Coke (Sample B-4) as a Function of pH.

pH	Relative Zeta Potential
1.47	-9.4
1.53	-18.5
2.04	3.4
2.50	2.7
2.52	1.6
2.99	1.2
3.00	0.8
3.26	0.9
3.59	0.9
3.92	-0.1
4.34	-1.1
4.86	-1.9
5.44	-2.3
6.50	-2.3
7.35	-2.0
8.12	-3.7
8.40	-27.0

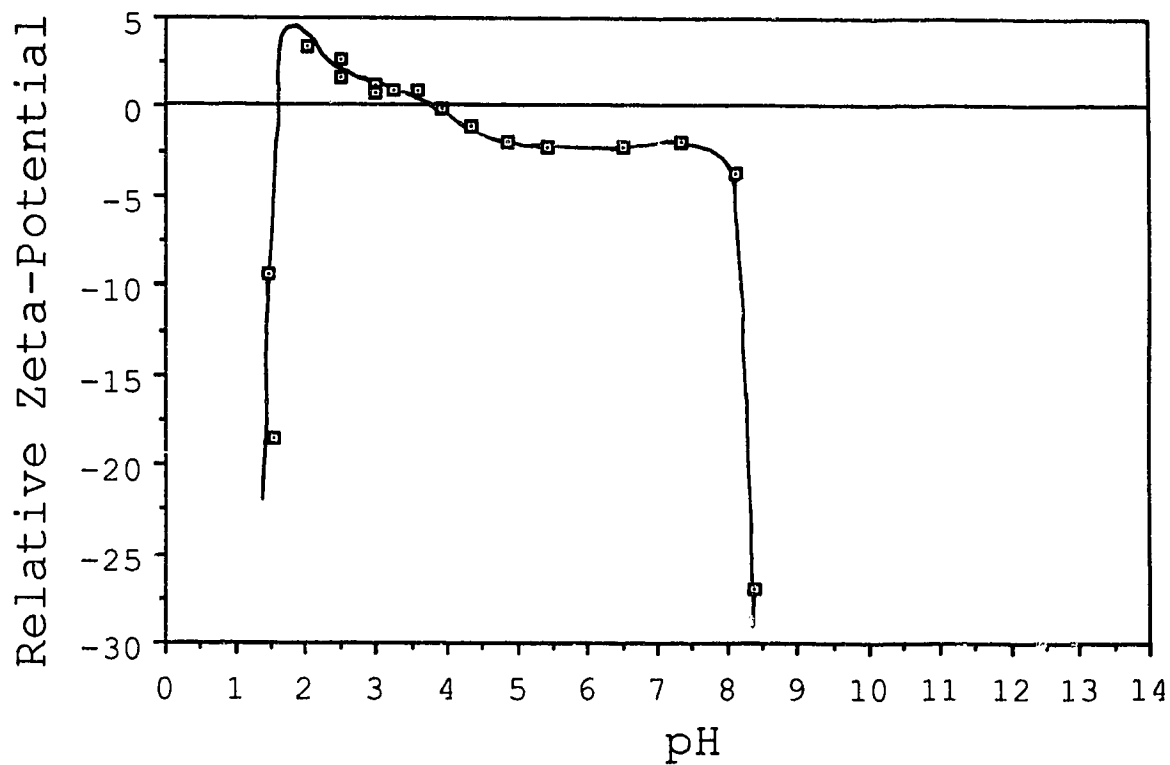


Figure 33. The Relative Zeta Potential of
Untreated Activated Coke (Sample B-4)
as a Function of pH.

TABLE 16

Zeta Potential of Potassium Activated
Coke (Sample B-7) as a Function of pH.

pH	Relative Zeta Potential
1.68	-7.00
2.04	4.06
2.52	1.55
2.91	1.36
3.12	1.21
3.73	-0.50
4.09	0.63
4.31	0.75
4.94	-0.79
5.44	-1.09
5.93	-2.31
6.51	-2.14
7.50	-2.90
8.84	-3.59

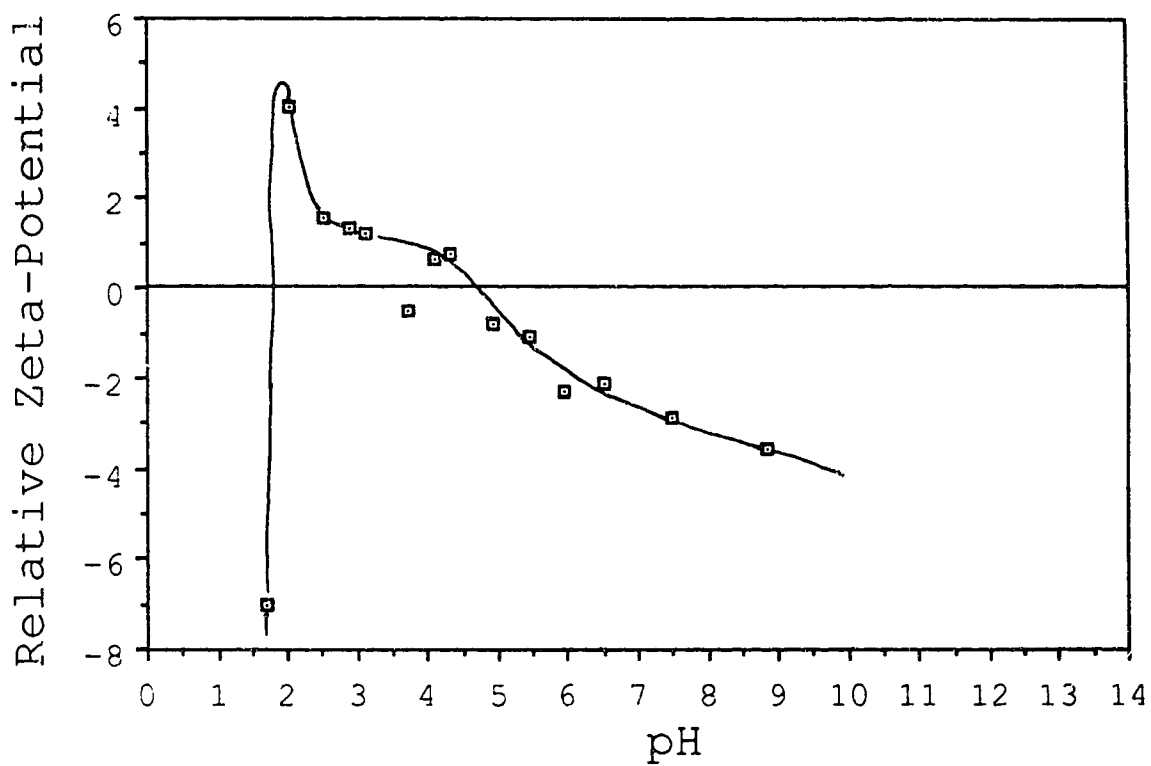


Figure 34. The Relative Zeta Potential of Potassium
Treated (4% KOH) Activated Coke
(Sample B-7) as a Function of pH.

TABLE 17

Zeta Potential of Fisher Coconut
Charcoal as a Function of pH.

pH	Relative Zeta Potential
1.58	0.37
2.10	0.15
2.65	0.92
3.29	0.85
3.85	-1.05
4.23	-1.74
4.77	-3.42
5.21	-2.23
5.88	-3.80
6.24	-4.70
6.75	-3.42
7.40	-4.01
8.80	-3.40
9.59	-3.55
10.13	-3.65
11.42	-3.15

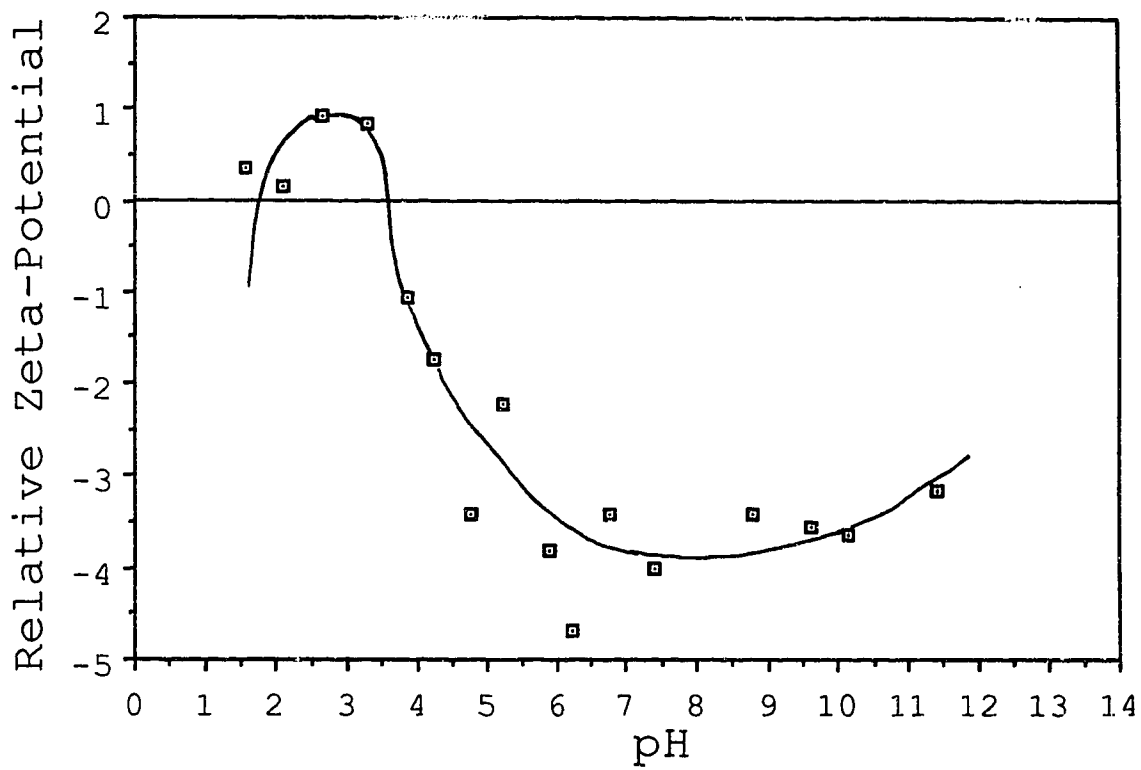
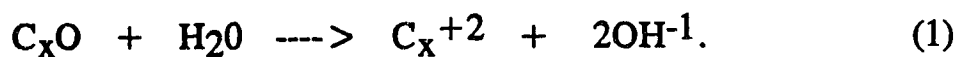


Figure 35. The Relative Zeta Potential of Fisher
Coconut Charcoal as a Function of pH.

The relative zeta potential of untreated activated coke versus pH as shown in Figure 33 indicates that the activated coke displays the Frumkin Phenomena [29]. This theory states that the activated coke acts as a gas (oxygen) electrode when adsorbing an electrolyte. The surface of the coke is covered with oxygen complexes or functional groups, either as a result of the activation procedure or atmospheric oxygen aging. Activated carbon is theorized to be active enough to oxidize water molecules. If the surface functional groups are designated as C_xO or C_xO_2 , activated carbon reacts with water by the following reaction:

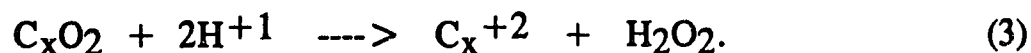
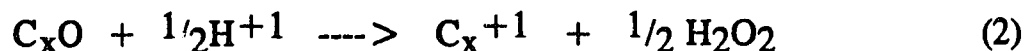


The surface of the coke develops a net positive charge and hydroxyl ions (OH^{-1}) diffuse into the bulk solution increasing the pH. The positively charged coke then non-specifically adsorbs anions as well as hydroxyl ions into the diffuse double layer surrounding the coke particle [29].

The zeta potential of the coke from a pH of 4.9 to 7.4 is relatively constant at -2.0 due to the action of the electrical double layer. Although the net charge on the particle is positive, as predicted by equation (1), the coke particle adsorbs a specific amount of anions thus keeping the zeta-potential relatively constant. At a pH of 8.4, the zeta potential increases dramatically to -27.0. The high zeta potential can be explained by the specific adsorption of the hydroxyl ions into and through the diffuse

layer into the pores of the activated coke particle. The high internal surface area of the coke particle enables enough anions to be adsorbed so that the net electrical charge of the coke particle is negative even though according to equation (1), the surface charge is positive.

As the pH of the bulk solution is decreased, hydroxyl ions are removed from the diffuse layer by hydrogen ions (H^{+1}). As hydrogen ions are added, the zeta potential decreases to 0.0, the iso-electric point. The iso-electric point for untreated activated coke occurs at a pH of 4.0. As the pH is lowered further, the addition of hydrogen ions brings on the Frumkin phenomenon [29], which describes how a particle obtains a positive zeta-potential. Hydrogen ions start combining with the oxygen complexes on the coke surface to form positively charged sites and produces hydrogen peroxide (H_2O_2) as a by-product according to the equations:



The zeta potential start increasing quickly to a maximum of 3.4 at about a pH of 2.0. As the pH is decreased below 2.0, the charge on the coke particle reverses quickly. When the pH decreases below 2.0 or a H^{+1} concentration of 10^{-2} N, the activated coke starts the specific

adsorption of Cl^{-1} ions. As these chlorine ions fill the pores, the negative charge increases quickly.

The zeta potential versus pH for activated potassium treated coke is illustrated in Figure 34. As the pH increases from 4.5 to 8.84, the zeta potential increases in a roughly linear manner. Unlike the untreated coke, there is no dramatic decrease in zeta potential at high pH. This indicates that the hydroxyl ions are being non-specifically adsorbed onto the electric double layer and not through the double layer into the pores. The zeta potential is thus a function of hydroxyl concentration.

The iso-electric point for potassium treated activated coke occurs at a pH of 4.5, compared to 4.0 for untreated coke. This would indicate that there are less surface oxygen complexes. The coke particles achieved the iso-electric point at a lower hydrogen ion concentration, and according to equation (2) and (3), this would indicate that there are more surface functional groups. At lower pH's past the iso-electric point, the zeta potential increases positively in a similar manner as the untreated coke and reaches a maximum positive zeta potential of about 4.0 at a pH of about 2.0. At a HCl concentration of 10^{-2} N, the zeta potential reverses and decreases quickly.

The zeta potential versus pH for Fisher coconut charcoal differs from the untreated and potassium treated activated cokes. The iso-electric

point occurs at a pH of 3.6, indicating more surface functional groups are present. At pH's greater than 3.6, the zeta potential reaches a minimum of 4.70 at a pH of 6.24 and then the zeta potential starts to increase slightly to 3.15 at a pH of 11.42. Below a pH of 3.6, the zeta potential increases to a maximum of 0.92 before reversing at a HCL concentration of 10^{-3} N. The coconut charcoal does not show any affinity for adsorbing Cl^{-1} ions at a low pH. The relatively high negative zeta potential at high pH's compared to the very low positive zeta potential at low pH's suggests that the coconut charcoal develops a very stable double electrical layer which does not allow the transmission of hydroxyl ions. At low pH's its surface functional groups are very efficient in neutralizing hydrochloric acid.

4.1.8 Aqueous Adsorption

The adsorption capacities were determined for raw coke, untreated activated coke, activated potassium coke and Fisher coconut charcoal, with respect to methylene blue and iodine. All adsorption data is summarized in Table 18.

The maximum adsorptive capacity of raw coke for methylene blue dye is 8.2 mg g^{-1} , and 28 mg g^{-1} for iodine.

The untreated activated coke used for the adsorptive tests with methylene blue dye and iodine was sample B-4. Sample B-4 was activated for 6 hours and has a burnoff of 67.5%, corresponding to a specific surface area of over $300 \text{ m}^2 \text{ g}^{-1}$.

The methylene blue adsorption ranges from 80 to 100 mg g^{-1} . A uncrushed sample was also tested to determine if the uncrushed sample has the same adsorptive capacity as the crushed activated coke. The uncrushed sample used was B-1, which was activated for 6 hours and has a burnoff of 68.5%. The adsorptive capacity for methylene blue was 75 mg g^{-1} thus suggesting only minor differences between the crushed and uncrushed samples. The adsorptive capacity of the crushed coke for iodine was 200 mg g^{-1} .

TABLE 18

Summary of Aqueous Adsorption
of Methylene Blue and Iodine.

Adsorption (mg g⁻¹)

	Raw Coke	Untreated Coke	Potassium Coke	Coconut Charcoal
Methylene Blue Dye	8.2	80 - 100	55	420
		(75) *		
Iodine	28.0	200	235 - 300	1100

* Uncrushed Sample

The potassium treated activated coke sample used for both methylene blue dye and iodine adsorption was sample B-7. Sample B-7 was activated for 4 hours with a burnoff of 53.7%, corresponding to a specific surface area of $167 \text{ m}^2 \text{ g}^{-1}$. The adsorptive capacity for methylene blue dye is 55 mg g^{-1} and ranges from 235 to 300 mg g^{-1} for iodine adsorption.

The adsorptive capacity of Fisher coconut charcoal for methylene blue dye is 420 mg g^{-1} and 1100 mg g^{-1} for iodine.

Coconut charcoal is one of the best activated carbons commercially available for liquid adsorption [154]. The adsorptive capacities of raw coke, untreated activated coke and potassium coke are compared below to the adsorptive properties of Fisher Coconut charcoal.

	Raw Coke	Untreated Activated Coke	Activated Potassium Coke
Methylene Blue Dye	2.0%	19.0 - 23.8%	13.1%
Iodine	2.5%	18.2%	21.4-27.3%

4.1.9 Gas Analysis

The exhaust gases from the steam activation of untreated coke were analyzed for composition with respect to nitrogen (N₂), carbon dioxide (CO₂), carbon monoxide (CO), methane (CH₄) and hydrogen sulphide (H₂S). The gases were sampled directly at the exit port of the reactor just before the water trap. The gas composition of the exhaust stream was determined on a dry gas volume basis. The gas composition of various activation times is given in Table 19 and illustrated in Figure 36.

The percentage of CH₄ increases slowly with activation time, with 1.6% at 0.5 hours and increasing to 3.2% at 4 to 5 hours of activation.

The H₂S content varies slightly with increasing activation time. At 0.5 hours, the H₂S content is 2.6%, then drops to 1.0% at 2.0 hours, then rises slowly to 3.5% at 5 hours of activation.

Carbon monoxide content increases with activation time while CO₂ declines with activation time. The CO content goes from 23.1% at 0.5 hours, to 54.4% at 5.0 hours, while CO₂ drops from 62.6% to 38.6% in the same time period. The change in CO/CO₂ ratio with time could be related to the increase in surface area with activation time. As more surface area is developed, more locations can open up on the coke where CO synthesis can occur in preference to CO₂.

TABLE 19

Gas Composition from the
Steam Activation of Untreated
Coke at 850°C.

Activation Run	Activation Time (h)	% Gas Composition				
		CO ₂	CO	CH ₄	H ₂ S	N ₂
A-6	0.5	62.6	23.1	1.6	2.6	10.1
A-7	2.0	43.6	51.8	1.8	1.0	1.8
	3.0	57.7	35.3	2.2	2.2	2.6
A-8	3.0	49.2	40.4	2.9	4.9	2.6
	4.0	45.4	47.7	3.2	3.3	0.4
	5.0	38.6	54.4	3.2	3.5	0.3

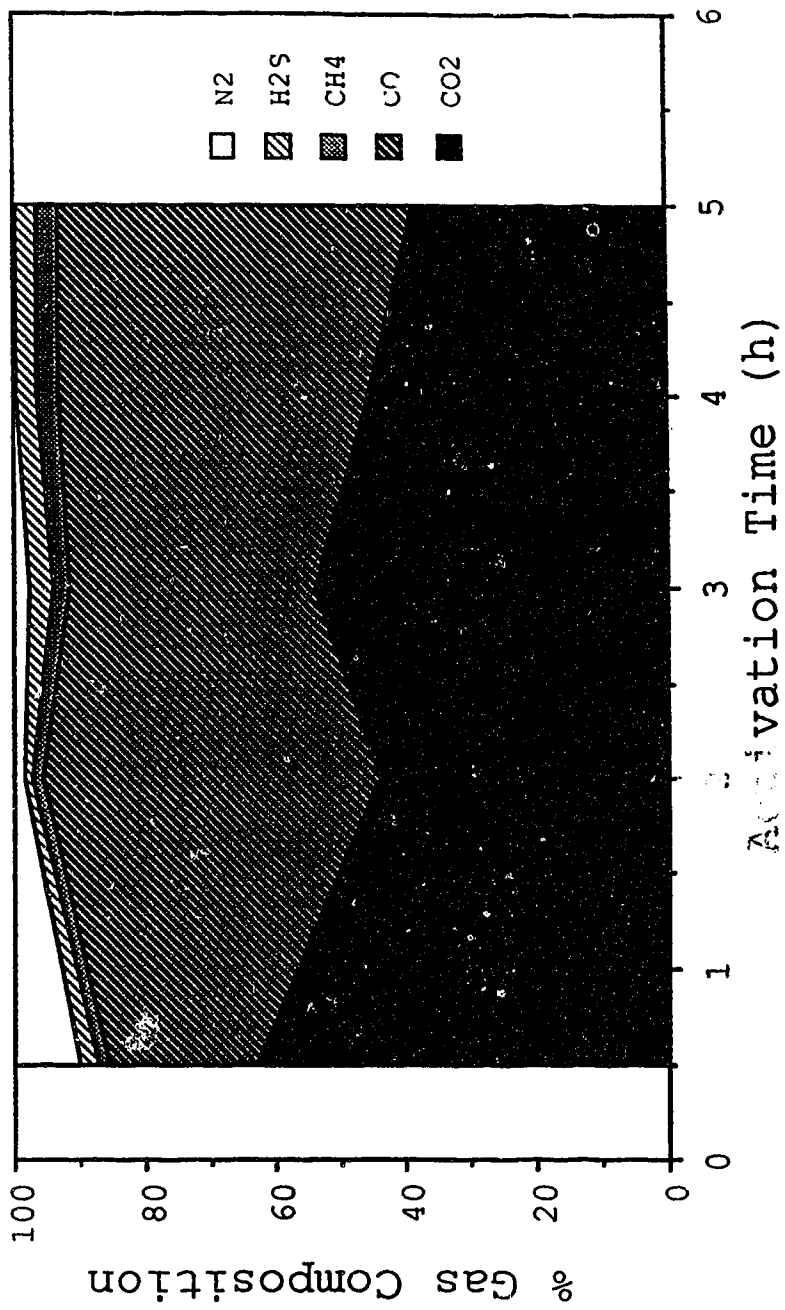


Figure 36. The Gas Composition from the Steam Activation of Untreated Coke at 850 C.

These gases, CO, CH₄ and H₂S can be used for fuel gas [77], thus the increase of CO with respect to CO₂ synthesis is beneficial. The percentage of usable gas goes from 27.3% to 61.1%.

The nitrogen flow was kept constant in the activations runs at 3000 cm³ hr⁻¹. Assuming no nitrogen reactions occurred at 850°C and the nitrogen released from the coke matrix was negligible, the actual volumes of the gases produced can be calculated. Converting the percentages to actual volumes, at 0.5 hours, 120 cm³ min⁻¹ (STP) of CO, CH₄ and H₂S were produced. At 5.0 hours, 1,320 cm³ min⁻¹ (STP) of the same gases were produced, an increase of 11 times. This is closely related to the surface area produced. From Figure 20, the specific surface area at 0.5 hours of activation is approximately 25 m² g⁻¹ and at 5.0 hours it is approximately 245 m² g⁻¹, an increase of 10 times. If a direct correlation between specific surface area and volume of gas produced is assumed, then approximately 5 cm³ of fuel gas is produced per minute for every m² of exposed coke surface area.

4.1.10 Scanning Electron Microscopy

The SEM micrographs were taken of raw, activated untreated and activated potassium treated coke. The activated untreated coke samples consisted of samples B-13, A-9, A-12, and A-17, which correspond to activation times of 0 (pyrolysis only), 2, 4, and 6 hours respectively. Similarly, the activated potassium coke samples consisted of samples A-11, A-14, and A-18, also with activation times of 2, 4, and 6 hours respectively. Magnifications of 200, 1000, and 5000 times were used for the micrographs. Typical coke particles were chosen for the micrographs but some atypical coke particles were photographed to illustrate some property not displayed by normal coke particles. Raw coke and sample B-13 particles were crushed with a mortar and pestle to obtain views of the interior structure.

4.1.10.1 Raw Fluid Coke

Plates 1 and 2 show a typical coke particle at a magnification of 200 and 1000 times. The coke particle is roughly spherical with a mottled, bumpy surface texture. No surface cracks were observed. At 200 times magnification, the surface bumps appear to be rounded and smooth. At 1000 times magnification, the bumps appear irregularly shaped with some sharp edges. Small vesicles and flakes about the size of 1 micron cover the surface of the particle. At 1000 magnification, the surface appears much rougher than at 200 magnification; scale-invariance [83],

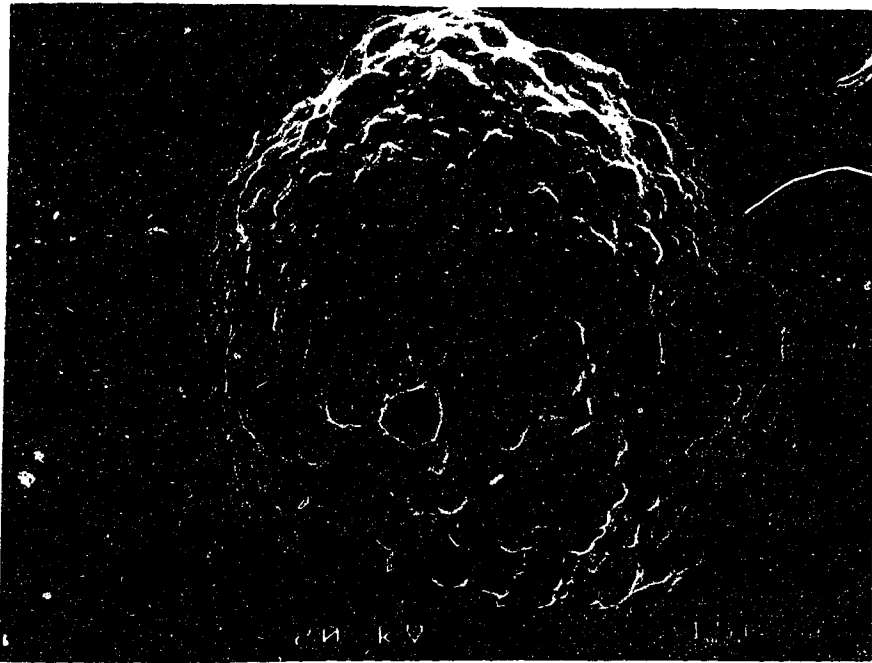


PLATE 1 SEM Micrograph of Raw Fluid Petroleum Coke, (x200).

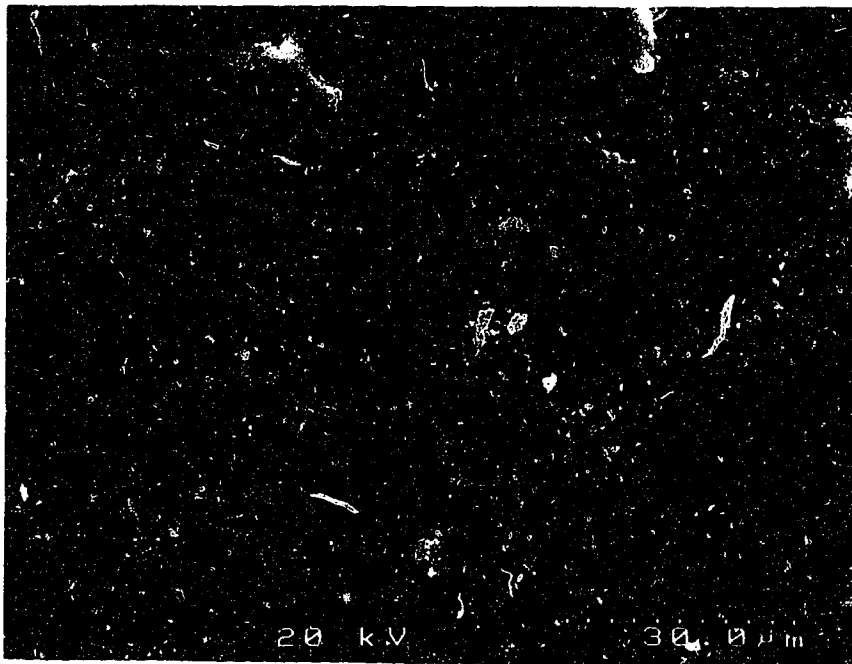


PLATE 2 SEM Micrograph of Raw Fluid Petroleum Coke, (x1000).

as determined visually, does not seem to apply to raw fluid coke despite earlier studies [83,84].

Plates 3 and 4 shows the interior of a raw coke particle at magnifications of 200 and 1000 times. The particle was split open in a mortar using compressive force. In Plate 3, the concentric layers of the coke structure are evident by fractures propagating along the interfaces. The fracturing is most likely caused by the splitting open of the particle and not present in a normal particles. The micrographs indicates that there may be from 4 to 5 distinct layers of coke. The central core of the particle was not split open but the other layers appear uniform in thickness and it can be assumed that the layers in the core are the same width. Plate 4 shows more detail of the interior structure. The fracture surface indicates an internal structure composed of concentric layers with the interfaces being difficult to pick out. Except for the cracking, no internal porosity was evident and the carbon appears uniform in composition or structure.

4.1.10.2 Activated Coke

Zero Hours Activation

Plates 5 and 6 show interior views of a coke particle that has undergone pyrolysis but no activation. The particle was fractured in a mortar in the same manner as the raw coke. Plate 5 shows a particle in the center of the



PLATE 3 SEM Micrograph of a Cross Section of Raw Fluid Petroleum Coke, (x200).

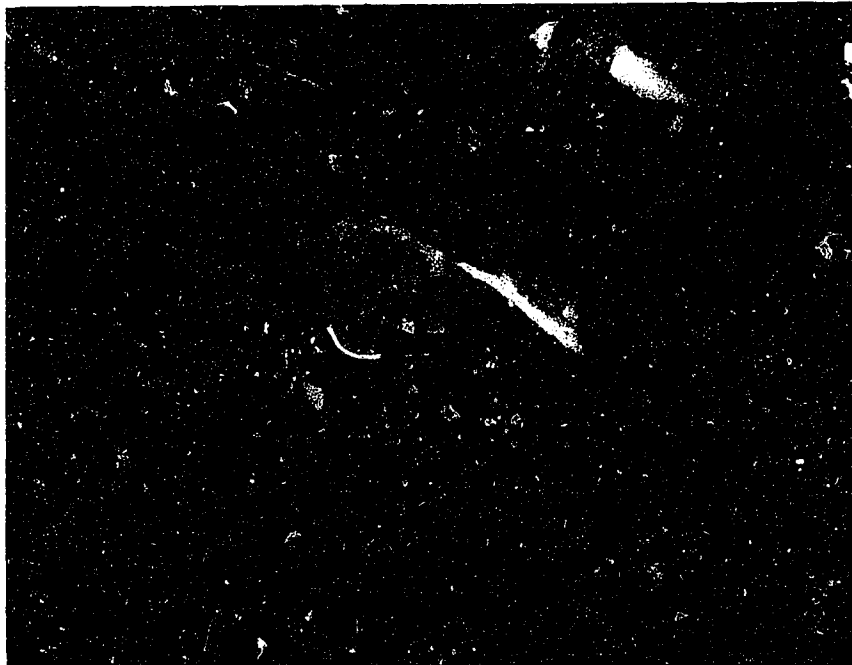


PLATE 4 SEM Micrograph of a Cross Section of Raw Fluid Petroleum Coke, (x1000).

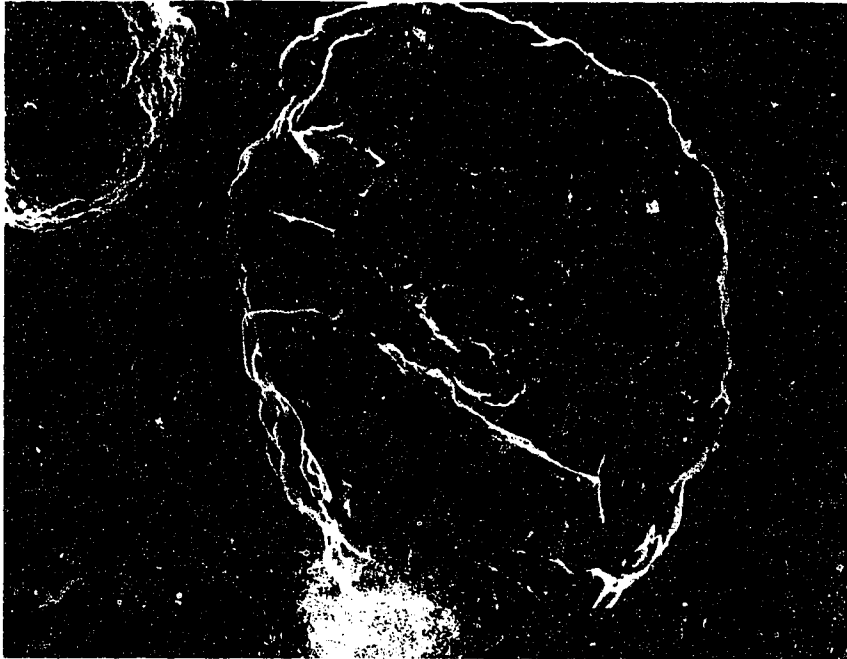


PLATE 5 SEM Micrograph of a Cross Section of Untreated Coke Activated for 0 Hours, Sample B-13, (x200).

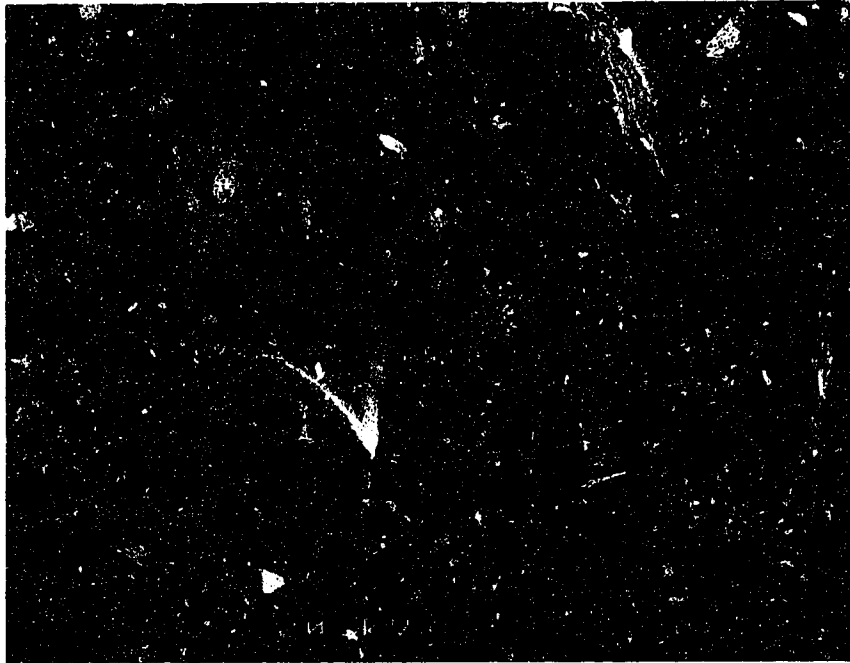


PLATE 6 SEM Micrograph of a Cross Section of Untreated Coke Activated for 0 Hours, Sample B-13, (x1000).

micrograph that has been split cleanly in half. The left hand corner of the micrograph there appears an external view of an unsplit particle. The external texture shows no difference between the raw coke and pyrolyzed coke. The internal view shows a circular orientation to the carbon structure similar to raw coke but individual layers or interfaces are impossible to differentiate due to the lack of fractures along the interfaces.

Plate 6 shows more detail of the carbon structure. The carbon is orientated in a circular pattern as shown by the orientation of the fracture surface but individual layers or interfaces are still not evident. The pyrolysis appears to have no effect on the overall structure of the coke particle. The only difference noted is that of the flakes of carbon sticking to the surface of the raw coke. The flakes of carbon attached to the raw coke as shown in Plate 4 are larger than the flakes attached to the pyrolyzed coke in Plate 6.

Two Hours Activation

Plates 7, 8, and 9 show the surface of a typical coke particle after 2 hours of activation. Surface cracking has appeared on a much smoother looking surface. The overall surface area appears smoother than raw coke at both 200 and 1000 magnification. The surface bumps appear less pronounced and more rounded with a glassy texture. At 1000 magnification,

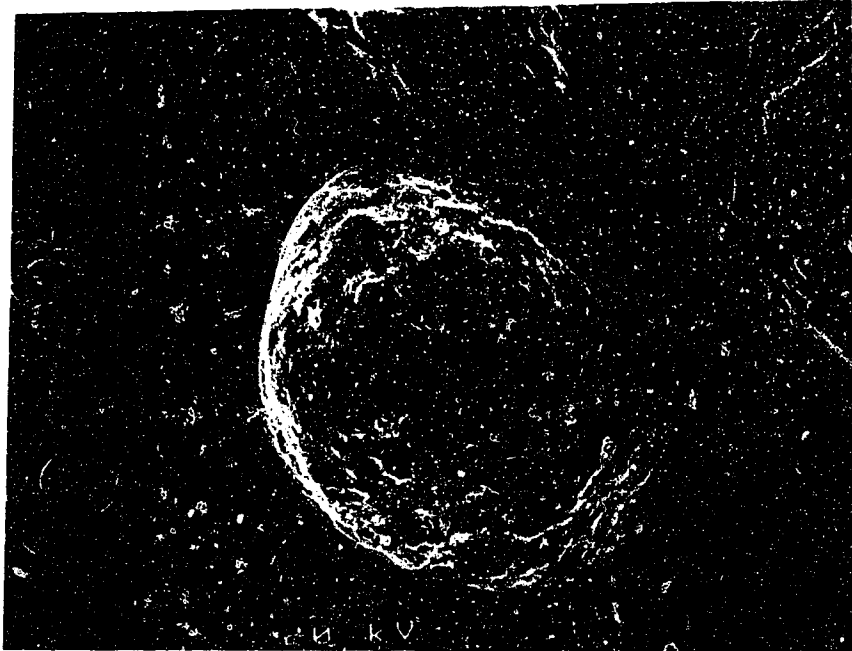


PLATE 7 SEM Micrograph of Untreated
Coke Activated for 2 Hours,
Sample A-9, (x200).

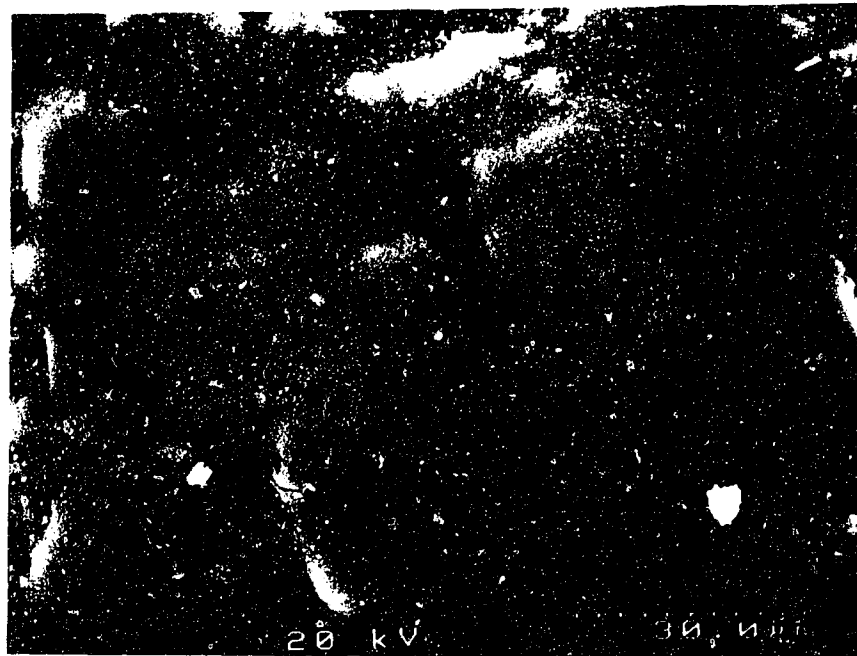


PLATE 8 SEM Micrograph of Untreated
Coke Activated for 2 Hours,
Sample A-9, (x1000).

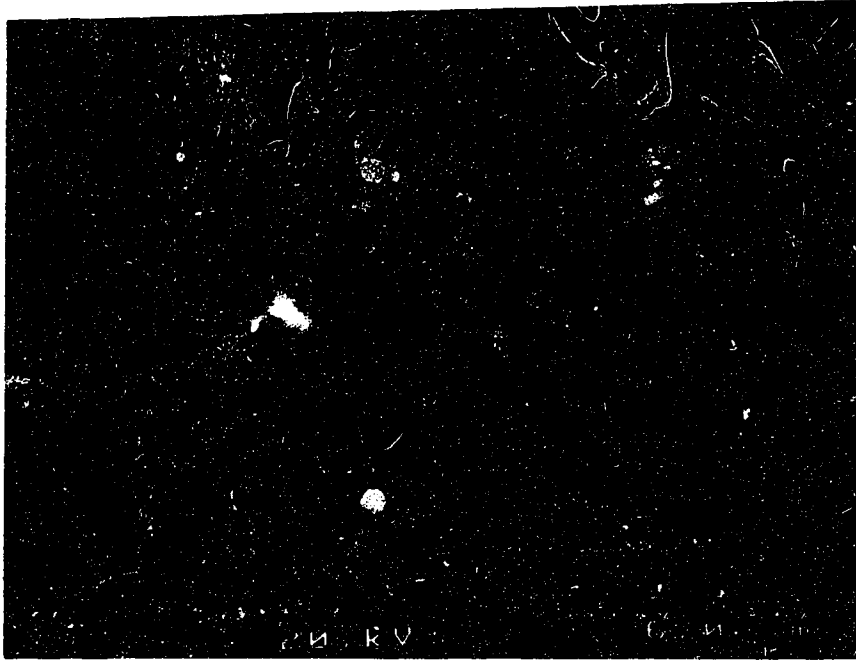


PLATE 9 SEM Micrograph of Untreated
Coke Activated for 2 Hours,
Sample A-9, (x5000).

no vesicles or flaking are evident. The glassy surface could be caused by surface burnoff and/or softening. Scale-invariance appears at all scales, the degree of roughness appears to be equal at all magnifications.

The cracks range in length from 3 to 15 microns and are thin and slightly curved. The maximum width appears to be about 1 micron. Plate 9 shows a typical looking crack at a magnification of 5000. The edges are jagged and fit together. The interior of the crack shows that both sides of the crack are connected to each other by small slivers of coke that did not fracture when the crack developed. This supports the view that this crack was caused by tension rather than burnoff. The nature of the cracks seems to indicate that the tension is caused either by shrinkage or expansion of the coke particle.

Four Hours Activation

Plates 10 and 11 show the exterior of a coke particle after 4 hours of activation. The coke particles are similar in appearance to the coke particles after 2 hours of activation except that the cracking is more extensive in frequency, width and length. Plate 10, at a magnification of 200 microns, shows one crack that appears to circle the particle along with numerous shorter cracks. Examining Plate 11, at a magnification of 1000, shows that the majority of cracks range from 1 to 30 microns in length with the majority being less than 10 microns long.

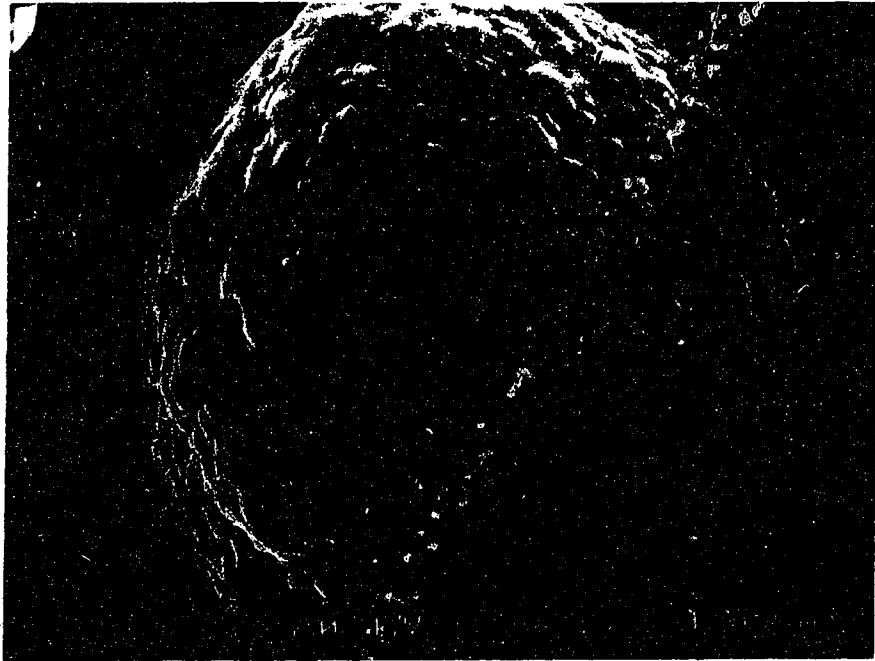


PLATE 10 SEM Micrograph of Untreated
Coke Activated for 4 Hours,
Sample A-12, (x200).

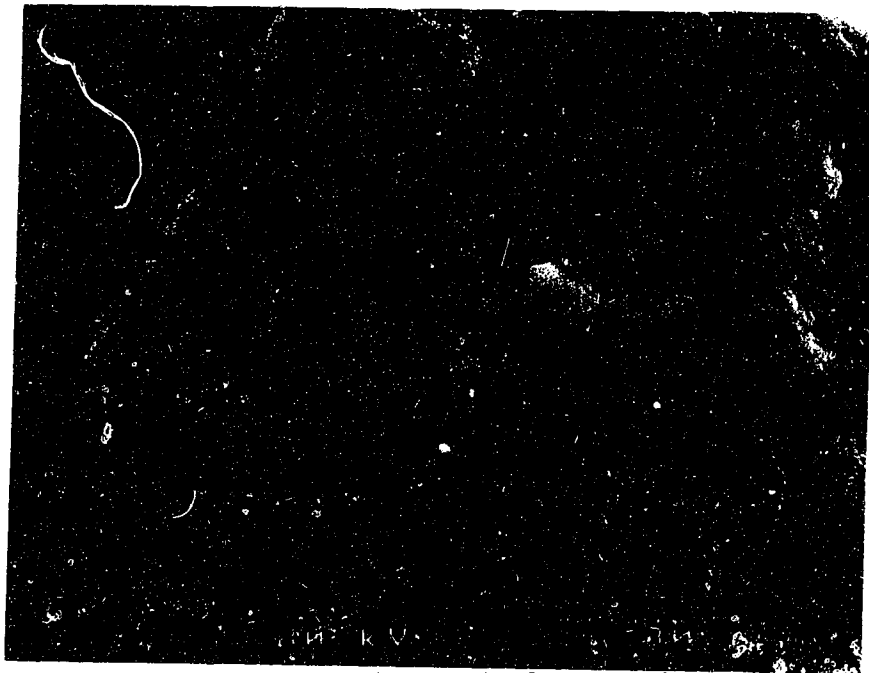


PLATE 11 SEM Micrograph of Untreated
Coke Activated for 4 Hours
Sample A-12, (x1000).

The surface at 1000 magnification appears rougher than at two hours of activation in part due to the numerous pits appearing on the surface. Except for the cracks and pits, the surface appears as glassy as the 2 hour activation, as shown in Plate 8.

The cracks still show signs that they were caused by tension, resulting from the shrinkage or expansion of the particle. The rougher surface indicates that the surface is not undergoing any softening at 4 hours of activation. Instead the carbon appears to be fully aromatized, hence the solidifying of the surface with activation etching pits in the surface. The larger bumps could be the result of uneven burnoff at the surface of the coke particle.

Six Hours Activation

The highest specific surface area developed was $318 \text{ m}^2 \text{ g}^{-1}$ with this specific sample. Plates 12 and 13 show a typical particle at 200 and 1000 magnification. The particle's dominating characteristic is the massive crisscrossing cracks. The cracks circle the particle and appear to run quite deep below the surface.

At a magnification of 1000, as shown in Plate 13, the surface appears much more bumpier than at 4 hours of activation. The bumps are more pronounced and contrast with the shallow depressions. The surface texture appears less glassy and the pitting noticed at 4 hours of activation is

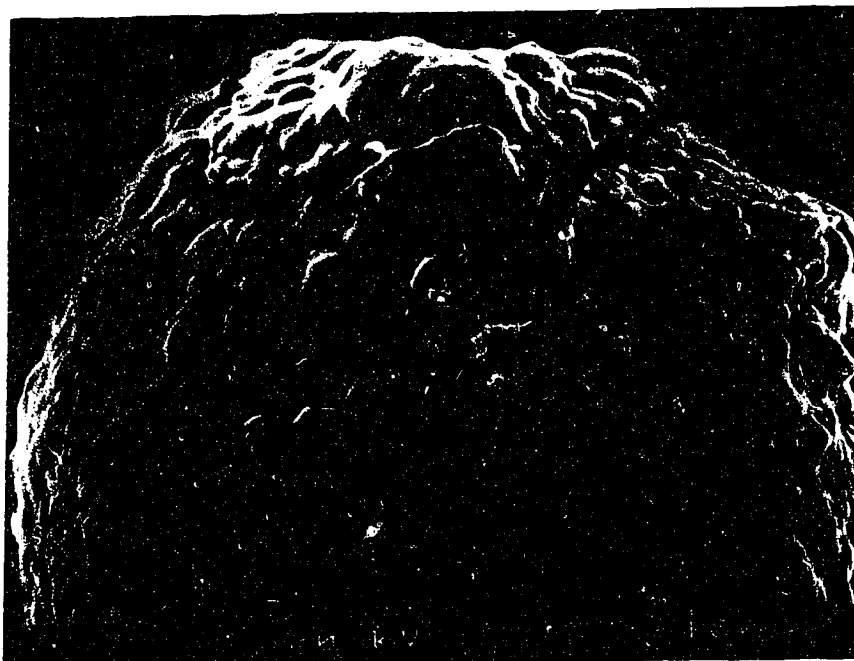


PLATE 12 SEM Micrograph of Untreated
Coke Activated for 6 Hours,
Sample A-17, (x200).

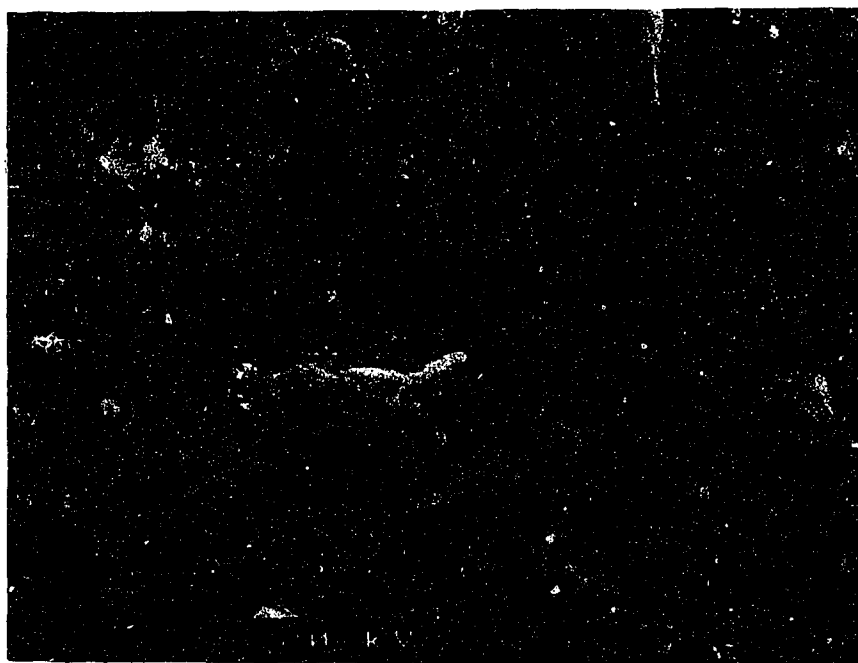


PLATE 13 SEM Micrograph of Untreated
Coke Activated for 6 Hours,
Sample A-17, (x1000).

absent. The scale-invariance appears to be equal at both scales.

The major cracks are at least 10 microns wide and extend deep into the coke particle. The crack edges are sharp and fit together. No burnoff or softening of the edges seems to have occurred. The overall appearance of the the cracks indicate that they formed by tension cracking caused either by shrinkage or expansion of the coke particle. The size analysis did indicate that after six 6 hours of activation, the overall size of the coke particles expanded by 3.8%.

4.1.10.3 Activated Potassium Coke

Two Hours Activation

Potassium coke that has undergone 2 hours of activation is similar in appearance to untreated coke after 4 hours of activation. Plates 14 and 15 show a typical particle at 200 and 1000 magnification respectively. At 200 times magnification, a major crack appears to circle the particle but there are not as many smaller cracks as in the 4 hour activated coke. As with the other sample, the cracking seems to be a result of surface tension caused by expansion.

The surface texture at 200 magnification, Plate 14, also resembles the surface texture of 4 hour activated coke, shown in Plate 10. The bumps

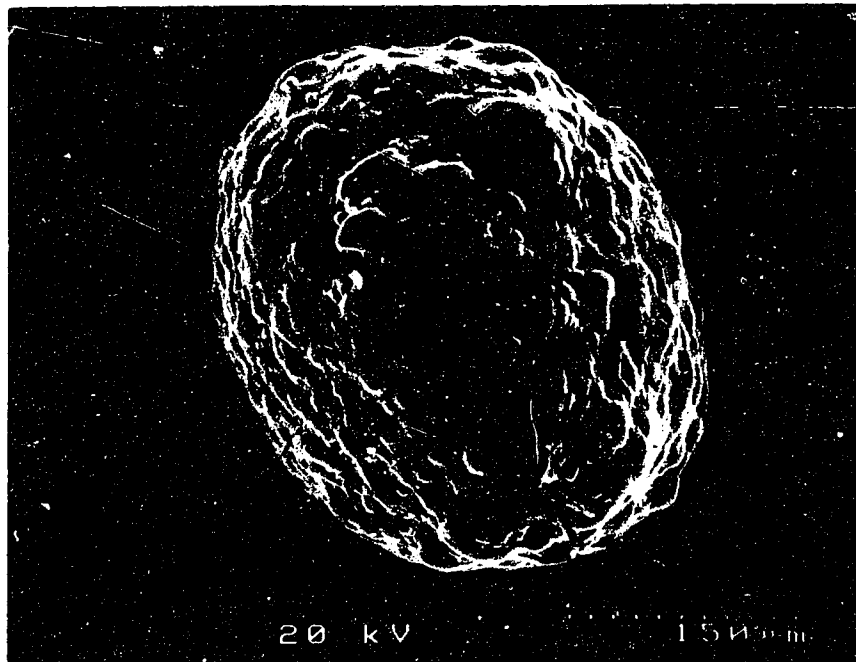


PLATE 14 SEM Micrograph of Potassium Treated (4% KOH) Coke Activated for 2 Hours, Sample A-11, (x200).

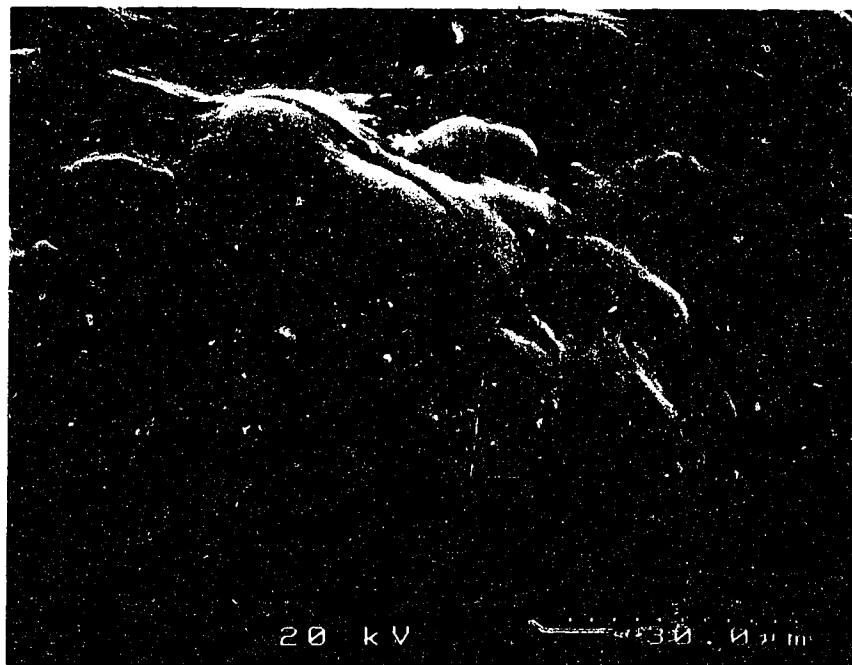


PLATE 15 SEM Micrograph of Potassium Treated (4% KOH) Coke Activated for 2 Hours, Sample A-11, (x1000).

are similarly shaped and rounded. At the higher magnification of 1000, in Plate 15, the surface appears very smooth and glassy, similar to the appearance of 2 hour activated untreated coke, Plate 8. At both scales, the surface roughness does appear to be similar.

Plate 16 shows an atypical particle which has been split open before activation. The particle may have been split open before activation but it is more likely it was split apart by handling after activation. The internal structure consists of concentric layers of coke 10 to 20 microns thick, nestled together but separated from each other. Large aligned cracks appear to intersect the layers. The internal surfaces of the layers appear very rough and covered with flakes of carbon.

The individual layers have separated from each other suggesting that during activation either burnoff occurs along the interfaces or the layers expand at different rates and the interfaces split apart. This suggests that the interfaces are more reactive or not tightly bonded to each other. The size of the hollow in the center of the particle suggests that there are 4 to 5 separate layers in a particle of this size, approximately 200 microns in diameter. In comparison to the exteriors of the other particles, Plates 14 and 15, the interior surface is much rougher with a sandy texture containing numerous flakes of carbon.



PLATE 16 SEM Micrograph of a Cross Section of Potassium Treated (4% KOH) Coke Activated for 2 Hours, Sample A-11, (x250).

Four Hours Activation

The four hour activated potassium coke is similar in some ways to the 6 hour activated untreated coke. Plates 17 and 18, show a typical particle at 200 and 1000 magnification. The particle is crisscrossed with major cracking at least 10 microns wide. The overall surface texture is characterized by a very bumpy texture with shallow depressions, similar in appearance to the six hour activated coke.

The 1000 magnification micrograph, Plate 18, shows a major crack and numerous smaller cracks on the surface. The major crack is highly fragmented with sharp edges, suggesting that the crack developed very quickly and explosively. The surface appears smooth and glassy but covered with small clumps of potassium salts, 0.5 to 6 microns in size.

Six Hours Activation

Plates 19 and 20 show a typical activated potassium coke particle after 6 hours of activation. The burnoff at this point is 85.4%, thus 14.6% of the original particle mass remains. At 200 magnification, Plate 19, the major characteristic is the large branching cracks that seem to circle the particle. The cracks appear to have formed by tension caused by expansion of the coke particle. The surface area has a few very large bumps that seem to be formed by uneven burnoff of the surface. Some bumps appear to be forming into mushroom shaped bumps, as at the lower left hand edge of

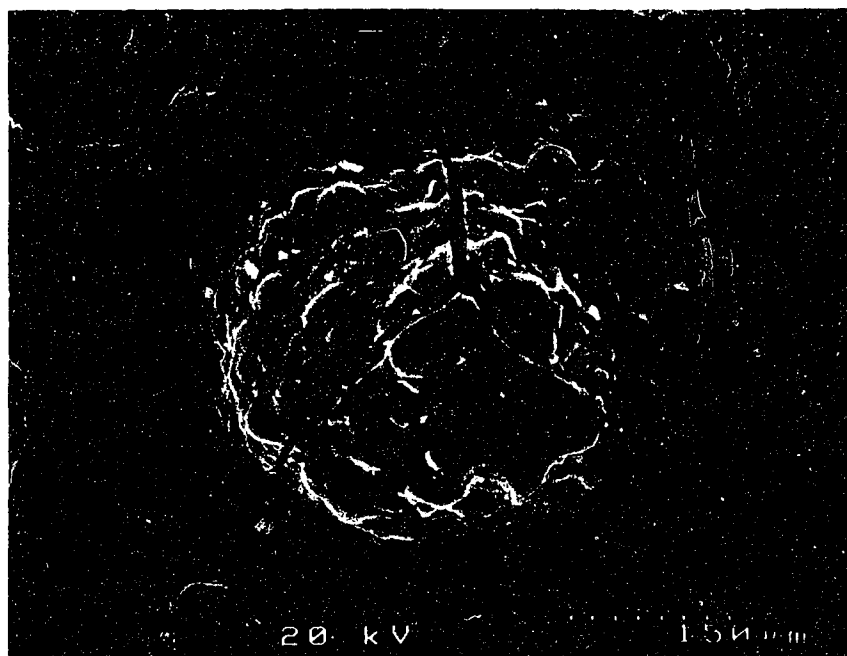


PLATE 17 SEM Micrograph of Potassium Treated (4% KOH) Coke Activated for 4 Hours, Sample A-14, (x200).

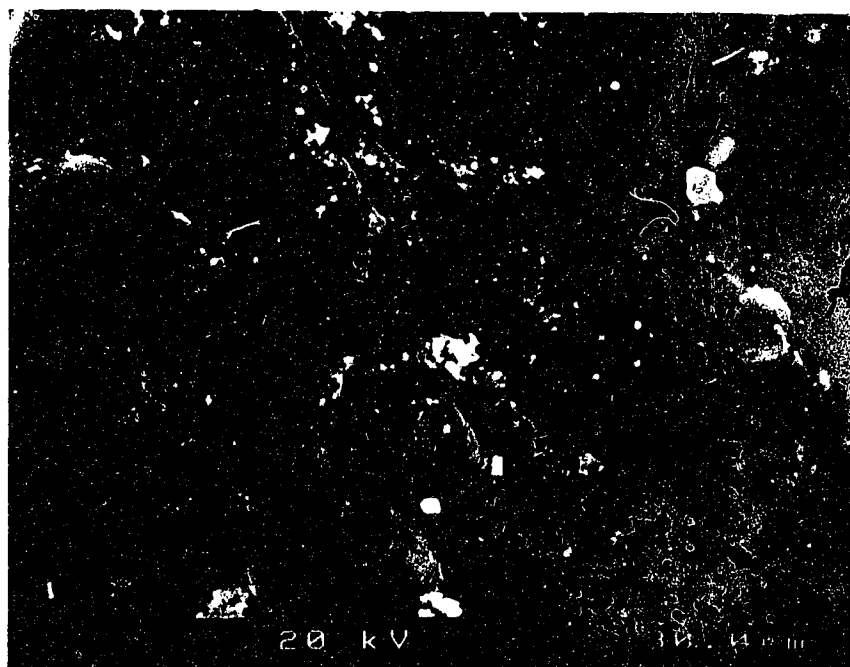


PLATE 18 SEM Micrograph of Potassium Treated (4% KOH) Coke Activated for 4 Hours, Sample A-14, (x1000).

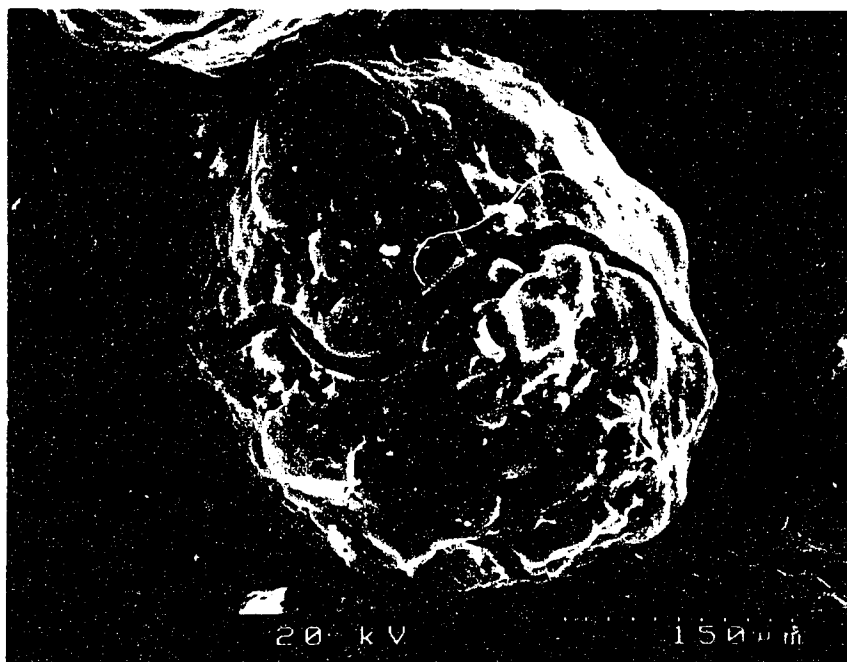


PLATE 19 SEM Micrograph of Potassium Treated (4% KOH) Coke Activated for 6 Hours, Sample A-18, (x200).

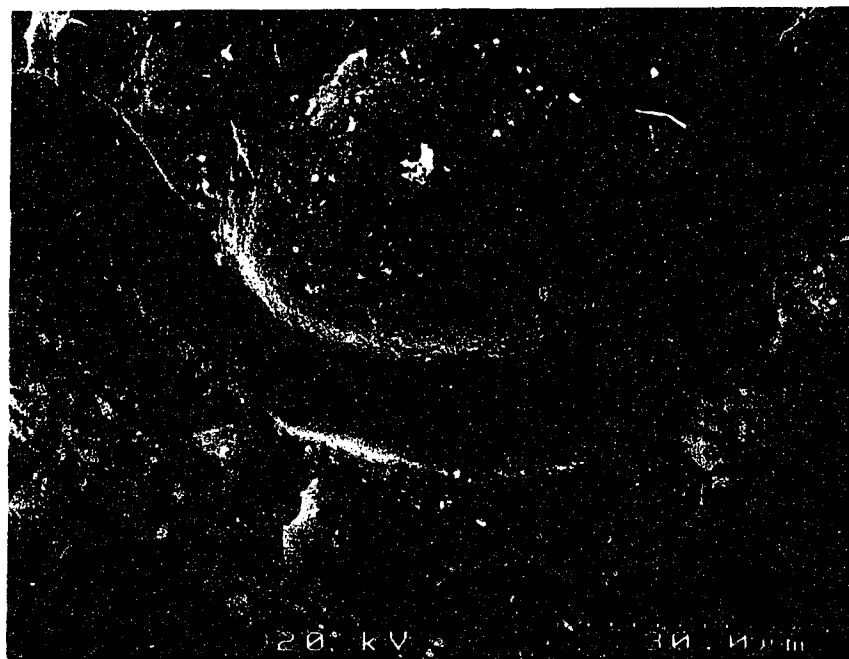


PLATE 20 SEM Micrograph of Potassium Treated (4% KOH) Coke Activated for 6 Hours, Sample A-18, (x1000).

the particle in Plate 19.

Plate 20 shows the detail around the major crack. The surface area appears rougher and duller than the surface at 4 hours of activation. Visible observation of the particles indicated that they were covered with ash, having a dull grey color. The ash appears to adhere to the particles and not fall off. At 1000 magnification, Plate 20, the surface appears rough at the very small scale of less than 1 micron. In the lower left hand corner of the micrograph, there are deep pits most likely caused by differential burnoff.

Also in Plate 20, it is possible to see some structure in the coke particle. Looking into the crack, layering can be discerned on the sides of the crack walls. The layering is extremely thin, 1 to 2 microns and parallel to each other. This layering is similar to the layering observed in the cross section of the raw coke, Plates 3 and 4.

Plate 21 shows another atypical activated potassium coke particle that has been split in half. The particle is composed of 4 concentric layers of coke, roughly 10 microns thick. Compared to a previous micrograph of another split particle, Plate 16, the surface appears smoother at the submicron level and a lot clearer of flaky material.

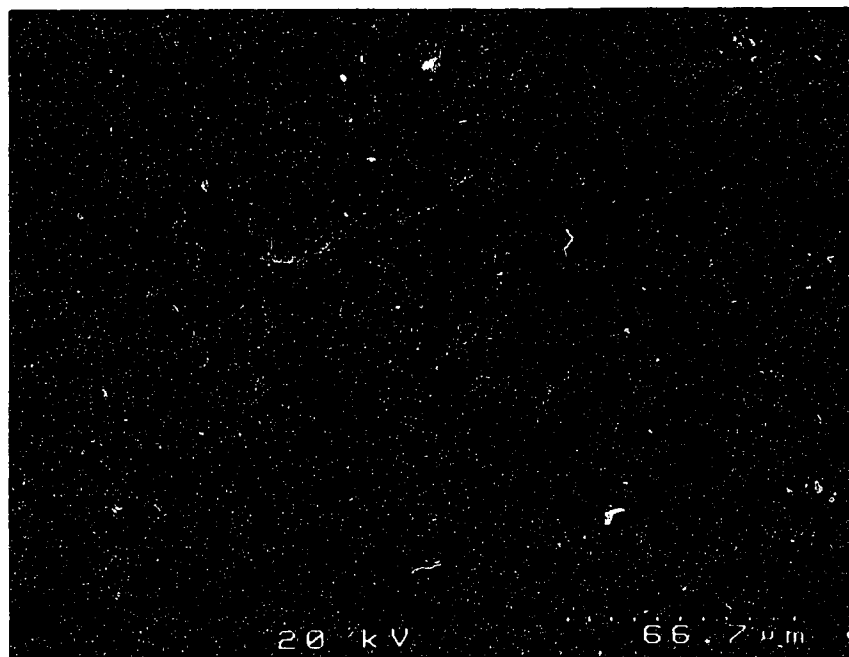


PLATE 21 SEM Micrograph of a Cross Section of Potassium Treated (4% KOH) Coke Activated for 6 Hours, Sample A-18, (x445).

4.2 General Discussion

4.2.1 Evolution of Pore Structure

The physical structure of any activated carbon depends on two main factors: the nature of the raw material, and the method of activation. The physical structure of fluid coke consists of concentric layers of carbon forming an "onion-like structure" [75]. The method of coke formation, as documented in the literature describes how bitumen is sprayed onto a fluidized bed of hot coke to induce cracking [75] which in turn causes successive layers of carbon to attached onto the coke particle. Some authors such as Metrailler [81] claim fluid coke has 30 to 100 different layers but the SEM micrographs of activated Syncrude coke indicated that there were 3 to 5 distinct layers of carbon.

The particle size analysis indicated that there is very little particle size difference between raw coke and activated cokes. In fact some slight size increases in certain size ranges have been noted, such as sample B-2, Table 7 and Figure 11. Even with high burnoffs of 60 to 70%, the particle sizes and distribution are relatively constant. With activation, the bulk density steadily decreases as shown in Figures 12 and 14. With the coke particles remaining the same size, all carbon losses can be assumed to come from the interior of the particles. The layered structure of the activated coke suggests that the interfaces between layers are the most reactive portions of

the coke particles. This reactivity plays a major role in the formation of porosity which leads to a novel mechanism of pore formation.

The SEM micrographs and size analyses revealed that in the first two hours of activation the coke particles did not change significantly in appearance or size. The surface appeared a little smoother indicating some carbon loss and/or softening but the most important feature was the appearance of small cracks. The cracks are reminiscent of tension cracks probably caused by thermal stresses and the loss of volatiles. In the first two hours, 25% of the coke mass was removed by activation. The material must have originated from the interior of the coke particle. These small tension cracks intersected the underlying interfaces of the coke layers and exposed these interfaces to burnoff.

Two likely scenarios are possible for the formation of porosity. The first scenario is that tension in the coke particle caused by thermal stress and loss of volatiles caused the layers to separate from each other along the interfaces exposing surface area. The separating of layers caused the coke particle to expand slightly which in turn caused the tension cracks on the surface to appear. Activating gas entered the surface cracks and reacted with the interfaces widening the space between individual layers. A second scenario is that thermal stress and loss of volatiles caused tension cracks to intersect the underlying interfaces. Activating gas entered the cracks and attacked the interfaces. Activation proceeded along the interfaces until the

individual layers separated from each other. Subsequent activation in both scenarios would have removed carbon from the exposed surfaces.

Plates 16 and 21 show the internal structure of potassium treated coke at 2 and 6 hours of activation respectively. Plates 5 and 6 show the internal structure of coke that has been pyrolyzed just before activation was started. The pyrolyzed coke shows no separation along its interfaces. The separation of the individual layers occurs after 2 hours of activation, as shown in Plate 16. The surface of the interfaces appears rough in texture and the distance between the interfaces is relatively thin. The surface of the interface surfaces appears smoother after 6 hours of activation, as shown in Plate 21. The gap between each interface, as measured from the micrograph appears to be of equal distance as the interface gaps of the two hour activation but the surfaces are free of carbon flakes and appear smoother. The rough surface at 2 hours of activation indicates that the surface roughness was caused by the layers splitting apart from each other. The debris on the surfaces are likely fragments of carbon broken off when the layers separated or were etched out. The smooth surface after six hours of activation is a result of the activation acting on the surface material removing debris and smoothing out the roughness.

In potassium activated coke, the maximum surface area is reached after 4 hours of activation and then remains constant even with extensive burnoff. The surface cracking steadily increases in size and extent with

activation. The roughness of the interfaces after 2 hours of activation, as shown in Plate 16, and the smoothness after 6 hours, as shown in Plate 21 indicates that the specific surface area is both a function of the gross surface area exposed by the layer separation and the surface roughness. A rough surface is expected to have more surface area than a smooth surface [82,83]. Syncrude coke has 3 to 5 separate carbon layers and a quick calculation indicates that if the surfaces of the interfaces were completely smooth, then their exposure would only increase the total surface area by a factor of 3 to 4. Since the surface area increased by a factor of 63, the roughness of the surfaces and micropores must make up a large portion of the surface area.

The mode of pore formation can therefore be summarized as follows:

- 1) Initial pyrolysis and activation causes tension in the coke particle which leads to small cracks on the surface to appear,
- 2) Tension may or may not cause the interfaces to separate from each other,
- 3) Activating gas enters the coke particle through cracks and either attacks the exposed interfaces or attacks the closed interfaces opening them up by removing carbon.

- 4) After the layers are separated, activation acts on the surfaces generally smoothing them out,
- 5) Maximum surface area for activated coke occurs at 6 hours of activation, where 60% of the coke particle is removed from the interior,
- 6) Excessive burnoff smooths out the interior surfaces decreasing the specific surface area,
- 7) The addition of potassium hydroxide causes much faster burnoff; the surface areas are exposed much faster but also burned off faster. By the time the internal structure is developed the surfaces are too smooth for maximum surface area, and
- 8) The untreated activated coke burns off at a slower rate, thus the cracks appear later than the potassium coke. This slower evolution allows the right amount of interface area to be exposed at the right time for the proper amount of activation to take place at the micropore level which increases the overall surface area.

4.2.2 Surface Chemistry

The pH analysis indicated that the untreated activated coke, as demonstrated by sample B-1 is a H carbon. It has a greater abundance of basic functional groups than acidic functional groups attached to its surface. This is to be expected due to the high activation temperature of 850°C [29] which tends to disassociate acidic functional groups. The most likely basic functional groups present are a) chromene or b) pyrone-like structure as shown below in Figure VIII.

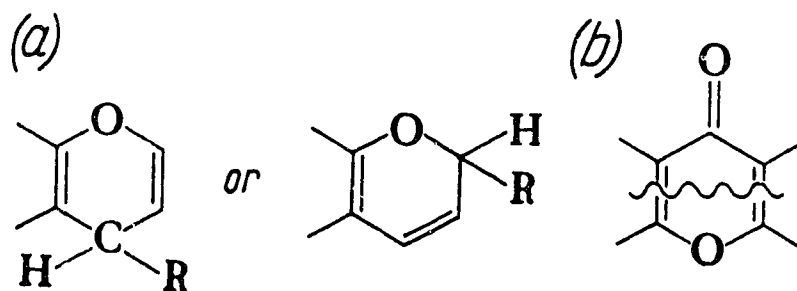


Figure VIII. Chromene (a) and pyrone-like (b) functional groups, from Mattson *et al* [29].

Subsequent oxidation caused by exposure to atmospheric oxygen would tend to form acidic functional groups so that the overall surface chemistry would become acidic over time.

5. CONCLUSIONS

The production of activated carbon from synthetic petroleum coke was demonstrated using a simple two-step pyrolysis/activation procedure. Steam was used as an activating gas at a temperature of 850°C, atmospheric pressure and a flow rate of 50% of the mass of coke per hour. A specific surface area of 318 m² g⁻¹ was achieved after six hours of activation.

The activation of untreated and potassium coke was compared. Untreated coke increased specific surface area steadily with activation time but the potassium coke achieved its maximum specific surface area after 4 hours of activation and then leveled off. It was discovered that while potassium hydroxide increased the activation rate, this did not lead to an increase in surface area development when compared to untreated coke. In addition, the formation of insoluble potassium compounds made it impossible to recover approximately half of the potassium for recycling and reuse. This would be a major disadvantage for a large scale commercial venture.

The activated coke particles retained their shape and size after activation. The activated coke particles were physically stable when agitated in a test solution and separated easily from the test water after use. They were physically and chemically stable in water.

The bulk density of the activated coke decreased linearly with burnoff while absolute density displayed non-linear behavior versus burnoff. The decrease in bulk density was a function of carbon loss while the change in absolute density was a function of carbon loss and structural changes in the coke during activation.

Untreated activated coke made an adequate activated carbon for the treatment of wastewater. The activated coke was able to adsorb large organic molecules and small ions such as iodine from water. The surface chemistry of the untreated activated coke consists of basic functional groups and thus is expected to perform well in an acidic environment.

The porosity was formed by a novel mechanism not previously reported in the literature. Instead of porosity being caused by the selective etching of the carbon, the activation induced stresses in the coke particle which caused the individual layers of carbon to split apart in the interior of the coke particle. Activating gases entered the particle via surface cracks and reacted with the interfaces. At a burnoff of approximately 50%, the carbon structure underwent a structural change. The final activated coke particle consisted of a coke particle covered with surface cracking and composed of independent concentric spheres of carbon in its interior.

The production of activated coke produced fuel-gas as a by-product. The activation procedure is actually the same chemical process as the

steam gasifications of carbon substances such as coal. The fuel-gas produced contained carbon monoxide, hydrogen sulphide, methane and possibly hydrogen.

Synthetic crude coke is a viable feedstock for the production of activated carbon. With stricter environmental laws and regulations becoming the norm, activated carbon has the potential to become an inexpensive and satisfactory solution for water and air treatment. By utilizing petroleum coke which is presently treated as a waste product, two problems can be solved at once.

The study of activated carbon covers a diverse range of materials, techniques and uses. This study concludes that activated carbon produced from synthetic coke can also be added to this body of knowledge.

6. REFERENCES

1. TORREGROSA, R. and MARTIN-MARTINEZ, J.M., Activation of lignocellulosic materials: a comparison between chemical, physical and combined activation in terms of porous texture; *FUEL*, Vol. 70, Oct., pp. 1173 - 1180, 1991.
2. RODRIGUEZ-MIRASOL, J., CORDERO, T., and RODRIQUEZ, J.J., Activated carbons from CO₂ partial gasification of eucalyptus kraft lignin; *ENERGY & FUELS*, Vol. 7, pp. 133 - 138, 1993.
3. WILSON, J., Active carbons from coals; *FUEL*, Vol. 60, Sept., pp. 823 - 831, 1981.
4. PETROV, N., GERGOVA, K., and ESER, S., Effect of water vapour on the porous structure of activated carbon from lignite; *FUEL*, Vol. 73(7), pp. 1197 - 1201, 1994.
5. DURIE, R.A., and SCHAFER, H.N.S., The production of active carbon from brown coal in high yields; *FUEL*, Vol. 58, June, pp. 472 - 476, 1979.
6. LIZZIO, A.A., and ROSTAM-ABADI, M., Production of carbon molecular sieves from Illinois coal; *AMERICAN CHEMICAL SOCIETY - DIVISION OF FUEL CHEMISTRY*, Vol. 37(2), pp. 512 - 523, 1992.
7. DERBYSHIRE, F.J., JAGTOYEN, M., McENANEY, B., SETHURAMAN, A.R., STENCEL, J.M., TAULBEE, D., and THWAITES, M.W., The production of activated carbons from coals by chemical activation; *AMERICAN CHEMICAL SOCIETY - DIVISION OF FUEL CHEMISTRY*, Vol. 36(3), pp. 1072 - 1080, 1991.
8. MUNOZ-GUILLENA, M.J., ILLAN-GOMEZ, M.J., MARTEN- MARTINEZ, J.M., LINARES-SOLANO, A., and SALINAS-MARTINEZ de LECEA C., Activated carbons from Spanish coals. 1. Two stage CO₂ activation; *ENERGY & FUELS*, Vol. 6(1), pp. 9 - 15, 1992.
9. KLOSE, E. and BORN, M., Partial gasification of lignite coke with steam in a rotary kiln for activated carbon production; *FUEL*, Vol. 64, Sept., pp. 1313 - 1316, 1985.

10. GERGOVA, K., ESER, S., and SCHOBERT, H.H, Preparation and characterization of activated carbons from anthracite; ENERGY & FUELS, Vol. 7, pp. 661 - 668, 1993.
11. POKONOVA, Y.V., and FAINBERG, V.S., The production of carbon adsorbents from shale oil phenols; FUEL SCIENCE and TECHNOLOGY INT'L., Vol. 8(1), pp. 27 - 38, 1990.
12. YAMAGUCHI, T., Preparation of activated carbon and light oil from petroleum asphaltenes. An attempt for the utilization of heavy oils; FUEL, Vol. 59, June, pp. 444 - 445, 1980.
13. POKONOVA, Y.V., and FAINBERG, V.S., The production of carbon materials from shale oil; FUEL SCIENCE and TECHNOLOGY INT'L., Vol. 7(7), pp. 951 - 967, 1989.
14. POKONOVA, J.V., Carbon adsorbents prepared with the use of petroleum residues; FUEL SCIENCE and TECHNOLOGY INT'L., Vol. 11(9), pp. 1149 - 1159. 1993.
15. POKONOVA, J.V., Carbon adsorbents from shale resin; FUEL SCIENCE and TECHNOLOGY INT'L., Vol. 11(8), pp. 1017 - 1023, 1993.
16. POKONOVA, Y.V., Preparation of crushed adsorbents from residues; FUEL SCIENCE and TECHNOLOGY INT'L., Vol. 11(5&6), pp. 713 - 719, 1993.
17. POKONOVA, Y.V., Carbon adsorbents from petroleum residues; FUEL SCIENCE and TECHNOLOGY INT'L., Vol. 11(7), pp. 875 - 882. 1993.
18. POKONOVA, Y.V., and GRABOVSKII, A.I., Carbonic adsorbents from fossil fuel processing products; KHIMIYA TVERDOGO TOPLIVA, Vol. 25(3), pp. 103 - 107, 1991.
19. POKONOVA, Y.V., Utilization of petroleum residues for production of carbon adsorbents; FUEL SCIENCE and TECHNOLOGY INT'L., Vol. 10(1), pp. 95 - 107, 1992.
20. POKONOVA, Y.V., ZAVERTKINA, L.I., and GRABOVSKII, A.I., Carbon adsorbents from solid fuel refining products; KHIMIYA TVERDOGO TOPLIVA, Vol. 24(3), pp. 80 - 85, 1990.

21. KOCHETKOVA, R.P., VORONKOV, V.V., SORKIN, E.I., POLYAKOV, V.V., KOROBENIKOVA, M.G., and APASOV, V.L., Production of a carbonaceous sorbent from wastes obtained in the vortex combustion of fuel in the boiler units of thermoelectric power stations; *KHIMIYA TVERDOGO TOPLIVA*, Vol. 23(2), pp. 139 -144, 1989.
22. GRAHAM, U.M., EKINCI, E., HUTTON, A., DERBYSHIRE, F., ROBL, T., STEWART, M.L., and RUBEL, A.M., Derivation of adsorbent carbons from oil shale residues; *AMERICAN CHEMICAL SOCIETY - DIVISION OF FUEL CHEMISTRY*, Vol. 38(3), pp. 915 - 919, 1993.
23. FEI, Y.Q., DERBYSHIRE, F., and ROBL, T., Carbon fibers and activated carbon fibers from residual shale oil; *AMERICAN CHEMICAL SOCIETY - DIVISION OF FUEL CHEMISTRY*, Vol. 38(2), pp. 427 - 433, 1993.
24. GIAVARINI, C., Active carbon from scrap tyres; *FUEL*, Vol. 64, Sept., pp. 1331-1332, 1985.
25. TENG, H., SERIO, M.A., BASSILAKIS, R., MORRISON, Jr., P.W., and SOLOMON, P.R., Reprocessing of used tires into activated carbon and other products; *AMERICAN CHEMICAL SOCIETY - DIVISION OF FUEL CHEMISTRY* Vol. 37(2), pp. 553 - 547, 1992.
26. JANKOWSKA, H., SWIATKOWSKI, A., and CHOMA, J., Active Carbon; KEMP, T.J. (Editor), Ellis Horwood Limited, New York, 1991.
27. DUBININ, M.M., Chemistry and physics of carbons; P.L. WALKER (Editor), Vol. 2, Marcel Dekker, Inc., New York, 1966.
28. COOKSON, Jr., J.T., Adsorption mechanisms: The chemistry of organic adsorption on activated carbon; Chapter 7, in *CARBON ADSORPTION HANDBOOK*, CHEREMISINOFF, P.N., and ELLERBUSCH, F.,(Editors) Ann Arbor Science Publishers Inc., Ann Arbor, Michigan, 1978.
29. MATTSON, J.S., and MARK, Jr., H.B., Activated Carbon - Surface chemistry and adsorption from solution; Marcel Dekker, Inc., New York, 1971.
30. BANSAL, R.C., DONNET, J-P., and STOECKLI, F., Active carbon; Marcel Dekker, Inc., New York, 1988.

31. DERBYSHIRE, F., JAGTOYEN, M., FEI, Y.Q., and KIMBER, G., The production of materials and chemicals from coal; AMERICAN CHEMICAL SOCIETY - DIVISION OF FUEL CHEMISTRY, Vol. 39(1), pp. 113 - 120, 1994.
32. RUBEL, A.M., STENCEL, J.M., and AHMED, S.N., Activated carbon for selective removal of nitrogen oxide from combustion flue gas; Vol. 38(2), pp. 726 - 733. 1992.
33. DAVINI, P., Adsorption of sulphur dioxide on thermally treated active carbon; FUEL, Vol 68, Feb., pp. 145 - 148, 1989.
34. AHMED, S.N., STENCEL, J.M., DERBYSHIRE, F.J., and BALDWIN, R.M., Activated carbons for the removal of nitric oxide; FUEL PROCESSING TECHNOLOGY, Vol. 34, pp. 123 - 136, 1993.
35. KISAMORI, S., KAWANO, S., and MOCHIDA, I., SO₂ and NO_x removal at ambient temperatures using activated carbon fibers; AMERICAN CHEMICAL SOCIETY - DIVISION OF FUEL CHEMISTRY, Vol. 38(2), pp. 421 - 426, 1992.
36. KNOBLAUCH, K., RICHTER, E., and JUNTGEN, H., Application of active coke in processes of SO₂- and NO_x- removal from flue gases; FUEL, Vol. 60, Sept., pp. 832 - 838, 1981.
37. FUJITSU, H., MOCHIDA, I., VERHEYEN, T.V., PERRY, G.J., and ALLARDICE, D.J., The influence of modifications to the surface groups of brown coal chars on their flue gas cleaning ability; FUEL, Vol. 72, Jan., pp. 109 - 113, 1993.
38. AHMED, S.N., STENCEL, J., DERBYSHIRE, F., and BALDWIN, B., Activated carbons for the removal of nitric oxides; AMERICAN CHEMICAL SOCIETY - DIVISION OF FUEL CHEMISTRY, Vol. 37(2), pp. 548 - 555, 1992.
39. CARRASCO-MARIN, F., UTRERA-HIDALGO, E., RIVERA-UTRILLA, J., and MORENO-CASTILLA, C., Adsorption of SO₂ in flowing air onto activated carbons from olive stones; FUEL, Vol. 71, May, pp. 575 - 578, 1992.
40. FERRAZ, M.C.A., Preparation of activated carbon for air pollution control; FUEL, Vol. 67, Sept., pp. 1237 - 1241, 1988.

41. GUO, S., LI, L., and WANG, A., Molecular sieve carbon from coals for air separation; FUEL SCIENCE and TECHNOLOGY INT'L., Vol. 8(5), pp. 545 - 561, 1990.
42. JUNTGEN, H., KNOBLAUCH, K., and HARDER, K., Carbon molecular sieves: production from coal and application in gas separation; FUEL, Vol. 60, Sept., pp. 817 - 822, 1981.
43. PATWARDHAN, S.N.V., VIJAYALAKSHMI, S, and GANGADHAR, B., Synthesis of carbon molecular sieves by activation and coke deposition; FUEL, Vol. 72(4), pp. 551 -555, 1993.
44. LIZZIO, A.A., and ROSTAM-ABADI, M., Production of carbon molecular sieves from Illinois coal; FUEL PROCESSING TECHNOLOGY, Vol. 34, pp. 97 - 122, 1993.
45. MATRANGA, K.R., MYERS, A.L., and GLANDT., E.D., Storage of natural gas by adsorption on activated carbon; CHEMICAL ENGINEERING SCIENCE, Vol. 47(7), pp. 1569 - 1579, 1992.
46. QUINN, D.F., MacDONALD, J.A., and SOSIN, K., Microporous carbons as adsorbents for methane storage; AMERICAN CHEMICAL SOCIETY - DIVISION OF FUEL CHEMISTRY, Vol. 39(2), pp. 451 - 455, 1994.
47. PETERSEN, F.W., and VAN DEVENTER, J.S.J, The influence of pH, dissolved oxygen and organics on the adsorption of metal cyanides on activated carbon; CHEMICAL ENGINEERING SCIENCE, Vol. 46(12), pp. 3053 - 3065, 1991.
48. SUN, T.M., and YEN, W.T., Kinetics of gold chloride adsorption onto activated carbon; MINERALS ENGINEERING, Vol. 6(1), pp. 17 - 29, 1993.
49. MENG, X., and HAN, K.N., Adsorption of gold from iodide solution by activated carbon; MINERALS AND METALLURGICAL PROCESSING, Feb., pp. 31 - 36, 1994.
50. ZYGOURAKIS, K., Effect of Pyrolysis conditions on the macropore structure of coal-derived chars; ENERGY & FUELS, Vol. 7, pp. 33 - 41, 1993.
51. CHITSORA, C.T., MUHLEN, H.J., VAN HEEK, K.H., and JUNTGEN, H., The influence of pyrolysis conditions on the reactivity of char in H₂O; FUEL PROCESSING TECHNOLOGY, Vol. 15, pp. 17 - 29, 1987.

52. SPENCER, D.H.T., and WILSON, J., Porosity studies on active carbons from anthracite; FUEL, Vol. 55, Oct., pp. 291 - 296, 1976.
53. JAGTOYEN, M, TOLES, C., and DERBYSHIRE, F., Activated carbons from bituminous coals; a comparison of H₃PO₄ and KOH activants; AMERICAN CHEMICAL SOCIETY - DIVISION OF FUEL CHEMISTRY, Vol 38(2), pp. 400 - 407, 1993.
54. JAGTOYEN, M., GROPPPO, J., and DERBYSHIRE, F., Activated carbons from bituminous coals by reaction with H₃PO₄: The influence of coal cleaning; FUEL PROCESSING TECHNOLOGY, Vol. 34, pp. 85 - 96, 1993.
55. JAGTOYEN, M., McENANEY, B., STENCEL, J., THWAITES, M., and DERBYSHIRE, F., Activated carbons from bituminous coals by reaction with H₃PO₃: Influence of coal cleaning; AMERICAN CHEMICAL SOCIETY - DIVISION OF FUEL CHEMISTRY, Vol. 37(2), pp. 505 - 511, 1992.
56. YANIK, J., SAGLAM, M., USTUN, G., and YUKSEL, M., Effects of MgCl₂ and ZnCl₂ additives on the porosity of formed coke; FUEL, Vol. 71, June, pp. 712 - 713, 1992.
57. WILDMAN, J., and DERBYSHIRE, F., Origins and functions of macroporosity in activated carbons from coal and wood precursors; FUEL, Vol. 70, May, pp. 655 - 661, 1991.
58. RIST, L.P., and HARRISON, D.P., Surface area and pore development during lignite activation; FUEL, Vol. 64, pp. 291 - 296, 1985.
59. SERGEEV, V.P., SOKOLOVSKII, V.N., KLEVTSOV, V.N., LUKASHEV, V.K., PIMONENKO, N.Y., MISHCHENKO, N.I., and TANTSYURA, T.P., Development of a porous structure on the activation of carbonaceous fibrous materials; KHIMIYA TVERDOGO TOPLIVA, Vol. 23(1), pp. 116 - 120, 1989.
60. LU, G.Q., Evolution of pore structure of high-ash char during activation; FUEL, Vol. 73(1), pp. 145 - 147, 1994.
61. ALVIM FERRAZ, M.C.M., Micropore volume determination in activated carbons; FUEL, Vol. 68, May, pp. 635 - 640, 1989.
62. STOECKLI, F., and BALLERINI, L., Evolution of microporosity during activation of carbon; FUEL, Vol. 70, April, pp. 557 - 559, 1991.

63. TOMKOW, K., SIEMIENIEWSKA, T., CZECHOWSKI, F., and JANKOWSKA, A., Formation of porous structures in activated brown-coal chars using O₂, CO₂, and H₂O as activating agents; FUEL, Vol. 56, April, pp. 121 - 124, 1977.
64. YANOVSKII, L.V., and SHCHIPKO, M.L., Water steam activation of brown coal semicokes produced by various methods; KHIMIYA TVERDOGO TOPLIVA, Vol. 24(3), pp. 103 - 106, 1990.
65. EHRBURGER, P., ADDOUN, A., ADDOUN, F., and DONNET, J-B., Carbonization of coals in the presence of alkaline hydroxides and carbonates: Formation of activated carbons; FUEL, Vol. 65, Oct., pp. 1447 - 1449, 1986.
66. KAPTEIJN, F., and MOULIJN, J.A., Kinetics of the potassium carbonate-catalysed CO₂ gasification of activated carbon; FUEL, Vol. 62, Feb., pp. 221-225, 1983.
67. MARSH, H., WILKINSON, A., and MACHNIKOWSKI, J., Study of the reaction of cokes with KOH under nitrogen; FUEL, Vol. 61, Sept., pp. 834 - 839, 1982.
68. GOMEZ-SERRANO, V., SANCHEZ-INIGUEZ, F., and VALENZUELA-CALAHORRO, C., Penetration of sodium catalysts in activated carbon: effect on the porous structure and reactivity in air, carbon dioxide, and steam; FUEL, Vol. 70, Sept., pp. 1083 - 1090, 1991.
69. SILVA, I.F., and LOBO, L.S., Study of CO₂ gasification of activated carbon catalysed by molybdenum oxide and potassium carbonate; FUEL, Vol. 65, Oct., pp. 1400 - 1403, 1986.
70. MORENO-CASTILLA, C., CARRASCO-MARIN, F., and RIVERA-UTRILLA, J., Air gasification of activated carbons and chars catalysed by Cr₂O₃ and MoO₂; FUEL, Vol. 69, March, pp. 354 - 361, 1990.
71. GRZYBEK, T., The influence of the support structure on the iron distribution for Fe³⁺-active carbon catalysts; FUEL, Vol. 69, May, pp. 604 - 607, 1990.
72. VERHUYAN, V., JAGTOYEN, M., and DERBYSHIRE, F., Formed activated carbons from bituminous coals by KOH activation; AMERICAM CHEMICAL SOCIETY - DIVISION OF FUEL CHEMISTRY, Vol. 38(2), pp. 414 - 420, 1993.

73. FOUHY, K., Legislation scrubs fluegas emissions; **CHEMICAL ENGINEERING**, June, pp. 31 -35, 1992.
74. ITYOKUMBUL, M.T., and KASPERSKI, K.L., Reactivity of caustic treated oil sand coke residues; **FUEL PROCESSING TECHNOLOGY**, Vol. 37, pp. 281 - 294, 1994.
75. JACK, T.R., SULLIVAN, E.A., and ZAJIC, J.E., Comparison of the structure and composition of cokes from the thermal cracking of Athabasca Oil Sands bitumen; **FUEL**, Vol. 58, Aug., pp. 585 - 588, 1979.
76. BRYERS, R.W., Utilization of petroleum cokes for steam raising; **AMERICAN CHEMICAL SOCIETY - DIVISION OF FUEL CHEMISTRY**, Vol. 38(4), pp. 1237 - 1244, 1993.
77. WATKINSON, A.P., CHENG, G., and FUNG, D.P.C., Gasification of oil sand coke; **FUEL**, Vol. 68, Jan., pp. 4 - 10, 1989.
78. MAJID, A., RATCLIFFE, C.I., and RIPMEESTER, J.A., Demineralization of petroleum cokes and fly ash samples obtained from the upgrading of Athabasca oil sands bitumen; **FUEL SCIENCE & TECHNOLOGY INT'L**, Vol. 7(5-6), pp. 879 - 895, 1989.
79. KUMAR, A., SPARKS, B.D., and MAJID, A., Recovery of organics from tailings pond sludge using coke for agglomeration; **35th CANADIAN CHEMICAL ENGINEERING CONFERENCE**, Vol. 1, pp. 214 - 219, Calgary, 1985.
80. HALL, E.S., and TOLLEFSON, E.L, Sorption-scavenging methods for recovery of residual oil from oil sands tailings streams; **AOSTRA JOURNAL OF RESEARCH**, Vol. 4, pp. 7 - 18, 1987.
81. METRAILER, W.J.; U.S. Patent 3,840,476; Oct. 8, 1974; assigned to ESSO Research and Engineering Company.
82. FAIRBRIDGE, C., NG, S.H., and PALMER, A.D., Fractal analysis of gas adsorption on Syncrude coke; **FUEL**, Vol. 65, Dec., pp. 1759 - 1762, 1986.
83. JARONIEC, M., Evaluation of the fractal dimension of microporous activated carbons; **FUEL**, Vol. 69, Dec., pp. 1573 - 1574, 1990.
84. FURIMSKY, E., Gasification reactivities of cokes derived from Athabasca bitumen; **FUEL PROCESSING TECHNOLOGY**, Vol. 11, pp. 167 - 182, 1985.

85. MOSCHOPEDIS, S.E., SCHULZ, K.F., SPEIGHT, J.G., and MORRISON, D.N., Surface-active materials from Athabasca oil sands; FUEL PROCESSING TECHNOLOGY, Vol. 3, pp. 55 - 61, 1980.
86. FAIRBRIDGE, C., PALMER, A.D., NG, S.H., and FURIMSKY, E., Surface structure and oxidation reactivity of oil sand coke particles; FUEL, Vol. 66, May, pp. 688 - 691, 1987
87. KOTLYAR, L.S., RIPMEESTER, J.A., SPARKS, B.D., and MONTGOMERY, D.S., Characterization of oil sands closely associated with Athabasca bitumen; FUEL, Vol. 67, June, pp. 808 - 814, 1988.
88. O'GRADY, T.M., and WENNERBERG, A.N., High-surface-area active carbon; in PETROLEUM-DERIVED CARBONS, BACHA, J.D., NEWMAN, J.W., and WHITE, J.L., (Editors), American Chemical Society, Washington, D.C., 1986.
89. TOLLEFSON, E.L., Removal of hydrocarbons from aqueous waste water from oil sands recovery operations; in CARBON ADSORPTION HANDBOOK, CHEREMISNOFF, P.N., and ELLERBUSCH, F., (Editors), Ann Arbor Science Publishers Inc., Ann Arbor, Michigan, 1978.
90. COOKSON, Jr., J.T., Adsorption mechanisms: The chemistry of organic adsorption on activated carbon; in CARBON ADSORPTION HANDBOOK, CHEREMISHOFF, P.N., and ELLERBUSCH, F., (Editors), Ann Arbor Science Publishers Inc., Ann Arbor, Michigan, 1978.
91. GREGG, S.J., and SING, K.S.W, Adsorption, Surface Area and porosity; Academic Press, New York, 1967.
92. LANGMUIR, I., The adsorption of gases on plane surfaces of glass, mica, and platinum; JOURNAL OF THE AMERICAN CHEMICAL SOCIETY, Vol. 40, pp. 1361 - 1403, 1918.
93. BRUNAUER, S., EMMETT, P.H., and TELLER, E., Adsorption of gases in multimolecular layers; JOURNAL OF THE AMERICAN CHEMICAL SOCIETY, Vol. 60, pp. 309 , 1938.
94. YEH, F., Activated Carbon - Manufacture and Regeneration; Noyes Data Corporation, New Jersey, 1978.
95. TAYLOR, R., and HENNAH, L., The nature of strength-controlling structural flaws in formed coke; FUEL, Vol. 71, Jan., 1992.

96. TAYLOR, J.W., Compaction and cementing of char particles with a tar-derived binder; FUEL, Vol. 67, Nov., 1988.
97. KLIEN, J.K., and HENNING, K-D., Catalytic oxidation of hydrogen sulphide on activated carbons; FUEL, Vol. 63, Aug., 1984.
98. LIPOVICH, V.G., KAPUSTIN, M.A., and BELOVA, T.Y., Influence of metal and carrier on properties of coated catalysts with activated carbon in decomposition of gas hydrogen sulfide; KHIMIYA TVERDOGO TOPLIVA, Vol. 25(4), p. 134 - 137, 1991.
99. BELOVA, T.Y., GARBER, Y.N., LIPOVICH, V.G., and KAPUSTIN, M.A., Hydrogen sulphide oxidation on coated catalysts with activated carbon; KHIMIYA TVERDOGO TOPLIVA, Vol. 25(3), pp. 108 - 113, 1991.
100. KUSAKABE, K., KASHIMA, M., MOROOKA, S., and KATO, Y., Rate of reduction of nitric oxide with ammonia on coke catalysts activated with sulphuric acid, FUEL, Vol. 67, May, pp. 714 - 718, 1988.
101. LEE, J.K., SUH, D.J., PARK, S., and PARK, D., Effects of pyrolysis conditions on the reactivity of char for the reduction of nitric oxide with ammonia; FUEL, Vol. 72(7), pp. 935 - 939, 1993.
102. MOCHIDA, I., OGAKI, M., YOSHINOBU, K., and IDA, S., Catalytic activity of coke activated with sulphuric acid for the reduction of nitric oxide; FUEL, Vol. 62, July, pp. 867 - 868, 1983.
103. MOCHIDA, I., OGAKI, M., FUJITSU, H., KOMATSUBARA, Y., and IDA, S., Reduction of nitric oxide with activated PAN fibres; FUEL, Vol. 64, Aug., pp. 1054 - 1057, 1985.
104. MOCHIDA, I., KISAMORI, S., HIRONAKA, M., and KAWANO, S., Oxidation of NO into NO₂ over activated carbon fibers; AMERICAN CHEMICAL SOCIETY - DIVISION OF FUEL CHEMISTRY, Vol. 39(1), pp. 219 - 222, 1994.
105. ILLAN-GOMEZ, M.J., LINARES-SOLANO, A., and SALINAS-MARTINEZ de LECEA, C., NO reduction by activated carbons. 1. The role of carbon porosity and surface area; ENERGY & FUELS, Vol. 7, pp. 146 - 154, 1993.
106. JUNTGEN, H., Activated carbon as catalyst support; FUEL, Vol. 65, Oct., pp. 1436 - 1446, 1986.

107. POHL, J.H., The influence of mineral matter on the rate of coal char combustion; AMERICAN CHEMICAL SOCIETY - DIVISION OF FUEL CHEMISTRY, Vol. 29(4), pp. 295 - 300, 1984.
108. TOMITA, A., MAHAJAN, O.P., and WALKER Jr., P.L., Catalysis of char gasification by minerals; AMERICAN CHEMICAL SOCIETY - DIVISION OF FUEL CHEMISTRY, Vol. 22(1), pp. 4 - 11, 1977.
109. EHRBURGER, P., ADDOUN, F., and DONNET, J-B., Effect of mineral matter of coals on the microporosity of charcoals; FUEL, Vol. 67, Sept., pp. 1228 - 1231, 1988.
110. VALENZUELA CALAHORRO, C., CHAVES CANO, T., and GOMEZ SERRANO, V., Effect of acid and heat treatments on surface area and porosity of a Spanish coal with high mineral matter content; FUEL, Vol. 66, April, pp. 479 - 485, 1987.
111. SOUSA J.C., MAHAMUD, M., PARRA, J.B., and PIS, J.J., PAJARES, J.A., Effect of operation variables in the obtention of tailored active carbons from coals; FUEL PROCESSING TECHNOLOGY, Vol. 36, pp. 333 - 339, 1993.
112. TOLES, C., RIMMER, S.M., DERBYSHIRE, F., and JAGTOYEN, M., Production of activated carbons from a vitrain concentrate from the Stockton coal; AMERICAN CHEMICAL SOCIETY - DIVISION OF FUEL CHEMISTRY, Vol. 39(2), pp. 596 - 600, 1994.
113. GOW, A.S., and PHILLIPS, J., Calorimetric study of oxygen adsorption on a high surface area polymer-derived carbon; ENERGY & FUELS, Vol. 6, pp. 184 - 188, pp. 184 - 188, 1992.
114. PETIT, J.C., A calorimetric investigation of the low temperature oxidation of coal and activated carbon; FUEL, Vol. 69, July, pp. 861 - 866, 1990.
115. RASHID KHAN, M., Significance of char active surface area for appraising the reactivity of low- and high- temperature chars; FUEL, Vol. 66, Dec., pp. 1626 - 1634, 1987.
116. HURT, R.H., SOROFIM, A.F., and LONGWELL, J.P., Effect of nonuniform surface reactivity on the evolution of pore structure and surface area during carbon gasification; ENERGY & FUELS, Vol. 5, pp. 463 - 468, 1991.

117. STEWART, M.L., and STENCEL, J.M., Treatment of activated carbons for densification; AMERICAN CHEMICAL SOCIETY - DIVISION OF FUEL CHEMISTRY, Vol. 38(2), pp. 408 - 413, 1993.
118. GUHA, O.K., ROY, J., and CHOUDHURY, A., Non-polar carbon adsorbents from coal: effect of coal rank studied by molecular probe chromatography; FUEL, Vol. 70, Jan., pp. 9 - 12, 1991.
119. POKONOVA, Y.V., VOROZHBITOVA, L.N., and ZAVERTKINA, L.I., A study of the sorptive properties of modified carbon adsorbents; KHIMIYA TVERDOGO TOPLIVA, Vol. 24(5), pp. 116 - 122, 1990.
120. THWAITES, M.W., McENANEY, B., BOTHA, F.D., McNEESE, B.E., and SUMNER, M.B., Synthesis and characterization of activated pitch-based carbon fibers; AMERICAN CHEMICAL SOCIETY - DIVISION OF FUEL CHEMISTRY, Vol. 37(2), pp. 497 - 504, 1992.
121. SALAS-PEREGRIN, M.A., CARRASCO-MARIN, F., LOPEZ-GARZON, F.J., and MORENO-CASTILLA, C., Adsorption of CO₂ on activated carbons from diluted ambient environments; ENERGY & FUELS, Vol. 8, pp. 239 - 243, 1994.
122. TINGE, J.T., and DRINKENBURG, A.A.H., Adsorption of gases into activated carbon-water slurries in a stirred cell; CHEMICAL ENGINEERING SCIENCE, Vol 47(6), pp. 1337 - 1345, 1992.
123. TINGE, J.T., OP'T ENDE, H.C., BERENDSEN, H.J.C., and A.A.H., DRINKENBURG, The adsorption of propane and ethene in slurries of activated carbon in water-II; CHEMICAL ENGINEERING SCIENCE, Vol. 46(1), pp. 343 - 350, 1991.
124. GINTER, D.M., SOMORJAI, G.A., and HEINEMANN, H., Factors affecting the reactivity of chars and cokes during low-temperature (640 C) steam gasification; ENERGY & FUELS, Vol. 7, pp. 393 - 398, 1993.
125. DHUPE, A.P., GOKARN, A.N., and DORAISWAMY, L.K., Investigations into the compensation effect at catalytic gasification of active charcoal by carbon dioxide; FUEL, Vol. 70, July, pp. 839 - 844, 1991.
126. KELEMEN, S.R., and FREUND, H., A comparison of CO₂ and O₂ gasification of glassy carbon; AMERICAN CHEMICAL SOCIETY - DIVISION OF FUEL CHEMISTRY, Vol. 30(1), pp. 286 - 293, 1985.

127. MAHAJAN, O.P., and WALKER Jr., P.L, Effect of inorganic matter removal from coals and chars on their surface areas; FUEL, Vol. 58, May, pp. 333 - 337, 1979.
128. JUNTGEN, H., RICHTER, E., and KUHL, H., Catalytic activity of carbon catalysts for the reaction of NO_x with NH₃; FUEL, Vol. 67, June, pp. 775 - 780, 1988.
129. VALENZUELA-CALAHORRO, C., FERNANDEZ-GONZALEZ, C., BERNALTE-GARCIA, A., and GOMEZ-SERRANO, V., Catalysis by alkali and alkaline-earth metals of the gasification in CO₂ and steam of chars from a semi-anthracite with high inorganic matter content; FUEL, Vol. 66, Feb., pp. 216 - 222, 1987.
130. TAKAYUKI, T., TAMAI, Y., and TOMITA, A., Effectiveness of K₂CO₃ and Ni as catalysts in steam gasification; Fuel, Vol. 65, May, pp. 679 - 683, 1986.
131. THOMSON, W.J., and SY, L.Y., Potassium catalysed gasification of Kentucky oil shale char; Fuel, Vol. 66, Feb., pp. 223 - 227, 1987.
132. MCKEE, D.W., Mechanisms of the alkali metal catalysed gasification of carbon; FUEL, Vol. 62, Feb., pp. 170 - 175, 1983.
133. RUDAKOV, E.S., METLOVA, L.P., CHUPRINA, V.S., and SUPUNOV, V.A., Oxidation of carbonic materials in the presence of alkaline metal hydroxides; KHIMIYA TVERDOGO TOPLIVA, Vol. 25(3), pp. 51 - 56, 1991.
134. VERA, M.J., and BELL, A.T., Effect of alkali catalysts on gasification of coal char; FUEL, Vol. 57, April, pp. 194 - 200, 1978.
135. CARRAZZA, J., SOMORJAI, G.A., and HEINEMANN, H., Steam gasification of carbonaceous solids catalyzed by a mixture of potassium and nickel oxides below 1000 K; AMERICAN CHEMICAL SOCIETY - DIVISION OF FUEL CHEMISTRY, Vol. 31(3), pp. 158 - 165, 1986.
136. RATCLIFFE, C.T., Kinetic and mechanistic aspects of CO₂ gasification on alkali treated carbon; AMERICAN CHEMICAL SOCIETY - DIVISION OF FUEL CHEMISTRY, Vol. 30(1), pp. 330 - 340, 1985.
137. LANG, R.J., and NEAVEL, R.C., Behavior of calcium as a steam gasification catalyst; FUEL, Vol. 61, July, pp. 620 - 626, 1982.

138. SALINAS-MARTINEZ de LECEA, C., ALMELA-ALARCON, M., and LINARES-SOLANO, A., Calcium-catalysed carbon gasification in CO₂ and steam; FUEL, Vol. 69, Jan., pp. 21 - 27, 1990.
139. PEREIRA, P., SOMORJAI, G.A., and HEINEMANN, H., Catalytic steam gasification of coals; ENERGY & FUELS, Vol. 6, pp. 407 - 410, 1992.
140. RADOVIC, L.R., WALKER Jr., P.L., and JENKINS, R.G., Catalytic coal gasification: use of calcium versus potassium; FUEL, Vol. 63, July, pp. 1028 - 1030, 1984.
141. FIGUEIREDO, J.L., ORFAO, J.J.M., and FERRAZ, M.C.A., Catalytic gasification of chars; FUEL, Vol. 63, Aug., pp. 1059 - 1060, 1984.
142. MORENO-CASTILLA, C., RIVERA-UTRILLA, J. and LOPEZ-PEINADO, A.J., Vanadium pentoxide as catalyst in the air gasification of chars; Fuel, Vol. 68, Aug., pp. 968 - 971, 1989.
143. MORENO-CASTILLA, C., LOPEZ-PEINADO, A., RIVERA-UTRILLA, J., FERNANDEZ-MORALES, I., and LOPEZ-GARZON, F.J., The striking behavior of copper catalysing the gasification reaction of coal in dry air; FUEL, Vol. 66, Jan., pp. 113 - 118, 1987.
144. CARRASCO-MARIN, F., RIVERA-UTRILLA, J., UTRERA-HIDALGO, E., and MORENO-CASTILLA, C., MoO₂ as catalyst in the CO₂ gasification of activated carbons and chars; Fuel, Vol. 70, Jan., pp. 13 - 16, 1991.
145. RATCLIFFE, C.T., and VAUGHN, S.N., Population and turnover number of active potassium sites on bituminous coals during gasification; AMERICAN CHEMICAL SOCIETY - DIVISION OF FUEL CHEMISTRY, Vol. 30(1), pp. 304 - 319, 1985.
146. MIMS, C.A., and PABST, J.K., Alkali catalysed carbon gasification I. Nature of the catalytic sites & II. Kinetics and mechanism; AMERICAN CHEMICAL SOCIETY - DIVISION OF FUEL CHEMISTRY, Vol. 25(3), pp. 258 - 268, 1980.
147. SPIRO, C.L., McKEE, D.W., KOSKY, P.G., and LAMBY, E.J., Observation of alkali catalyst particles during gasification of carbonaceous materials in CO₂ and steam; FUEL, Vol. 63, May, pp. 686 - 691, 1984.

148. MOULIJN, J.A., CERFONTAIN, M.B., and KAPTEIJN, F., Mechanism of the potassium catalysed gasification of carbon in CO₂; FUEL, Vol. 63, Aug., pp. 1043 - 1047, 1984.
149. GOMEZ-SERRANO, V., SANCHEZ-INIGUEZ, F., BERNALTE-GARCIA, A., and VALENZUELA-CALAHORRO, C., Penetration of Na compounds - catalysts of the gasification reaction - in activated carbon by heating between 380 and 950 C; FUEL, Vol. 69, March, pp. 391 - 394, 1990.
150. SPITZER, D.P., Effective surface areas of coals measured by dye adsorption; AMERICAN CHEMICAL SOCIETY - DIVISION OF FUEL CHEMISTRY, Vol. 33(4), pp. 789 - 796, 1988.
151. RODRIGUEZ, N.M., and MARSH, H., Surface structure of coals studied by iodine and water adsorption; AMERICAN CHEMICAL SOCIETY - DIVISION OF FUEL CHEMISTRY, Vol. 32(1), pp. 226 - 238, 1987.
152. SLOMKA, B.J., DAWSON, M.R., and BUTTERMORE, W.H., Characterization of mineral and coal surfaces by adsorption of dyes; AMERICAN CHEMICAL SOCIETY - DIVISION OF FUEL CHEMISTRY, Vol. 33(4), pp. 797 - 803, 1988.
153. BRUNO, G., BURONI, L., CARVANI, G., DEL PIERO, G., and PASSONI, G., Water-insoluble compounds formed by reaction between potassium and mineral matter in catalytic coal gasification; FUEL, Vol. 67, Jan., pp. 67 - 72, 1988.
154. HIEMENZ, P.C., Principles of colloid and surface chemistry, 2nd Edition; Marcel Dekker, Inc., New York, 1986.

6. APPENDIX A

Autosorb Data Summary for Raw Fluid Petroleum Coke, Sample C-1.

UNIVERSITY OF ALBERTA
Quantachrome Autosorb Automated Gas Adsorption System Report
ASORB2PC Version 1.03

Sample ID..... C-1
Sample Description..... Raw Coke
Comments..... No Activation
Gas Type..... NITROGEN
Cross-Sec Area.. 16.2 A² Corr Factor.. 6.580E-05 Molec Wgt.. 28.0134
Sample Weight... 0.6849 g P/Po Toler... 4 File Name.. ROB1.RAW
Analysis Time... 113.0 min Equil Time... 2 Operator... RDP
Outgas Time..... 4.0 hrs Outgas Temp.. 300 °C Station #.. 1
End of Run.....

AREA-VOLUME-PORE SIZE SUMMARY

SURFACE AREA DATA

Single-Point BET.....	4.750E+00	m ² /g
Multi-Point BET.....	4.575E+00	m ² /g
Langmuir Surface Area.....	1.004E+01	m ² /g
Meso Pore Area.....	1.106E+00	m ² /g
* t-Method Micro Pore Area.....	3.470E+00	m ² /g
* MP-Method Micro Pore Area.....	2.019E+00	m ² /g
DR-Method Micro Pore Area.....	7.368E+00	m ² /g
Cumulative Adsorption Surface Area.....	1.388E-01	m ² /g
Cumulative Desorption Surface Area.....	8.454E-02	m ² /g

PORE VOLUME DATA

Total Pore Volume for pores with Radius less than 15926.8 Å at P/Po = 0.9994.....	3.766E-03	cc/g
Cumulative Adsorption Pore Volume for pores in the range of 300.0 to 32.5 Å Radius.....	3.040E-04	cc/g
Cumulative Desorption Pore Volume for pores in the range of 300.0 to 22.5 Å Radius.....	1.478E-04	cc/g
* t-Method Micro Pore Volume.....	1.839E-03	cc/g
* MP-Method Micro Pore Volume.....	1.121E-03	cc/g

PORE SIZE DATA

Average Pore Radius.....	1.646E+01	Å
--------------------------	-----------	---

* Note: MP and t-Method values based on data points with t-Tags.

Adsorption and Desorption Isotherm Data For Figure 24,
Raw Fluid Coke, Sample C-1.

UNIVERSITY OF ALBERTA
Quantachrome Autosorb Automated Gas Adsorption System Report
ASORB2PC Version 1.03

```

Sample ID..... C-1
Sample Description..... Raw Coke
Comments..... No Activation
Gas Type..... NITROGEN
Cross-Sec Area.. 16.2 A2      Corr Factor.. 6.580E-05 Molec Wgt.. 28.0134
Sample Weight... 0.6849 g      P/Po Toler... 4      File Name.. ROB1.RAW
Analysis Time... 113.0 min     Equil Time... 2      Operator... RDP
Outgas Time..... 4.0 hrs      Outgas Temp.. 300 °C Station #.. 1
End of Run.....
    
```

ISOTHERM

P/Po	Volume cc/g STP
0.1070	1.389
0.2129	1.511
0.3137	1.590
0.4141	1.643
0.5144	1.683
0.6134	1.739
0.7149	1.771
0.8136	1.841
0.9134	1.907
0.9994	2.434
0.8844	1.952
0.7840	1.913
0.6842	1.894
0.5838	1.889
0.4840	1.873
0.3844	1.789
0.2847	1.748
0.1847	1.678
0.0849	1.572

Autosorb Data Summary for Raw Fluid Petroleum Coke, Sample C-2.

UNIVERSITY OF ALBERTA
Quantachrome Autosorb Automated Gas Adsorption System Report
ASORB2PC Version 1.03

```

Sample ID..... C-2
Sample Description..... Raw Coke
Comments..... No Activation
Gas Type..... NITROGEN
Cross-Sec Area.. 16.2  Å²      Corr Factor.. 6.580E-05  Molec Wgt.. 28.0134
Sample Weight... 0.8171  g      P/Po Toler... 4          File Name.. ROB2.RAW
Analysis Time... 124.2  min    Equil Time... 2          Operator... RDP
Outgas Time..... 4.0    hrs      Outgas Temp.. 300 °C    Station #.. 1
End of Run.....
    
```

AREA-VOLUME-PORE SIZE SUMMARY

SURFACE AREA DATA

```

Single-Point BET..... 5.688E+00  m²/g
Multi-Point BET..... 5.501E+00  m²/g
Langmuir Surface Area..... 1.095E+01  m²/g
Meso Pore Area..... 1.170E+00  m²/g
* t-Method Micro Pore Area..... 4.331E+00  m²/g
* MP-Method Micro Pore Area..... 2.848E+00  m²/g
DR-Method Micro Pore Area..... 8.770E+00  m²/g
Cumulative Adsorption Surface Area..... 1.219E-01  m²/g
Cumulative Desorption Surface Area..... 1.715E-01  m²/g
    
```

PORE VOLUME DATA

```

Total Pore Volume for pores with Radius
less than 15926.8 Å at P/Po = 0.9994..... 4.015E-03  cc/g
Cumulative Adsorption Pore Volume for pores
in the range of 300.0 to 32.5 Å Radius..... 2.740E-04  cc/g
Cumulative Desorption Pore Volume for pores
in the range of 300.0 to 22.5 Å Radius..... 1.583E-04  cc/g
* t-Method Micro Pore Volume..... 2.279E-03  cc/g
* MP-Method Micro Pore Volume..... 1.609E-03  cc/g
    
```

PORE SIZE DATA

```

Average Pore Radius..... 1.460E+01  Å
* Note: MP and t-Method values based on data points with t-Tags.
    
```

Adsorption and Desorption Data for Figure 25,
Raw Fluid Petroleum Coke, Sample C-2.

UNIVERSITY OF ALBERTA
Quantachrome Autosorb Automated Gas Adsorption System Report
ASORB2PC Version 1.03

```

Sample ID..... C-2
Sample Description..... Raw Coke
Comments..... No Activation
Gas Type..... NITROGEN
Cross-Sec Area.. 16.2   A2   Corr Factor.. 6.580E-05   Molec Wgt.. 28.0134
Sample Weight... 0.8171 g   P/Po Toler... 4           File Name.. ROB2.RAW
Analysis Time... 124.2 min   Equil Time... 2           Operator... RDP
Outgas Time..... 4.0    hrs   Outgas Temp.. 300 °C   Station #.. 1
End of Run.....
  
```

ISOTHERM

P/Po	Volume cc/g STP
0.0977	1.661
0.2100	1.822
0.3129	1.902
0.4132	1.962
0.5139	2.005
0.6140	2.050
0.7144	2.081
0.8140	2.129
0.9133	2.208
0.9994	2.595
0.8839	2.313
0.7840	2.280
0.6841	2.258
0.5843	2.245
0.4855	2.202
0.3846	2.099
0.2849	2.060
0.1847	2.010
0.0854	1.914

Autosorb Data Summary for Untreated Coke Activated for 2 Hours,

Sample A-9.

UNIVERSITY OF ALBERTA
 Quantachrome Autosorb Automated Gas Adsorption System Report
 ASSUREPC Version 1.03

Sample ID..... A-9
 Sample Description..... Untreated Coke
 Comments..... 2 Hours Activation
 Gas Type..... NITROGEN
 Cross-Sec Area.. 16.2 A² Corr Factor.. 6.580E-05 Molec Wgt.. 28.0134
 Sample Weight... 1.0838 g P/Po Toler.. 4 File Name.. ROB3.RAW
 Analysis Time... 291.6 min Equil Time... 2 Operator... RDP
 Outgas Time..... 4.0 hrs Outgas Temp.. 300 °C Station #.. 1
 End of Run.....

AREA-VOLUME-PORE SIZE SUMMARY

SURFACE AREA DATA

Multi-Point BET.....	1.188E+02	m ² /g
Langmuir Surface Area.....	2.254E+02	m ² /g
Meso Pore Area.....	2.707E+01	m ² /g
* t-Method Micro Pore Area.....	9.173E+01	m ² /g
* MP-Method Micro Pore Area.....	5.077E+01	m ² /g
DR-Method Micro Pore Area.....	1.829E+02	m ² /g
Cumulative Adsorption Surface Area.....	3.873E+00	m ² /g
Cumulative Desorption Surface Area.....	2.565E+00	m ² /g

PORE VOLUME DATA

Total Pore Volume for pores with Radius less than 1418.6 Å at P/Po = 0.9932.....	7.906E-02	cc/g
Cumulative Adsorption Pore Volume for pores in the range of 300.0 to 32.5 Å Radius.....	7.189E-03	cc/g
Cumulative Desorption Pore Volume for pores in the range of 300.0 to 25.0 Å Radius.....	2.569E-03	cc/g
* t-Method Micro Pore Volume.....	4.809E-02	cc/g
* MP-Method Micro Pore Volume.....	2.685E-02	cc/g

PORE SIZE DATA

Average Pore Radius..... 1.331E+01 Å

* Note: MP and t-Method values based on data points with t-Tags.

Adsorption and Desorption Isotherm Data for Figure 26,
 Untreated Coke Activated for 2 Hours, Sample A-9.

UNIVERSITY OF ALBERTA
 Quantachrome Autosorb Automated Gas Adsorption System Report
 ASORB2PC Version 1.03

Sample ID..... A-9
 Sample Description..... Untreated Coke
 Comments..... 2 Hours Activation
 Gas Type..... NITROGEN
 Cross-Sec Area.. 16.2 A² Corr Factor.. 6.580E-05 Molec Wgt.. 28.0134
 Sample Weight... 1.0838 g P/Po Toler... 4 File Name.. ROB3.RAW
 Analysis Time... 291.6 min Equil Time... 2 Operator... RDP
 Outgas Time..... 4.0 hrs Outgas Temp.. 300 °C Station #.. 1
 End of Run.....

ISOTHERM

P/Po	Volume cc/g STP
0.0967	36.094
0.1535	37.823
0.1996	38.855
0.2517	39.791
0.3036	40.591
0.3966	41.820
0.4991	42.956
0.6000	44.051
0.6992	45.163
0.7976	46.378
0.8995	48.014
0.9932	51.093
0.8938	50.293
0.7895	49.923
0.6893	49.583
0.5897	49.198
0.4970	48.635
0.4035	42.739
0.2921	41.355
0.1916	39.855
0.0964	37.727

**Autosorb Data Summary for Untreated Coke Activated for 4 Hours,
Sample A-12.**

**UNIVERSITY OF ALBERTA
Quantachrome Autosorb Automated Gas Adsorption System Report
ASORB2PC Version 1.03**

```

Sample ID..... A-12
Sample Description..... Untreated Coke
Comments..... 4 Hours Activation
Gas Type..... NITROGEN
Cross-Sec Area.. 16.2 A2   Corr Factor.. 6.580E-05 Molec Wgt.. 28.0134
Sample Weight... 0.9298 g   P/Po Toler... 4           File Name.. ROB7.RAW
Analysis Time... 260.0 min  Equil Time... 2           Operator... RDP
Outgas Time..... 4.0 hrs   Outgas Temp.. 300 °C     Station #.. 1
End of Run.....
  
```

AREA-VOLUME-PORE SIZE SUMMARY

SURFACE AREA DATA

```

Multi-Point BET..... 1.723E+02 m2/g
Langmuir Surface Area..... 4.134E+02 m2/g
Meso Pore Area..... 6.930E+01 m2/g
* t-Method Micro Pore Area..... 1.030E+02 m2/g
* MP-Method Micro Pore Area..... 7.942E+01 m2/g
DR-Method Micro Pore Area..... 2.650E+02 m2/g
Cumulative Adsorption Surface Area..... 1.319E+01 m2/g
Cumulative Desorption Surface Area..... 1.491E+01 m2/g
  
```

PORE VOLUME DATA

```

Total Pore Volume for pores with Radius
less than 1063.5 Å at P/Po = 0.9909..... 1.417E-01 cc/g
Cumulative Adsorption Pore Volume for pores
in the range of 300.0 to 32.5 Å Radius..... 2.750E-02 cc/g
Cumulative Desorption Pore Volume for pores
in the range of 300.0 to 25.0 Å Radius..... 1.685E-02 cc/g
* t-Method Micro Pore Volume..... 5.291E-02 cc/g
* MP-Method Micro Pore Volume..... 4.388E-02 cc/g
  
```

PORE SIZE DATA

```

Average Pore Radius..... 1.645E+01 Å
* Note: MP and t-Method values based on data points with t-Tags.
  
```

**Adsorption and Desorption Isotherm Data for Figure 27,
Untreated Coke Activated for 4 Hours, Sample A-12.**

**UNIVERSITY OF ALBERTA
Quantachrome Autosorb Automated Gas Adsorption System Report
ASORB2PC Version 1.03**

```

Sample ID..... A-12
Sample Description..... Untreated Coke
Comments..... 4 Hours Activation
Gas Type..... NITROGEN
Cross-Sec Area.. 16.2  Å²      Corr Factor.. 6.580E-05  Molec Wgt.. 28.0134
Sample Weight... 0.9298  g      P/Po Toler... 4      File Name.. ROB7.RAW
Analysis Time... 260.0  min    Equil Time... 2      Operator... RDP
Outgas Time..... 4.0    hrs    Outgas Temp.. 300 °C  Station #.. 1
End of Run.....
  
```

ISOTHERM

P/Po	Volume cc/g STP
0.0962	48.403
0.1472	51.398
0.2009	53.907
0.2526	56.043
0.3043	57.941
0.3969	61.036
0.4962	64.089
0.6011	67.503
0.7001	71.023
0.7989	75.443
0.8964	81.239
0.9909	91.611
0.8972	88.277
0.8001	86.017
0.7011	83.738
0.5952	81.010
0.4984	77.952
0.4003	62.033
0.2955	51.389
0.1952	54.569
0.0942	49.401

**Autosorb Data Summary for Untreated Coke Activated for 6 Hours,
Sample A-17.**

**UNIVERSITY OF ALBERTA
Quantachrome Autosorb Automated Gas Adsorption System Report
ASORB2PC Version 1.03**

Sample ID..... A-17
 Sample Description..... Untreated Coke
 Comments..... 6 Hours Activation
 Gas Type..... NITROGEN
 Cross-Sec Area.. 16.2 A² Corr Factor.. 6.580E-05 Molec Wgt.. 28.0134
 Sample Weight... 0.8652 g P/Po Toler... 4 File Name.. ROB4.RAW
 Analysis Time... 300.0 min Equil Time... 2 Operator... RDP
 Outgas Time..... 4.0 hrs Outgas Temp.. 0 °C Station #.. 1
 End of Run.....

AREA-VOLUME-PORE SIZE SUMMARY

SURFACE AREA DATA

Multi-Point BET.....	3.186E+02	m ² /g
Langmuir Surface Area.....	7.229E+02	m ² /g
Meso Pore Area.....	1.282E+02	m ² /g
* t-Method Micro Pore Area.....	1.904E+02	m ² /g
* MP-Method Micro Pore Area.....	1.542E+02	m ² /g
DR-Method Micro Pore Area.....	4.885E+02	m ² /g
Cumulative Adsorption Surface Area.....	2.115E+01	m ² /g
Cumulative Desorption Surface Area.....	1.722E+01	m ² /g

PORE VOLUME DATA

Total Pore Volume for pores with Radius less than 998.5 Å at P/Po = 0.9903.....	2.438E-01	cc/g
Cumulative Adsorption Pore Volume for pores in the range of 300.0 to 32.5 Å Radius.....	3.883E-02	cc/g
Cumulative Desorption Pore Volume for pores in the range of 300.0 to 25.0 Å Radius.....	1.750E-02	cc/g
* t-Method Micro Pore Volume.....	9.701E-02	cc/g
* MP-Method Micro Pore Volume.....	8.706E-02	cc/g

PORE SIZE DATA

Average Pore Radius.....	1.530E+01	Å
--------------------------	-----------	---

* Note: MP and t-Method values based on data points with t-Tags.

Adsorption and Desorption Isotherm Data for Figure 28,
 Untreated Coke Activated for 6 Hours, Sample A-17.

UNIVERSITY OF ALBERTA
 Quantachrome Autosorb Automated Gas Adsorption System Report
 ASORB2PC Version 1.03

Sample ID..... A-17
 Sample Description..... Untreated Coke
 Comments..... 6 Hours Activation
 Gas Type..... NITROGEN
 Cross-Sec Area.. 16.2 A² Corr Factor.. 6.580E-05 Molec Wgt.. 28.0134
 Sample Weight... 0.8652 g P/Po Toler... 4 File Name.. ROB4.RAW
 Analysis Time... 300.0 min Equil Time... 2 Operator... RDP
 Outgas Time..... 4.0 hrs Outgas Temp.. 0 °C Station #.. 1
 End of Run.....

ISOTHERM

P/Po	Volume cc/g STP
0.0972	88.931
0.1480	94.450
0.1971	98.856
0.2491	102.927
0.3009	106.558
0.3998	112.732
0.5000	118.426
0.5972	124.119
0.6966	130.064
0.7971	137.062
0.8967	145.130
0.9903	157.543
0.8443	153.626
0.7956	151.527
0.6974	149.278
0.6025	146.519
0.5014	142.519
0.4024	114.302
0.2945	107.105
0.1944	99.705
0.0960	90.004

**Autosorb Data Summary for Potassium Treated Coke Activated for 2 Hours,
Sample A-11.**

**UNIVERSITY OF ALBERTA
Quantachrome Autosorb Automated Gas Adsorption System Report
ASORB2PC Version 1.03**

```

Sample ID..... A-11
Sample Description..... Potassium Coke
Comments..... 2 Hours Activation
Gas Type..... NITROGEN
Cross-Sec Area.. 16.2  A*   Corr Factor.. 6.580E-05  Molec Wgt.. 28.0134
Sample Weight... 1.0191  g   P/Po Toler... 4           File Name.. ROB5.RAW
Analysis Time... 230.4   min  Equil Time... 2           Operator... RDP
Outgas Time..... 4.0    hrs  Outgas Temp.. 300 °C     Station #.. 1
End of Run.....
  
```

AREA-VOLUME-PORE SIZE SUMMARY

SURFACE AREA DATA

```

Multi-Point BET..... 8.747E+01  m²/g
Langmuir Surface Area..... 1.916E+02  m²/g
Meso Pore Area..... 2.575E+01  m²/g
* t-Method Micro Pore Area..... 6.172E+01  m²/g
* MP-Method Micro Pore Area..... 3.757E+01  m²/g
DR-Method Micro Pore Area..... 1.358E+02  m²/g
Cumulative Adsorption Surface Area..... 4.717E+00  m²/g
Cumulative Desorption Surface Area..... 5.175E+00  m²/g
  
```

PORE VOLUME DATA

```

Total Pore Volume for pores with Radius
less than 1087.1 Å at P/Po = 0.9911..... 6.887E-02  cc/g
Cumulative Adsorption Pore Volume for pores
in the range of 300.0 to 32.5 Å Radius..... 1.174E-02  cc/g
Cumulative Desorption Pore Volume for pores
in the range of 300.0 to 25.0 Å Radius..... 8.277E-03  cc/g
* t-Method Micro Pore Volume..... 3.248E-02  cc/g
* MP-Method Micro Pore Volume..... 2.044E-02  cc/g
  
```

PORE SIZE DATA

```

Average Pore Radius..... 1.575E+01  Å
* Note: MP and t-Method values based on data points with t-Tags.
  
```

Adsorption and Desorption Isotherm Data for Figure 29,
Potassium Treated Coke Activated for 2 Hours, Sample A-11.

UNIVERSITY OF ALBERTA
Quantachrome Autosorb Automated Gas Adsorption System Report
ASORB2PC Version 1.03

```

Sample ID..... A-11
Sample Description..... Potassium Coke
Comments..... 2 Hours Activation
Gas Type..... NITROGEN
Cross-Sec Area.. 16.2   A*   Corr Factor.. 6.580E-05   Molec Wgt.. 28.0134
Sample Weight... 1.0191 g   P/Po Toler... 4   File Name.. ROB5.RAW
Analysis Time... 230.4   min   Equil Time... 2   Operator... RDP
Outgas Time..... 4.0    hrs   Outgas Temp.. 300 °C   Station #.. 1
End of Run.....
  
```

ISOTHERM

P/Po	Volume cc/g STP
0.1016	26.139
0.1515	27.366
0.2043	28.385
0.2567	29.239
0.3078	29.966
0.4036	31.147
0.5039	32.263
0.6029	33.392
0.7016	34.585
0.7962	36.049
0.8946	38.393
0.9911	44.507
0.9016	41.971
0.7915	40.519
0.6971	39.558
0.5961	38.652
0.4974	37.743
0.4009	31.742
0.2903	30.339
0.1900	28.881
0.0932	26.885

**Autosorb Data Summary for Potassium Treated Coke Activated for 4 Hours,
Sample A-14.**

**UNIVERSITY OF ALBERTA
Quantachrome Autosorb Automated Gas Adsorption System Report
ASORB2PC Version 1.03**

Sample ID..... A-14
 Sample Description..... Potassium Coke
 Comments..... 4 Hours Activation
 Gas Type..... NITROGEN
 Cross-Sec Area.. 16.2 A² Corr Factor.. 6.580E-05 Molec Wgt.. 28.0134
 Sample Weight... 0.9122 g P/Po Toler... 4 File Name.. ROBB.RAW
 Analysis Time... 258.5 min Equil Time... 2 Operator... RDP
 Outgas Time..... 4.0 hrs Outgas Temp.. 300 °C Station #.. 1
 End of Run.....

AREA-VOLUME-PORE SIZE SUMMARY

SURFACE AREA DATA

Multi-Point BET.....	1.674E+02	m ² /g
Langmuir Surface Area.....	3.521E+02	m ² /g
Meso Pore Area.....	4.355E+01	m ² /g
* t-Method Micro Pore Area.....	1.239E+02	m ² /g
* MP-Method Micro Pore Area.....	8.113E+01	m ² /g
DR-Method Micro Pore Area.....	2.576E+02	m ² /g
Cumulative Adsorption Surface Area.....	7.541E+00	m ² /g
Cumulative Desorption Surface Area.....	7.699E+00	m ² /g

PORE VOLUME DATA

Total Pore Volume for pores with Radius less than 978.6 Å at P/Po = 0.9901.....	1.304E-01	cc/g
Cumulative Adsorption Pore Volume for pores in the range of 300.0 to 32.5 Å Radius.....	2.255E-02	cc/g
Cumulative Desorption Pore Volume for pores in the range of 300.0 to 25.0 Å Radius.....	1.504E-02	cc/g
* t-Method Micro Pore Volume.....	6.413E-02	cc/g
* MP-Method Micro Pore Volume.....	4.351E-02	cc/g

PORE SIZE DATA

Average Pore Radius.....	1.557E+01	Å
--------------------------	-----------	---

* Note: MP and t-Method values based on data points with t-Tags.

Adsorption and Desorption Isotherm Data for Figure 30,
Potassium Treated Coke Activated for 4 Hours, Sample A-14.

UNIVERSITY OF ALBERTA
Quantachrome Autosorb Automated Gas Adsorption System Report
ASORB2PC Version 1.03

Sample ID..... A-14
 Sample Description..... Potassium Coke
 Comments..... 4 Hours Activation
 Gas Type..... NITROGEN
 Cross-Section Area.. 16.2 Å² Corr Factor.. 6.580E-05 Molec Wgt.. 28.0134
 Sample Weight... 0.9122 g P/Po Toler... 4 File Name.. ROBB.RAW
 Analysis Time... 258.5 min Equil Time... 2 Operator... RDP
 Outgas Time..... 4.0 hrs Outgas Temp.. 300 °C Station #.. 1
 End of Run.....

ISOTHERM

P/Po	Volume cc/g STP
0.0985	49.530
0.1507	52.061
0.2042	54.030
0.2512	55.445
0.3020	56.764
0.4040	58.953
0.4969	60.615
0.5955	62.297
0.7072	64.278
0.8012	66.411
0.9013	70.484
0.9901	84.250
0.8975	78.397
0.8007	76.057
0.6949	74.353
0.5915	72.996
0.5024	71.818
0.3976	59.624
0.2968	57.395
0.1985	54.747
0.0973	50.612

**Autosorb Data Summary for Potassium Treated Coke Activated for 6 Hours,
Sample A-18.**

**UNIVERSITY OF ALBERTA
Quantachrome Autosorb Automated Gas Adsorption System Report
ASORB2PC Version 1.03**

Sample ID..... A-18
 Sample Description..... Potassium Coke
 Comments..... 6 Hours Activation
 Gas Type..... NITROGEN
 Cross-Sec Area.. 16.2 A² Corr Factor.. 6.580E-05 Molec Wgt.. 28.0134
 Sample Weight... 0.7819 g P/Po Toler... 4 File Name.. ROB6.RAW
 Analysis Time... 250.3 min Equil Time... 2 Operator... RDP
 Outgas Time..... 4.0 hrs Outgas Temp.. 300 °C Station #.. 1
 End of Run.....

AREA-VOLUME-PORE SIZE SUMMARY

SURFACE AREA DATA

Multi-Point BET.....	1.763E+02	m ² /g
Langmuir Surface Area.....	4.406E+02	m ² /g
Meso Pore Area.....	6.783E+01	m ² /g
* t-Method Micro Pore Area.....	1.085E+02	m ² /g
* MP-Method Micro Pore Area.....	9.393E+01	m ² /g
DR-Method Micro Pore Area.....	2.720E+02	m ² /g
Cumulative Adsorption Surface Area.....	1.221E+01	m ² /g
Cumulative Desorption Surface Area.....	1.527E+01	m ² /g

PORE VOLUME DATA

Total Pore Volume for pores with Radius less than 978.6 Å at P/Po = 0.9901.....	1.635E-01	cc/g
Cumulative Adsorption Pore Volume for pores in the range of 300.0 to 32.5 Å Radius.....	3.805E-02	cc/g
Cumulative Desorption Pore Volume for pores in the range of 300.0 to 25.0 Å Radius.....	3.339E-02	cc/g
* t-Method Micro Pore Volume.....	5.510E-02	cc/g
* MP-Method Micro Pore Volume.....	5.300E-02	cc/g

PORE SIZE DATA

Average Pore Radius.....	1.855E+01	Å
--------------------------	-----------	---

* Note: MP and t-Method values based on data points with t-Tags.

Adsorption and Desorption Isotherm Data for Figure 31,
Potassium Treated Coke Activated for 2 Hours, Sample A-18.

UNIVERSITY OF ALBERTA
Quantachrome Autosorb Automated Gas Adsorption System Report
ASORB2PC Version 1.03

```

Sample ID..... A-18
Sample Description..... Potassium Coke
Comments..... 6 Hours Activation
Gas Type..... NITROGEN
Cross-Sec Area.. 16.2 A²      Corr Factor.. 6.580E-05 Molec Wgt.. 28.0134
Sample Weight... 0.7819 g      P/Po Toler... 4      File Name.. ROB6.RAW
Analysis Time... 250.3 min     Equil Time... 2      Operator... RDP
Outgas Time..... 4.0 hrs      Outgas Temp.. 300 °C Station #.. 1
End of Run.....
  
```

ISOTHERM

P/Po	Volume cc/g STP
0.1032	49.343
0.1526	52.360
0.2043	54.974
0.2561	57.236
0.3005	58.978
0.4013	62.397
0.5013	65.397
0.6020	68.307
0.7002	71.227
0.8011	74.981
0.8981	81.207
0.9901	105.671
0.9002	90.444
0.7987	85.169
0.6957	81.801
0.5984	79.308
0.4991	76.892
0.4038	63.309
0.2950	59.313
0.1950	55.136
0.0935	49.409

Autosorb Data Summary for Fisher Coconut Charcoal.

**UNIVERSITY OF ALBERTA
Quantachrome Autosorb Automated Gas Adsorption System Report
ASORB2PC Version 1.03**

```

Sample ID..... Fisher 690B-B
Sample Description..... Commercial Activated Carbon
Comments..... 50 - 200 Mesh
Gas Type..... NITROGEN
Cross-Sec Area.. 16.2 A2      Corr Factor.. 6.580E-05 Molec Wgt.. 28.0134
Sample Weight... 0.3524 g      P/Po Toler... 4      File Name.. ROB9.RAW
Analysis Time... 430.4 min     Equil Time... 2      Operator... RDP
Outgas Time..... 4.0 hrs      Outgas Temp.. 300 °C  Station #.. 1
End of Run.....
    
```

AREA-VOLUME-PORE SIZE SUMMARY

SURFACE AREA DATA

```

Multi-Point BET..... 1.237E+03 m2/g
Langmuir Surface Area..... 2.208E+03 m2/g
Meso Pore Area..... 3.685E+02 m2/g
* t-Method Micro Pore Area..... 8.680E+02 m2/g
* MP-Method Micro Pore Area..... 1.167E+03 m2/g
DR-Method Micro Pore Area..... 1.823E+03 m2/g
Cumulative Adsorption Surface Area..... 3.384E+01 m2/g
Cumulative Desorption Surface Area..... 2.839E+01 m2/g
    
```

PORE VOLUME DATA

```

Total Pore Volume for pores with Radius
less than 950.2 Å at P/Po = 0.9898..... 7.678E-01 cc/g
Cumulative Adsorption Pore Volume for pores
in the range of 300.0 to 25.0 Å Radius..... 7.233E-02 cc/g
Cumulative Desorption Pore Volume for pores
in the range of 300.0 to 25.0 Å Radius..... 6.486E-02 cc/g
* t-Method Micro Pore Volume..... 4.164E-01 cc/g
* MP-Method Micro Pore Volume..... 6.083E-01 cc/g
    
```

PORE SIZE DATA

```

Average Pore Radius..... 1.242E+01 Å
    
```

* Note: MP and t-Method values based on data points with t-Tags.

Adsorption and Desorption Isotherm Data for Fisher Coconut Charcoal.

UNIVERSITY OF ALBERTA
 Quantachrome Autosorb Automated Gas Adsorption System Report
 ASORB2PC Version 1.03

Sample ID..... Fisher 690B-B
 Sample Description..... Commercial Activated Carbon
 Comments..... 50 - 200 Mesh
 Gas Type..... NITROGEN
 Cross-Sec Area.. 16.2 A² Corr Factor.. 6.580E-05 Molec Wgt.. 28.0134
 Sample Weight... 0.3524 g P/Po Toler... 4 File Name.. ROB9.RAW
 Analysis Time... 430.4 min Equil Time... 2 Operator... RDP
 Outgas Time..... 4.0 hrs Outgas Temp.. 300 °C Station #.. 1
 End of Run.....

ISOTHERM

P/Po	Volume cc/g STP	P/Po	Volume cc/g STP
0.0516	298.076	0.0464	295.216
0.0989	331.424		
0.1493	357.747		
0.1979	377.639		
0.2476	394.010		
0.2969	407.035		
0.3503	418.610		
0.3986	427.225		
0.4454	433.879		
0.4975	439.963		
0.5518	445.219		
0.5963	448.998		
0.6471	452.662		
0.6988	456.098		
0.7486	459.484		
0.7962	463.056		
0.8533	467.716		
0.8998	472.781		
0.9462	480.423		
0.9898	496.232		
0.9546	487.965		
0.9037	479.211		
0.8512	473.570		
0.8039	469.722		
0.7519	466.257		
0.6996	463.138		
0.6492	460.221		
0.5986	457.313		
0.5492	454.305		
0.5012	451.061		
0.4538	442.256		
0.4036	430.394		
0.3492	419.838		
0.2990	409.100		
0.2508	396.583		
0.1976	379.319		
0.1476	358.805		
0.0969	332.094		